Procurement Executive - Ministry of Defence

AWRE, Aldermaston

AWRE REPORT NO. 050/73

Theoretical P Wave Seismograms from Earthquake Source Models

A Douglas
J B Young
J A Hudson*

*Department of Applied Mathematics and Theoretical Physics,
University of Cambridge.

SBN 85518052 8

CONTENTS

		Page
	SUMMARY	3
1.	INTRODUCTION	3
2.	COMPUTATION OF SEISMOGRAMS	3
3.	HALFSPACE MODELS: M1 TO M5	9
4.	INTERPRETING MODELS WITH CRUSTAL LAYERING: M6 TO M27	26
5.	VERTICAL DIP SLIP AND VERTICAL STRIKE SLIP MODELS: M6 TO M11	29
6.	45° DIP SLIP MODELS - SLIP DIRECTION 90° TO STRIKE: M12 TO M22	48
7.	MODELS WITH SLIP ON PLANES DIPPING AT 45° OR 67.5°: SLIP DIRECTION - 45° TO STRIKE: M23 TO M27	82
	REFERENCES	98

SUMMARY

Theoretical P wave seismograms are shown, computed using an earthquake source model of finite size and fixed rupture velocity. The examples shown are chosen to illustrate the influence on the computed seismogram of crustal layering, recording system, anelastic attenuation and source size, shape and orientation.

1. INTRODUCTION

Short period P wave seismograms from earthquakes are usually difficult to interpret. Occasionally they show the classic pattern of direct P and the surface reflections pP and sP but more often they are either simpler or more complex than this. Douglas et al. [1] have shown that it is possible to reproduce many of the features of observed seismograms with simple theoretical models, but to obtain a fit between a model and any given seismogram is a tedious process because there are so many variables in the models and so little is known about detailed earth structure. Douglas et al. [2], however, have described a relatively simple observed seismogram which can be reproduced rather closely. In this report we make no attempt to match theory and observation but simply present theoretical seismograms for a range of models to show the variety of seismograms that can be produced by a very simple model of an earthquake source. We hope these will be helpful to others who try to interpret observed seismograms.

The major part of this work was done while AWRE was part of the UKAEA.

2. COMPUTATION OF SEISMOGRAMS

The method of computation is adequately described elsewhere [1] and is only repeated here in outline. The earthquake source is assumed to be a double couple type of source of finite size. The source model is based on that proposed by Savage [3]; a fracture is assumed to be initiated at a point and to spread with uniform velocity in all directions in a nodal plane of the double couple radiation pattern. The fracture finally comes to rest along a circular or elliptic contour. Fracture may be initiated at either the centre of the circle or ellipse or at a focus of the ellipse. Slip occurs instantaneously as the fracture passes through a point in the fault plane and, for the models described here, the displacement is largest at the centre of the fault and falls off towards the edge as $(1 - x^2/s^2)^{\frac{1}{2}}$, where x is the distance of any point from the centre and s is the distance of the edge of the fault from the centre along a radius through the point.

The motion of the source of radiation introduces a Doppler shift in the spectrum of the seismic pulse which is apparent in the pulse shape itself. If the source were a crack running down a line of length ℓ at speed v and with uniform amplitude, the pulse shape at a distant observer would be a box-car function of duration $\tau = \ell[(1/v) - (\cos\theta/\alpha)]$ and amplitude proportional to τ^{-1}, where θ is the angle between the line

of faulting and the direction of the observer and α is the wave speed. The corresponding spectrum has a peak at zero frequency of width $2\pi/\tau$. An observer in line with the approaching crack ($\theta = 0$) sees a short high amplitude pulse with a broad spectrum (a Doppler shift to high frequencies), whereas an observer in the opposite direction ($\theta = \tau$) sees a long, low amplitude pulse with a narrow, low frequency spectrum. Observers at intermediate positions would see something between the two extremes. If the crack ran from an initial point at the centre of the line, in both directions to the ends, an observer in line with the crack would see a superposition of the two cases above; a short high amplitude beginning, from the approaching section of crack, and a low amplitude tail, from the receding section. An observer at a point in the plane perpendicular to the crack ($\theta = \pi/2$), however, would see, as before, a simple box-car function of length $\ell/2v$.

The characteristics of the pulse shapes from an elliptic or circular fault are similar, but rather more complicated. Let us consider a circular fault with a crack moving out in a circle from the centre with speed v and uniform amplitude. In figure 1, AOB is a cross section through the fault plane. The fracture starts at 0 and spreads out towards A and B. An observer at P_2 sees the fracture approaching along OA, receding along OB, and moving with intermediate speeds in other directions in the fault plane. The pulse shape is therefore a steep wave-front with a high amplitude beginning and a long, low amplitude tail. The pulse length is $s[(1/v) + (1/\alpha)]$ where s is the radius of the circle. The nature of the circular fault smooths out the extremely abrupt character of the pulse from a line fault. An observer at P_1, on the other hand, receives at any instant radiation from a fracture contour which grows at a constant rate proportional to v. The leading edge of the pulse is therefore a ramp which drops to zero after a time s/v. The pulse is shorter than at P_2, has a less steep front, and high amplitudes appear at the rear, rather than at the beginning. For observers at positions between P_1 and P_2, the pulse shapes are intermediate between the two extremes with lengths between s/v and $s(v^{-1} + \alpha^{-1})$.

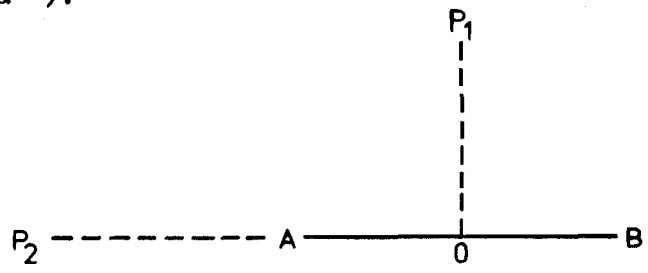

FIGURE 1. CROSS SECTION OF FAULT PLANE WITH OBSERVERS AT RIGHT ANGLES AND IN LINE WITH THE FAULT PLANE

Elliptic faults generate pulses of a similar kind. If the minor axis is much less than the major axis, the radiation will clearly be similar to that from a bilateral line fault, if the fracture initiates at the centre of the ellipse, or a unilateral line fault, if

the fracture starts at a focus. Figure 2 shows the geometrical relationship between the dip of the fault plane, the direction of slip on the fault and the azimuth of the observer.

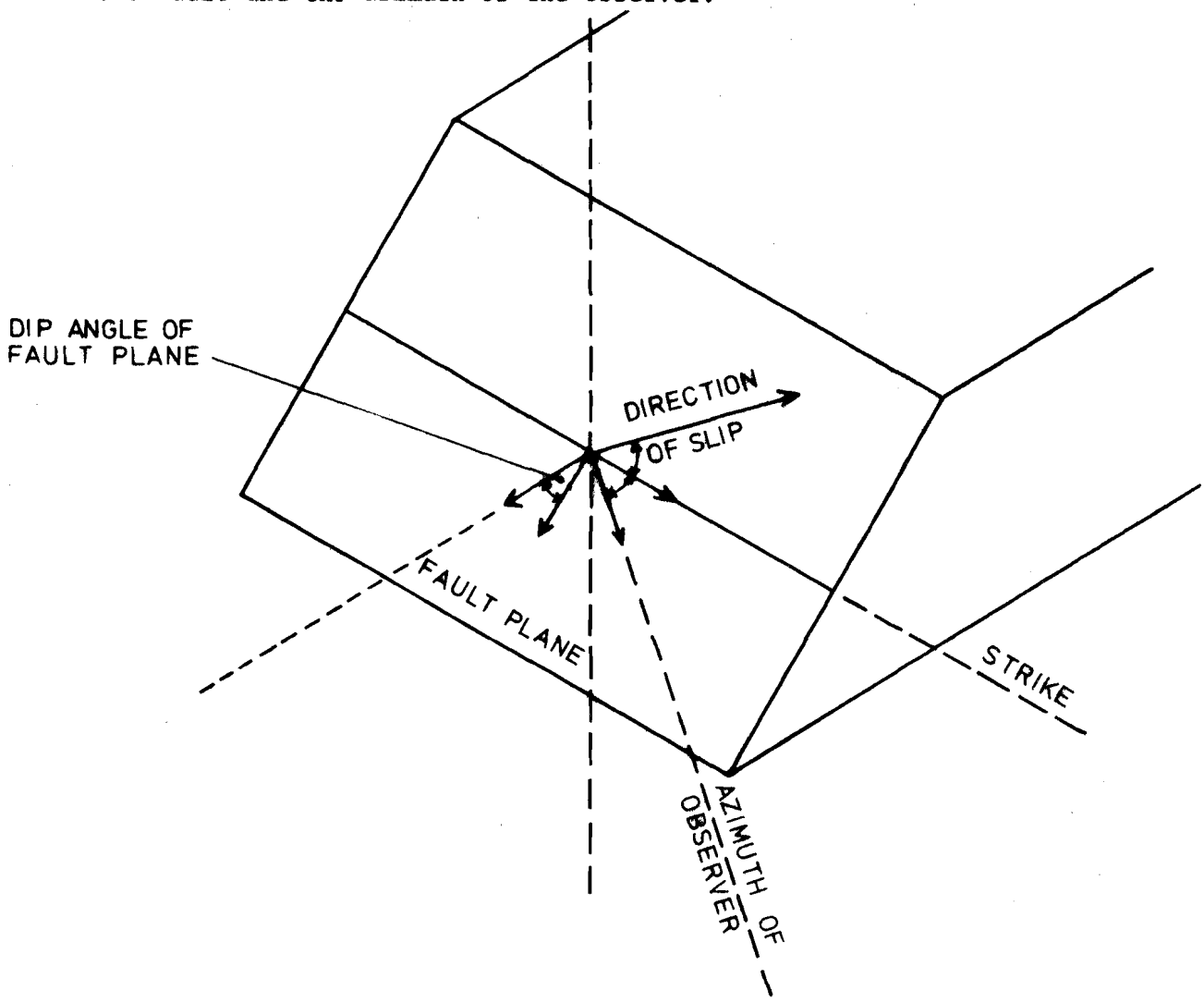

FIGURE 2. RELATIONSHIP BETWEEN DIP OF FAULT PLANE, DIRECTION OF SLIP ON THE FAULT AND THE AZIMUTH OF THE OBSERVER

The earth model used comprises three parts:-

(a) Crustal layers which contain the source.

(b) The earth's mantle which is allowed for simply by two terms, one a multiplier to allow for geometrical spreading of the wave-front, the other a term to allow for the effects of anelastic attenuation. The attenuation at each angular frequency w is assumed to be exp $(-wt^*/2)$ where $t^* = T/Q_{AV}$, T is the travel time between source and receiver and Q_{AV} the

average Q or quality factor. A small dispersion term has also to be introduced to satisfy causality. As Q_{AV} for the earth is only imperfectly known and is probably not the same for all ray paths, seismograms are given here for values of t* ranging from 0.0 to 2.0 which we hope covers the range of values in the earth.

(c) Crustal layers underlying the receiver.

The effects of source and receiver crustal layers are allowed for using Thomson-Haskell matrix methods.

The only other effect which will be taken into account is that of the recording equipment. We have looked at the effects of conventional (narrow band) long period (LP) and short period (SP) systems, and of broad band systems. Narrow band LP systems produce rather characterless records so only one example is shown here. Short period (UK array response) and broad band (Kirnos response) seismograms are shown for all models. The amplitude response of the three systems is shown in figure 3.

Two sets of seismograms are shown for all models; they are designated MnK for Kirnos seismograms and MnSP for SP seismograms, where Mn is the model number. Five seismograms are shown for each response, the top one (Channel 1) being the ground displacement at the receiver (for t* = 0.0), ie, before passing through the recording system and assuming no attenuation. The other four seismograms (Channels 2, 3, 4 and 5 reading from the top) are as recorded by the particular recording system for different values of t* (see table 1). Time is shown along the bottom of each figure, time marks being at intervals of 6 seconds.

To cut down the number of variables in the model some parameters have been kept constant throughout all the models. These parameters are listed in table 2.

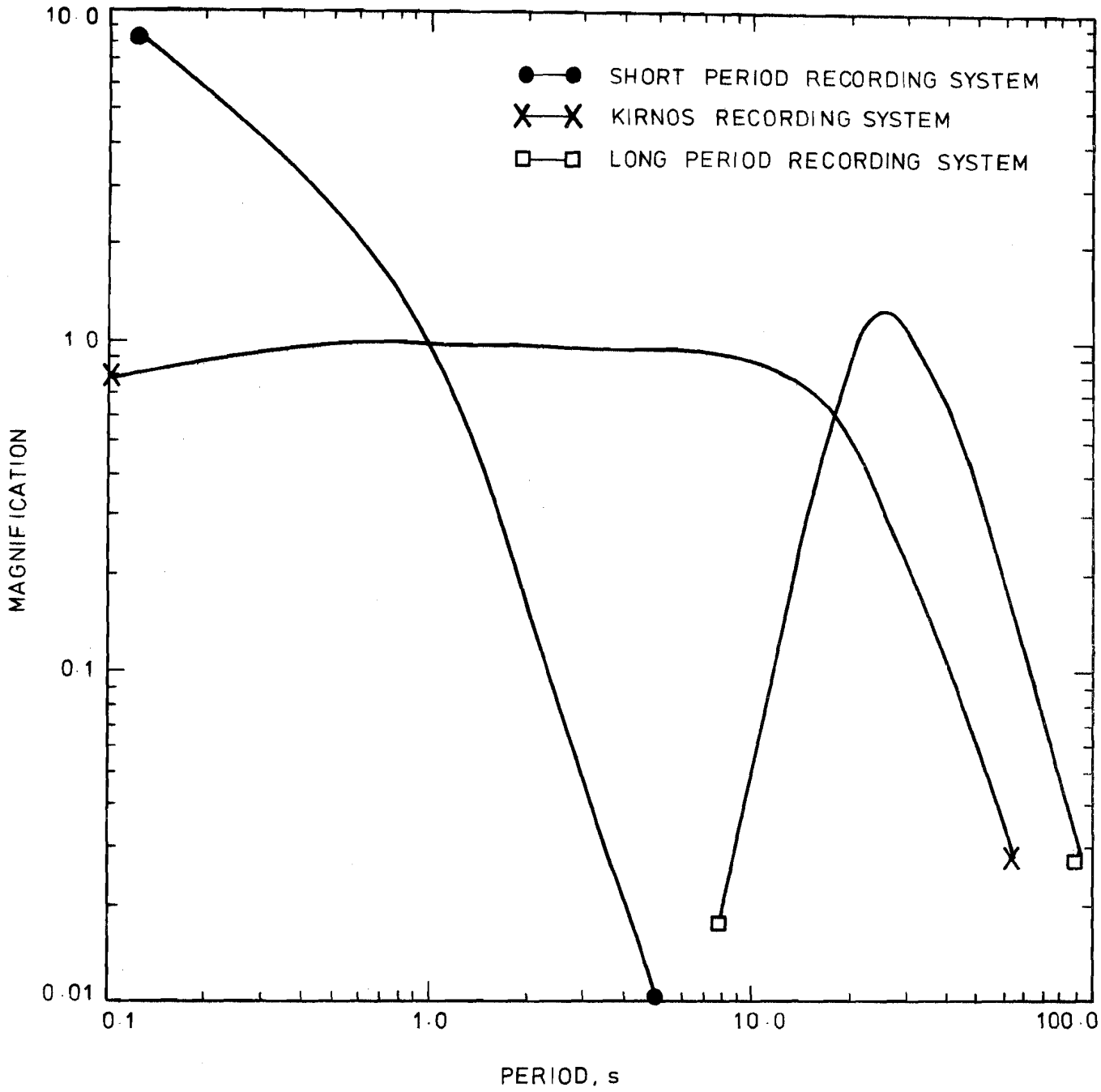

FIGURE 3. AMPLITUDE RESPONSE OF RECORDING SYSTEMS USED IN COMPUTATION OF THE SEISMOGRAMS

TABLE 1

Channels Computed for Each Model and Recording System

Channel 1:	Displacement at receiver before passing through recording system	$t^* = 0.0$
Channel 2:	Recorded seismogram	$t^* = 0.0$
Channel 3:	Recorded seismogram	$t^* = 0.2$
Channel 4:	Recorded seismogram	$t^* = 1.0$
Channel 5:	Recorded seismogram	$t^* = 2.0$

Time - time marks at intervals of 6 seconds.

TABLE 2

Parameters Kept Constant for all Models

Depth of focus	:	25 km
Epicentral distance, source to receiver	:	60° (take off angle for P at source 23.22° to vertical)
Fracture velocity	:	2.364 km s^{-1}
Stress drop	:	100 bars
Recording systems	:	(a) Kirnos (broad band) system (b) UK array system (SP)
Distribution of displacement over fault plane	:	Falls off as $(1 - x^2/s^2)^{\frac{1}{2}}$, where x is the distance of any point from the centre of the fault plane and s is the radius of the fault plane passing through the point

3. HALFSPACE MODELS: M1 TO M5

Models M1 to M5 have been computed assuming the source is in a halfspace with P wave velocity 6.7 km s^{-1}, S wave velocity 3.96 km s^{-1} and density 2.9 g cm^{-3} and that the receiver is also on a halfspace with the same properties. The only arrivals on these seismograms other than direct P are thus the free surface reflections pP and sP. These halfspace models are included to illustrate the influence of the shape and size of the fault plane and the position of initiation of fracture on the pulse shape uncomplicated by reflected and refracted arrivals from layering in the crust.

Model M1

Dip of fault plane	:	90°
Direction of slip on fault plane	:	vertical
Shape of fault plane	:	circular
Dimensions of fault plane	:	1 km radius
Azimuth	:	90° to strike

Figure 4 shows a cross section through the source in the plane of the observer. For all three phases P, pP and sP, the rays leave the source at relatively small angles to the fault plane. Thus, the leading edges of the pulses should be steeper than the trailing edges. This is only clearly seen for sP where the S wave velocity and the fracture velocity are not greatly different.

For this model only, a section of the LP seismogram is shown (shifted 6 seconds to the left relative to the broad band and SP seismograms). The almost sinusoidal form of the LP seismogram is typical of the LP seismograms.

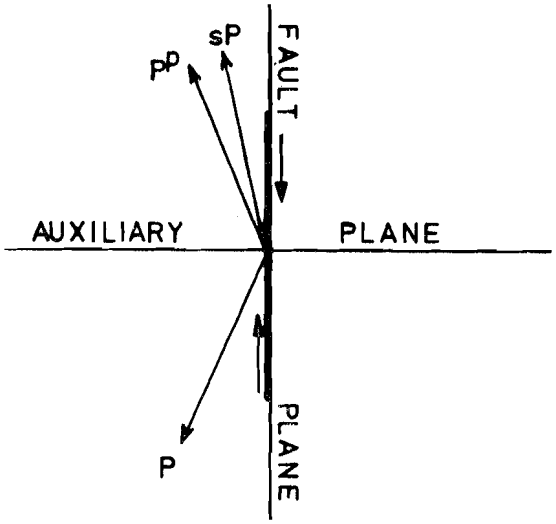

FIGURE 4

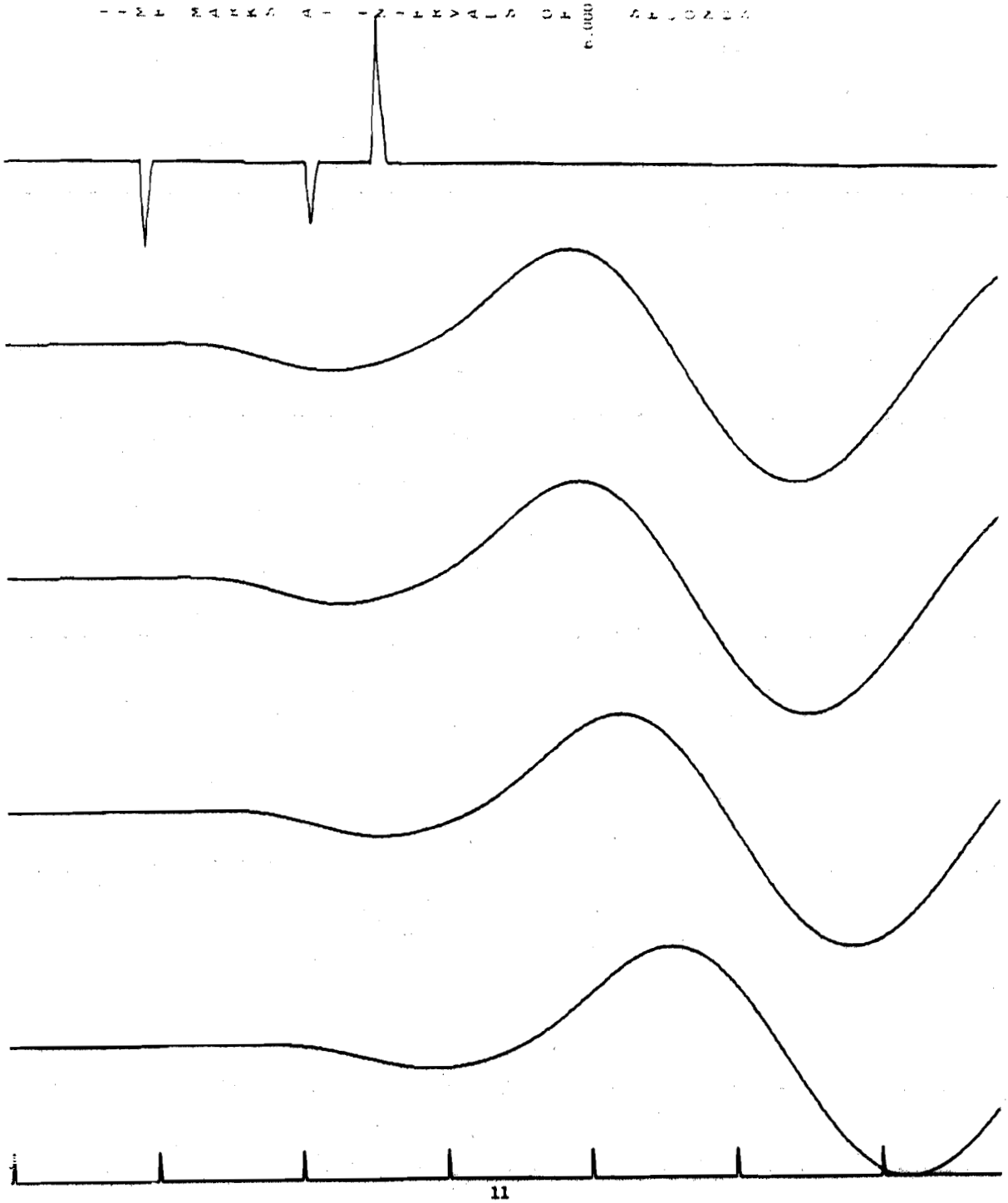

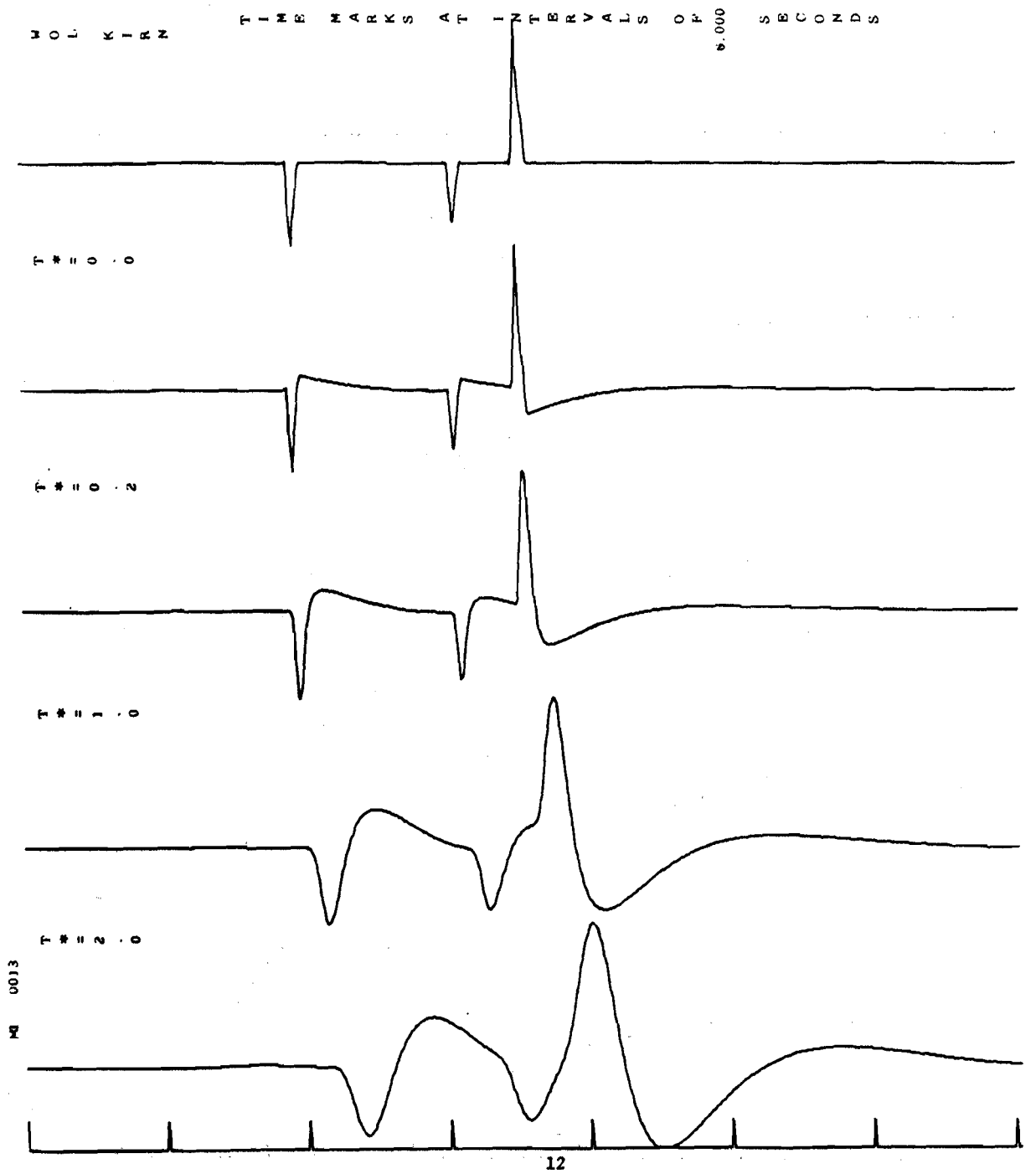
MOLI KIRN
TIME MARKS AT INTERVALS OF 0.000 SECONDS
T*=0.0
T*=0.2
T*=1.0
T*=2.0
MM 0013

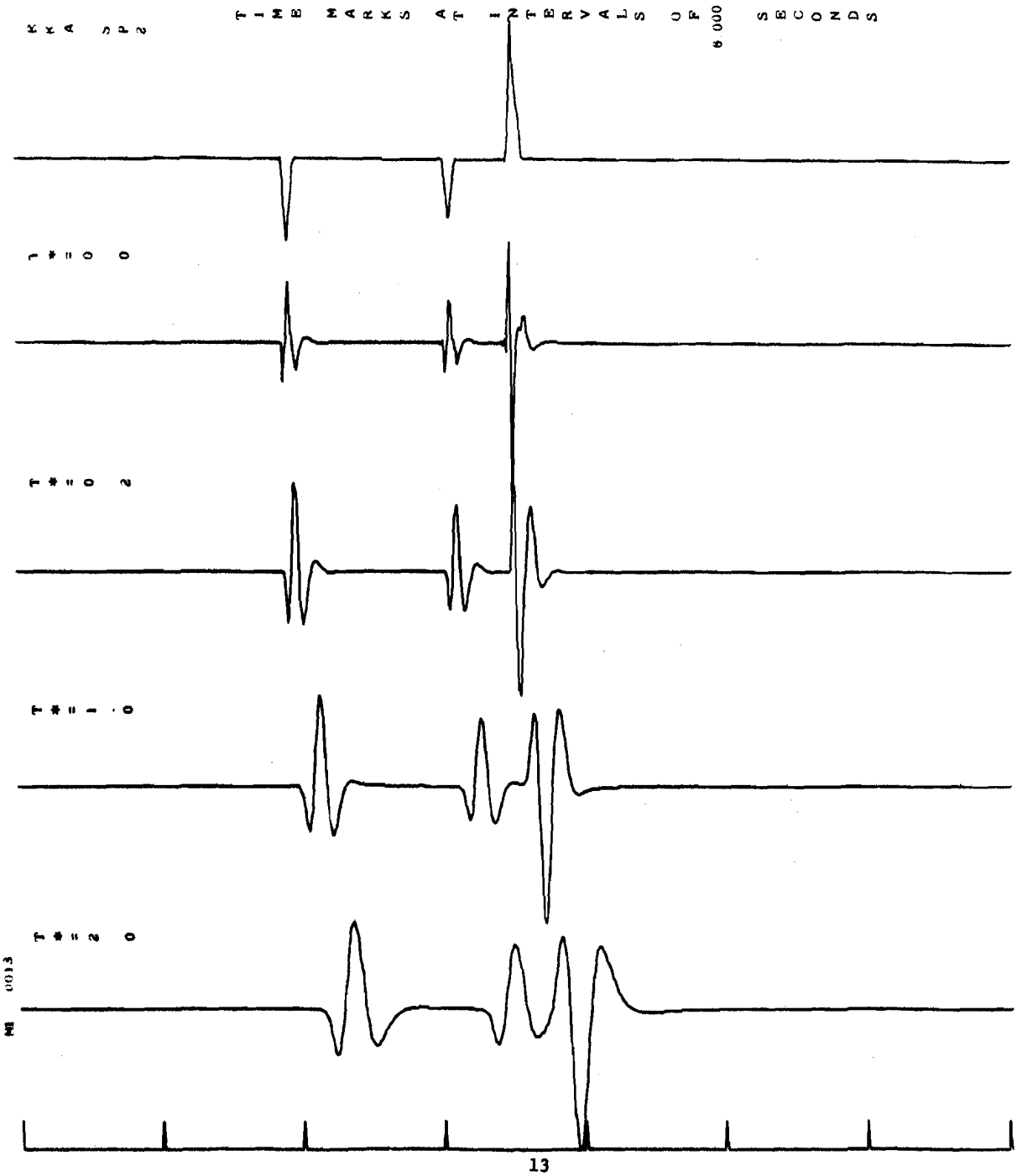
KKA SP2
TIME MARKS AT INTERVALS OF 6000 SECONDS
T*=0 0
T*=0 2
T*=-.0
T*=2 0
ME 0013

Model M2

Dip of fault plane	:	45°
Direction of slip on fault plane	:	90° to strike
Shape of fault plane	:	circular
Dimensions of fault plane	:	5 km radius
Azimuth	:	90° to strike

Figure 5 shows a cross section through the source in the plane of the observer. Direct P in this model is radiated in a direction that makes a relatively small angle with the fault plane so that the leading edge of the pulse is steeper than the trailing edge. For pP the direction in which the pulse leaves the source is more nearly at right angles to the fault plane. The leading edge of this pulse is thus less steep than the trailing edge. For sP, because the S velocity is much closer than the P velocity to the fracture velocity, the effects of the moving source in steepening the leading edge of the pulse are again clearly seen even though the angle between fault plane and sP ray paths is quite large.

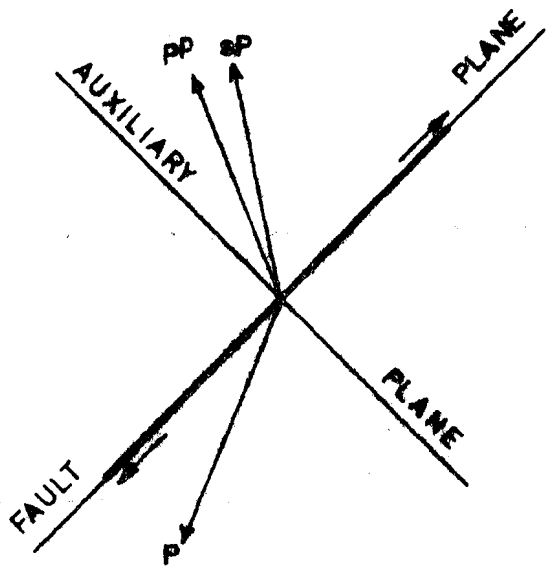

FIGURE 5

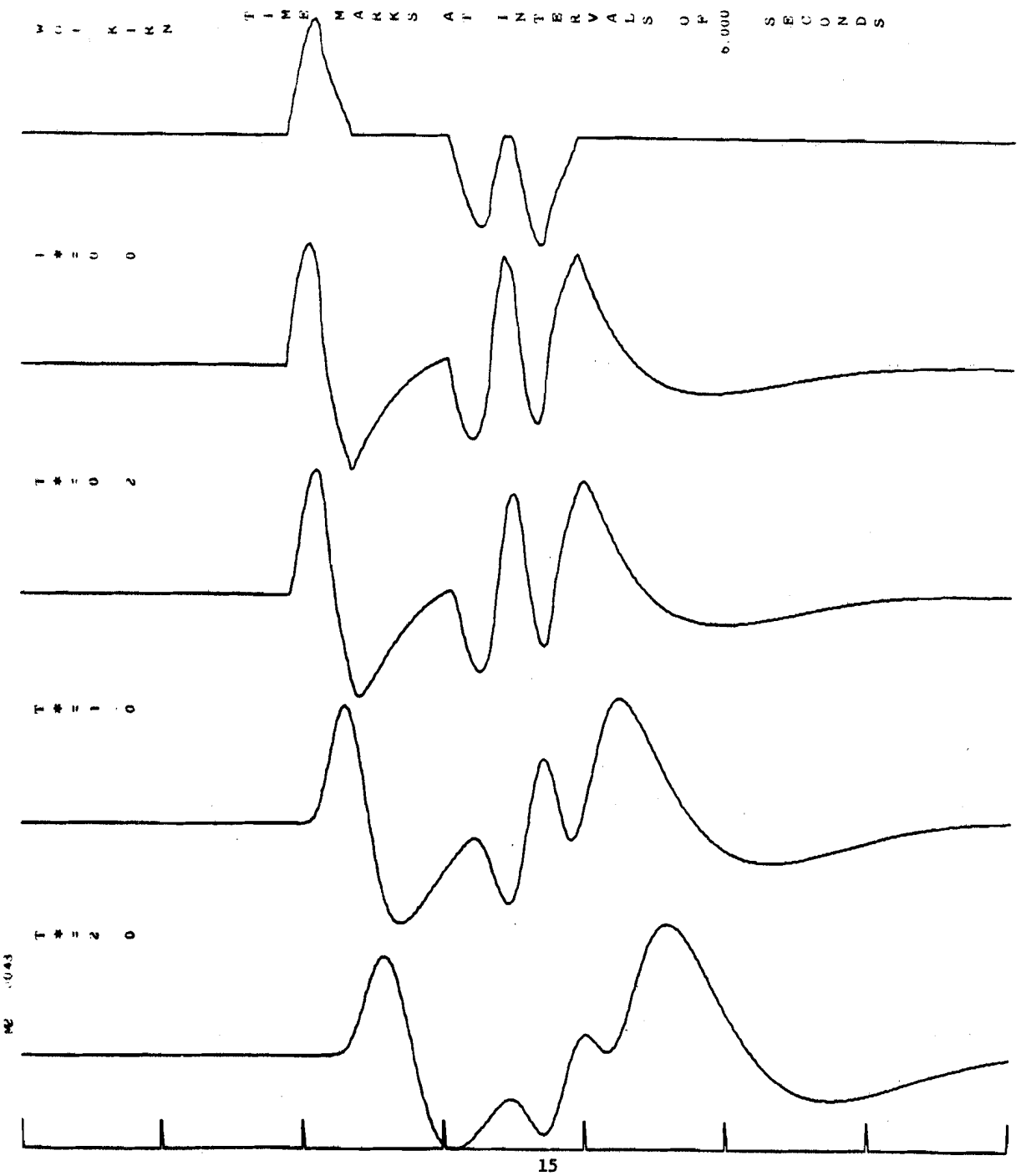
TIME MARKS AT INTERVALS OF 6.000 SECONDS

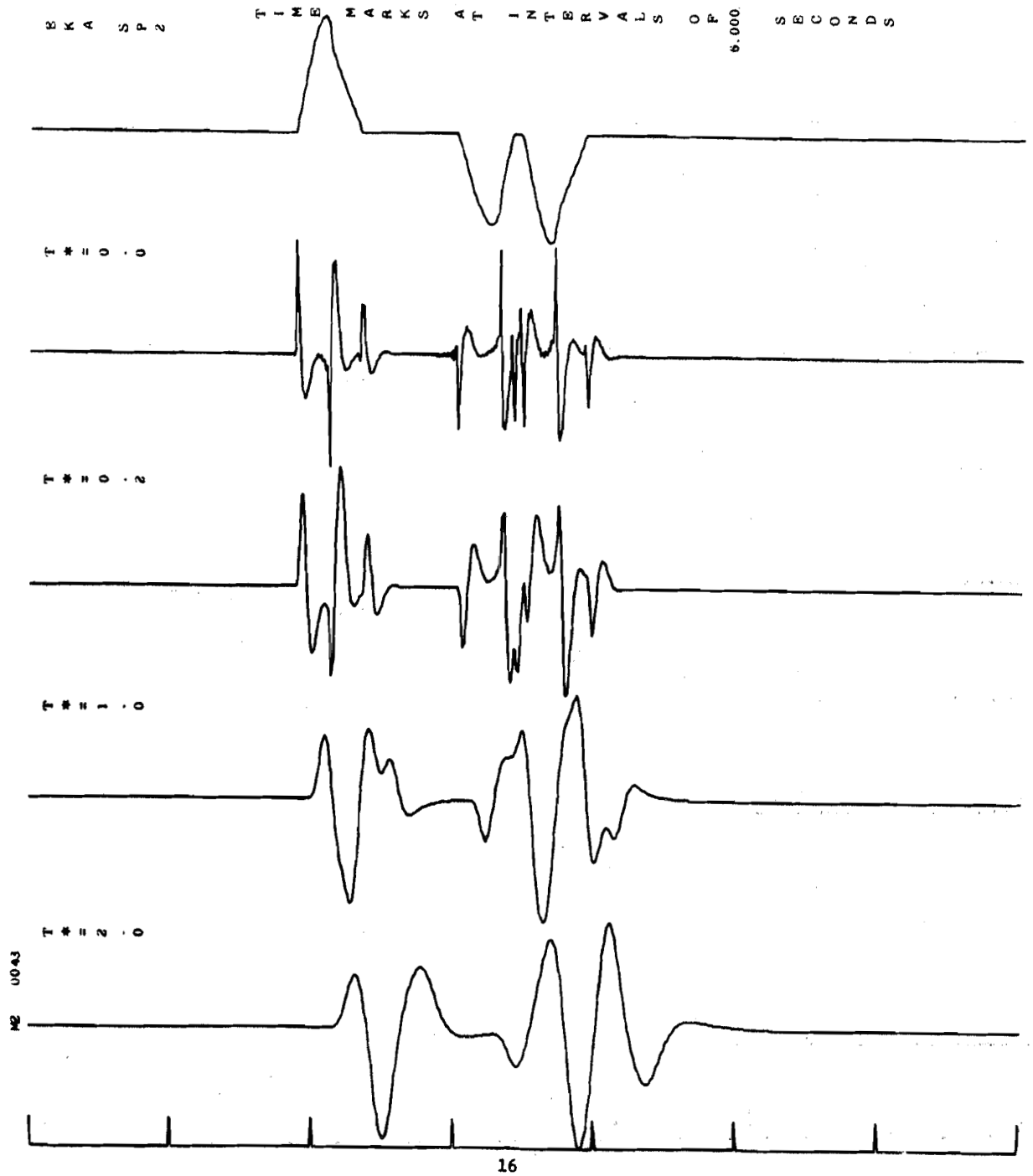
BKA SP2
TIME MARKS AT INTERVALS OF 6.000 SECONDS
T*=0.0
T*=0.2
T*=1.0
T*=2.0
M2 0043

Model M3

Dip of fault plane	:	90°
Direction of slip on fault plane	:	vertical
Shape of fault plane	:	elliptical
Dimensions of fault plane	:	2.5 × 2.0 km
Azimuth	:	90°
Orientation of major axis of ellipse	:	vertical
Point of initiation of fracture	:	upper focus

Figure 6 shows a cross section through the source in the plane of the observer. For direct P the source is effectively moving towards the observer during the whole time of fracturing. For pP and sP the fracture spreads towards the observer for only a short time (the time to travel from the upper focus to the upper limit of the ellipse) which gives a sharp front to the pulse. For the remainder of the time the fracture is moving away from the observer. pP and sP are thus much broader than the direct P pulse.

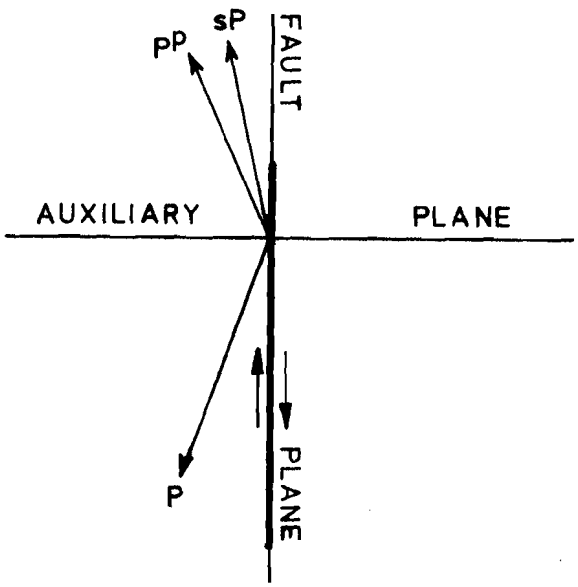

FIGURE 6

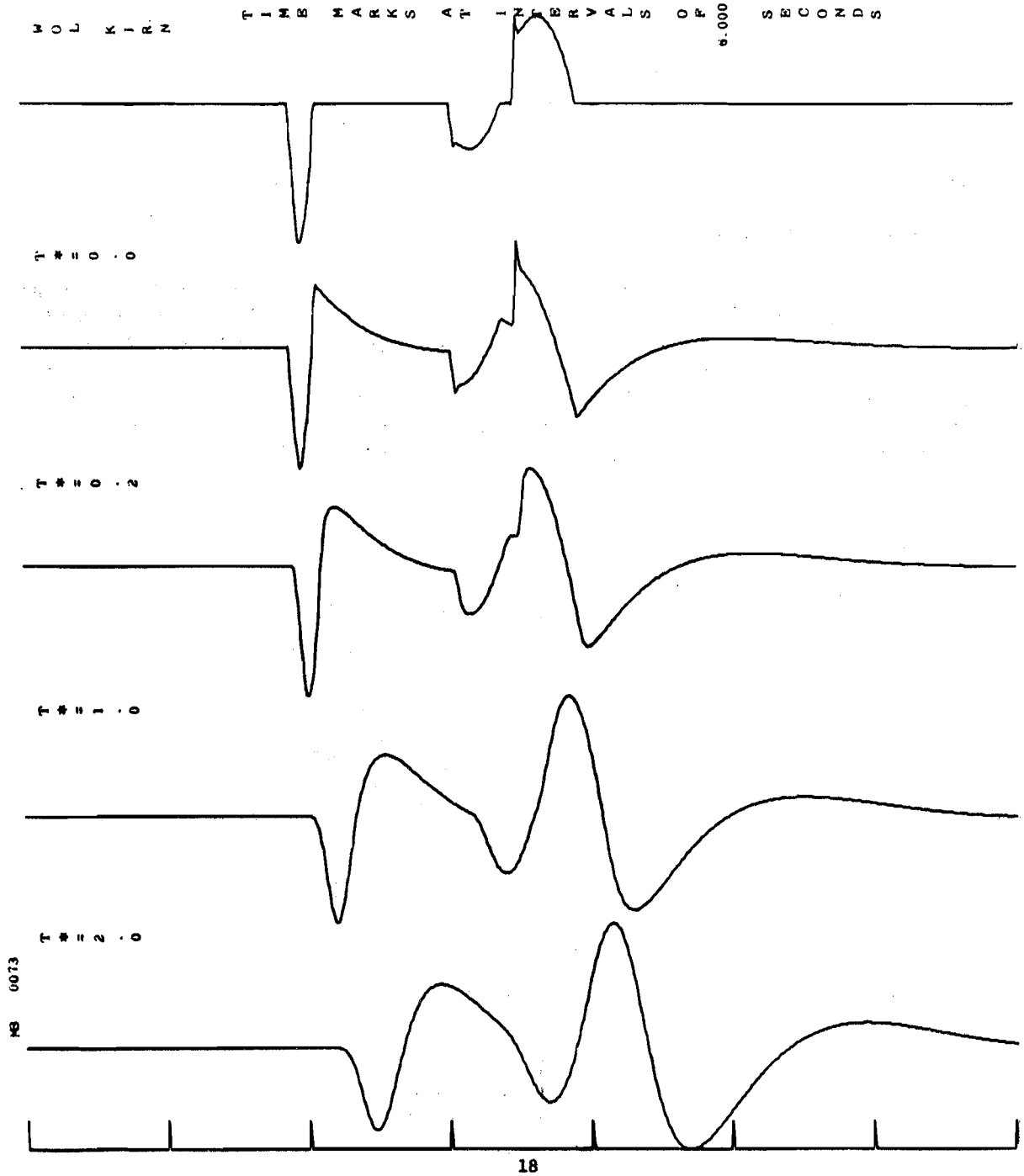
WOLKIRN
TIMB MARKS AT INTERVALS OF 0.000 SECONDS
t*=0.0
t*=0.2
t*=1.0
t*=2.0
MB 0073

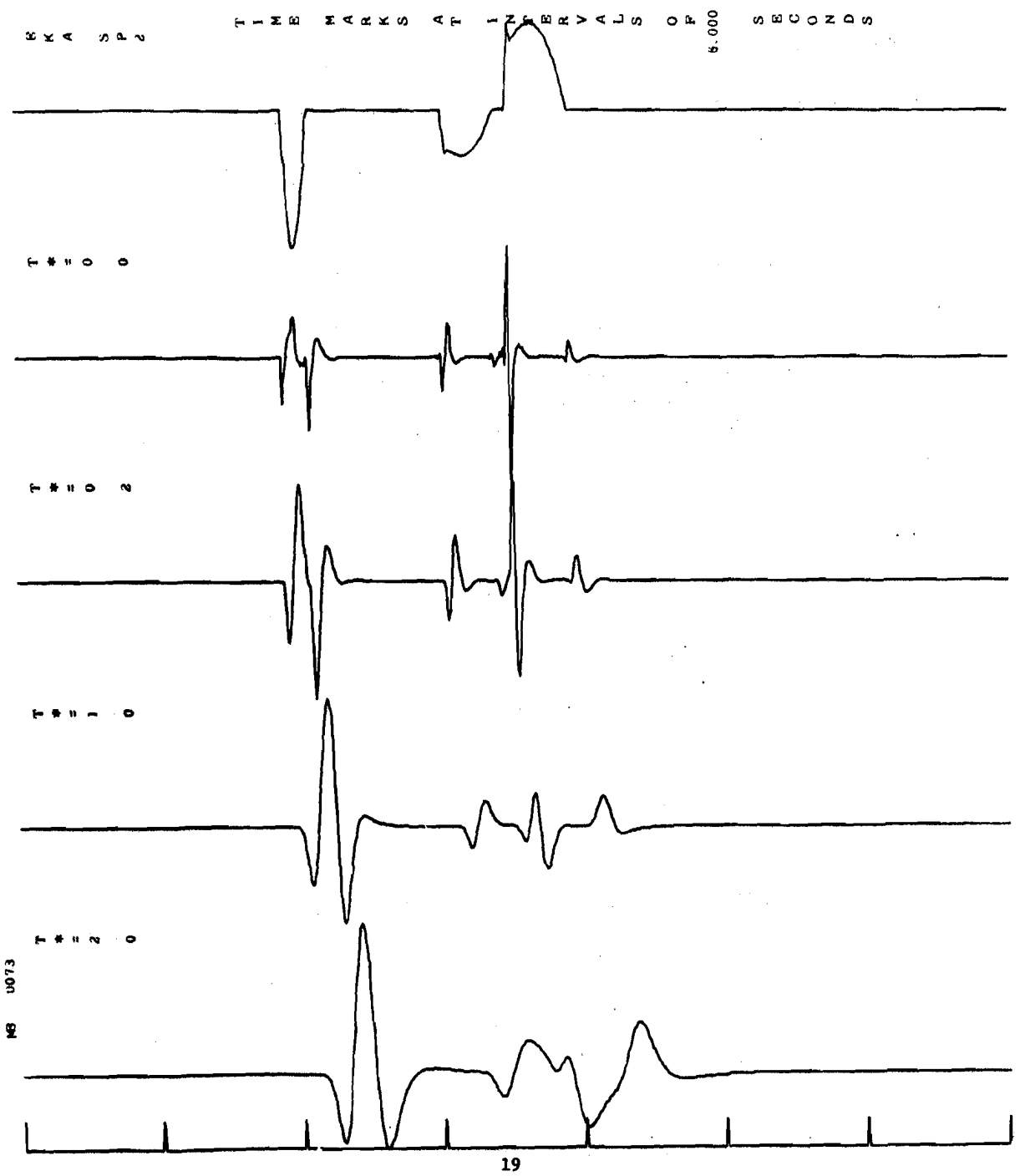
EKA SP2
TIME MARKS AT INTERVALS OF 5.000 SECONDS
T**=0 0
T**=0 2
T**=1 0
T**=2 0
MB U073

Model M4

Dip of fault plane	:	90°
Direction of slip on fault plane	:	vertical
Shape of fault plane	:	elliptical
Dimensions of fault plane	:	2.5 × 2.0 km
Azimuth	:	90°
Orientation of major axix	:	vertical
Point of initiation of fracture	:	lower focus

Figure 7 shows a cross section through the source in the plane of the observer. As fracturing begins at the lower focus it is the P pulse that is broadest and the pP and sP narrowest, the converse of Model M3.

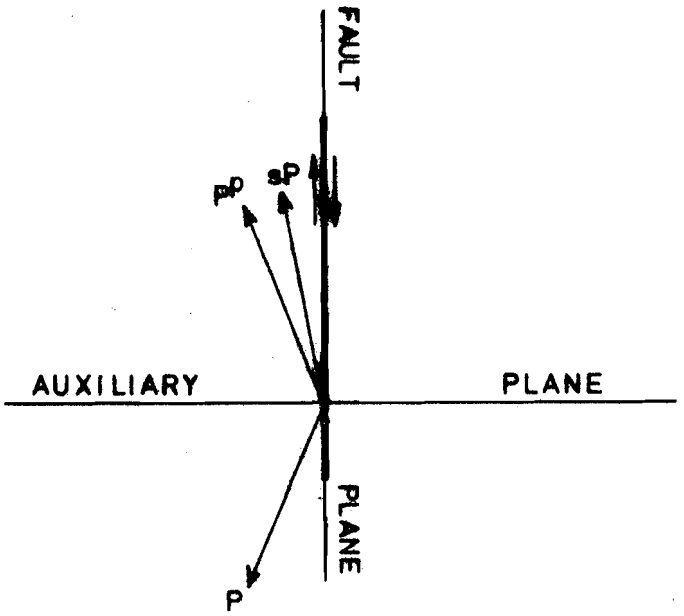

FIGURE 7

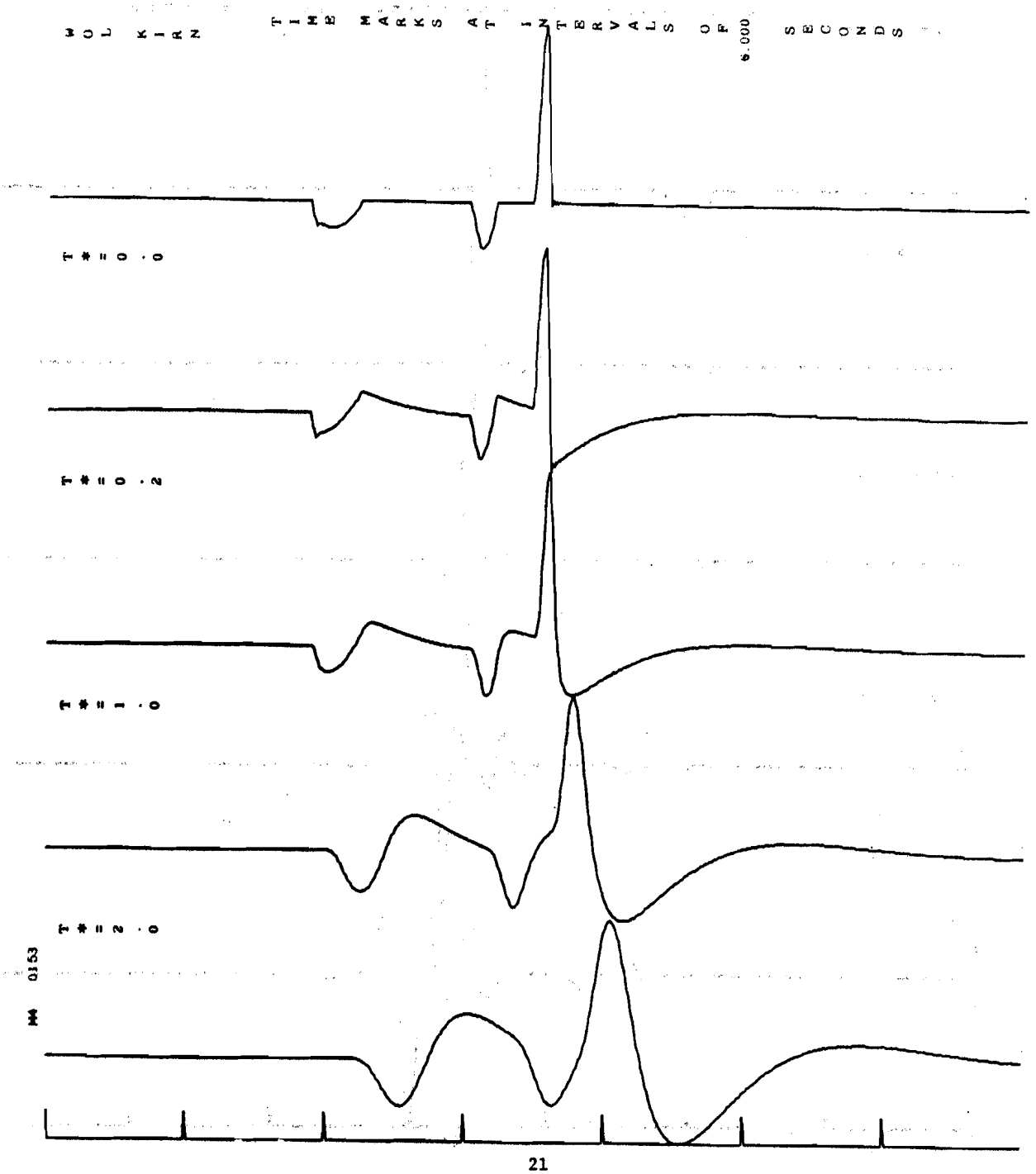
MOL KIRN
TIME MARKS AT INTERVALS OF 6.000 SECONDS
T*=0.0
T*=0.2
T*=1.0
T*=2.0
M4 0153

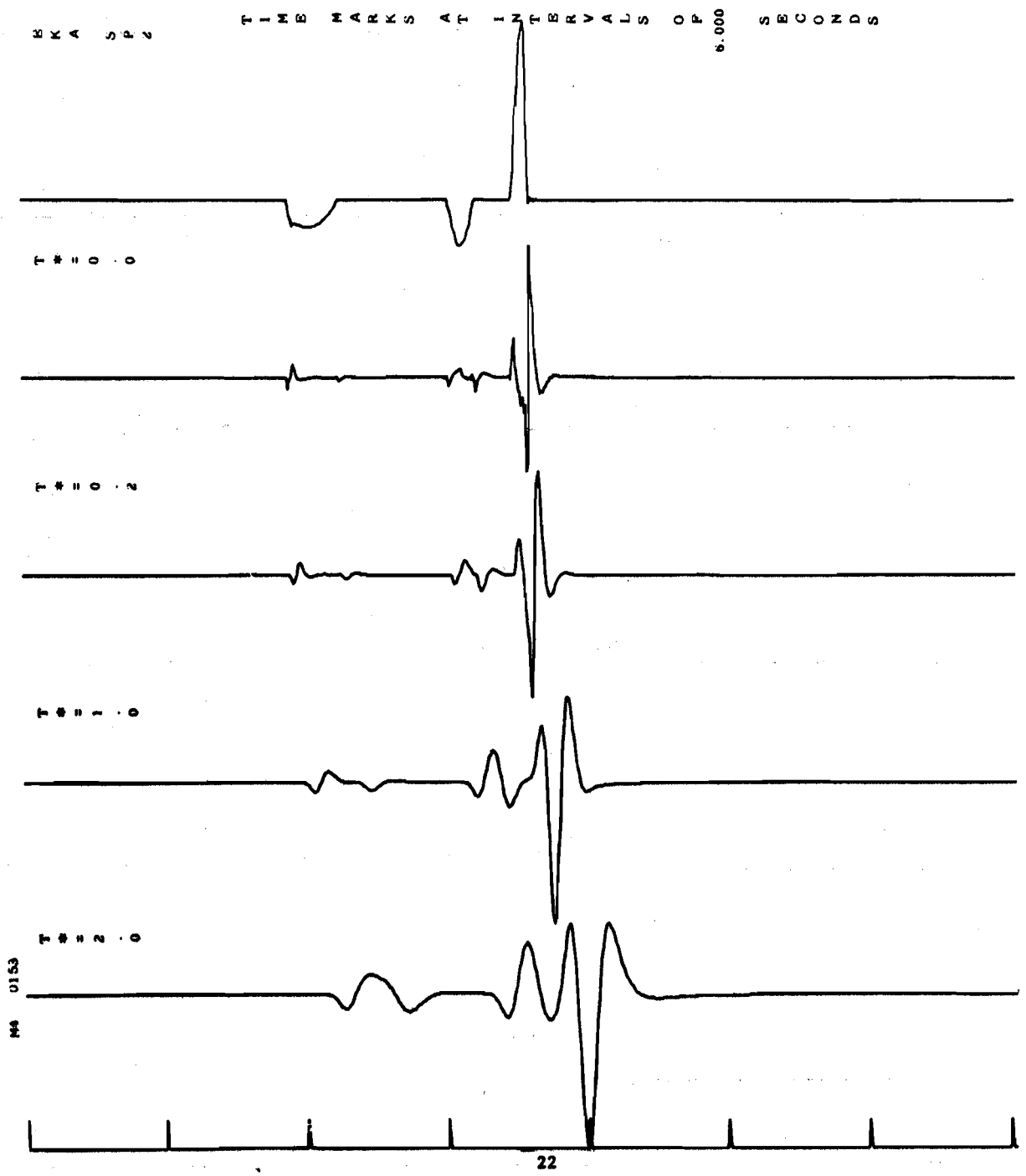
EKA SP2
TIME MARKS AT INTERVALS OF 6.000 SECONDS
T*=0.0
T*=0.2
T*=0.6
T*=2.0
M4 0153

Model M5

Dip of fault plane	:	90°
Direction of slip on fault plane	:	vertical
Shape of fault plane	:	elliptical
Dimensions of fault plane	:	2.5 × 2.0 km
Azimuth	:	90° to strike
Orientation of major axis of ellipse	:	horizontal
Point of initiation of fracture	:	a focus

Figure 8 shows a cross section through the source in the plane of the observer. As the major axis of the ellipse is horizontal the model is symmetrical for P and pP so the pulse shapes are identical. The sP pulse is very similar to, but slightly longer than, P and pP. All the pulses have a sharp front because initially they all have a component of fracture towards the observer. The main motion, however, is the fracture spreading across the field of the observer.

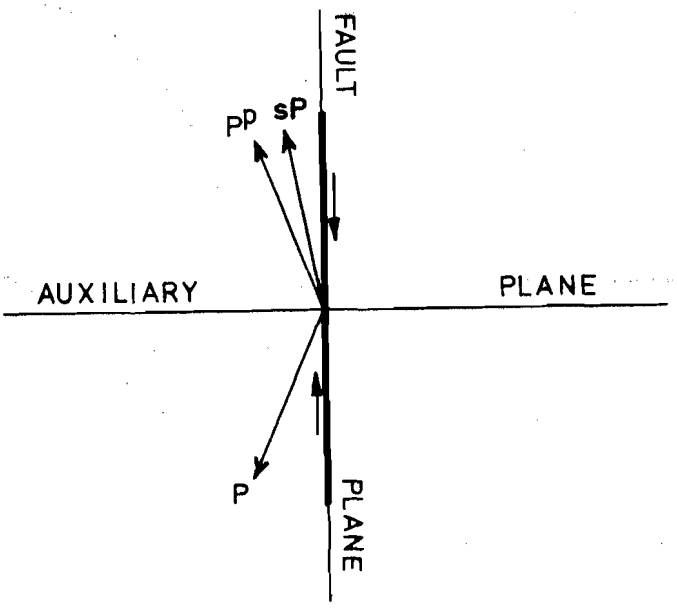

FIGURE 8

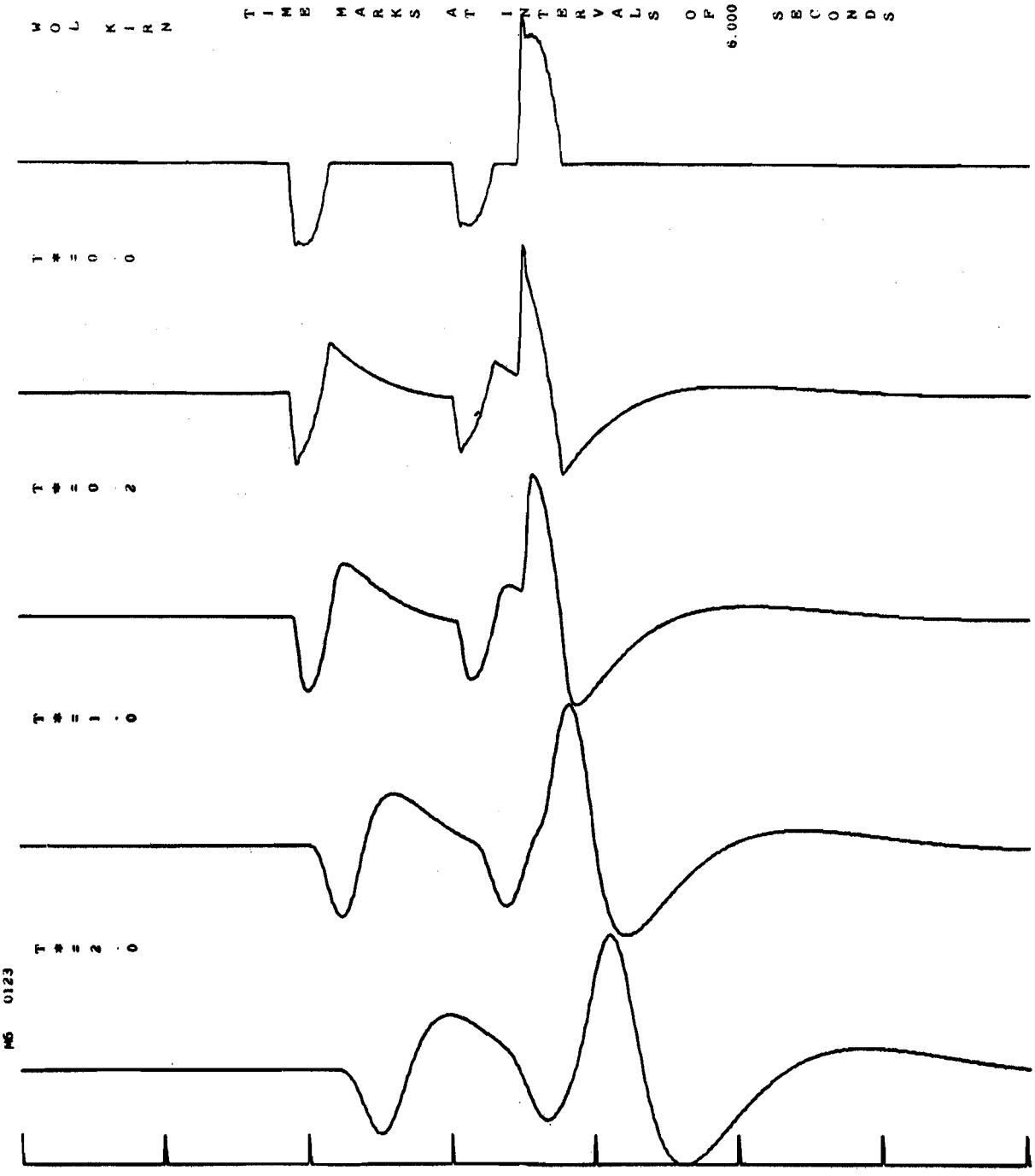
WOLKIRN
TIME MARKS AT INTERVALS OF 6.000 SECONDS
T*=0.0
T*=0.2
T*=1.0
T*=2.0
MS 0123

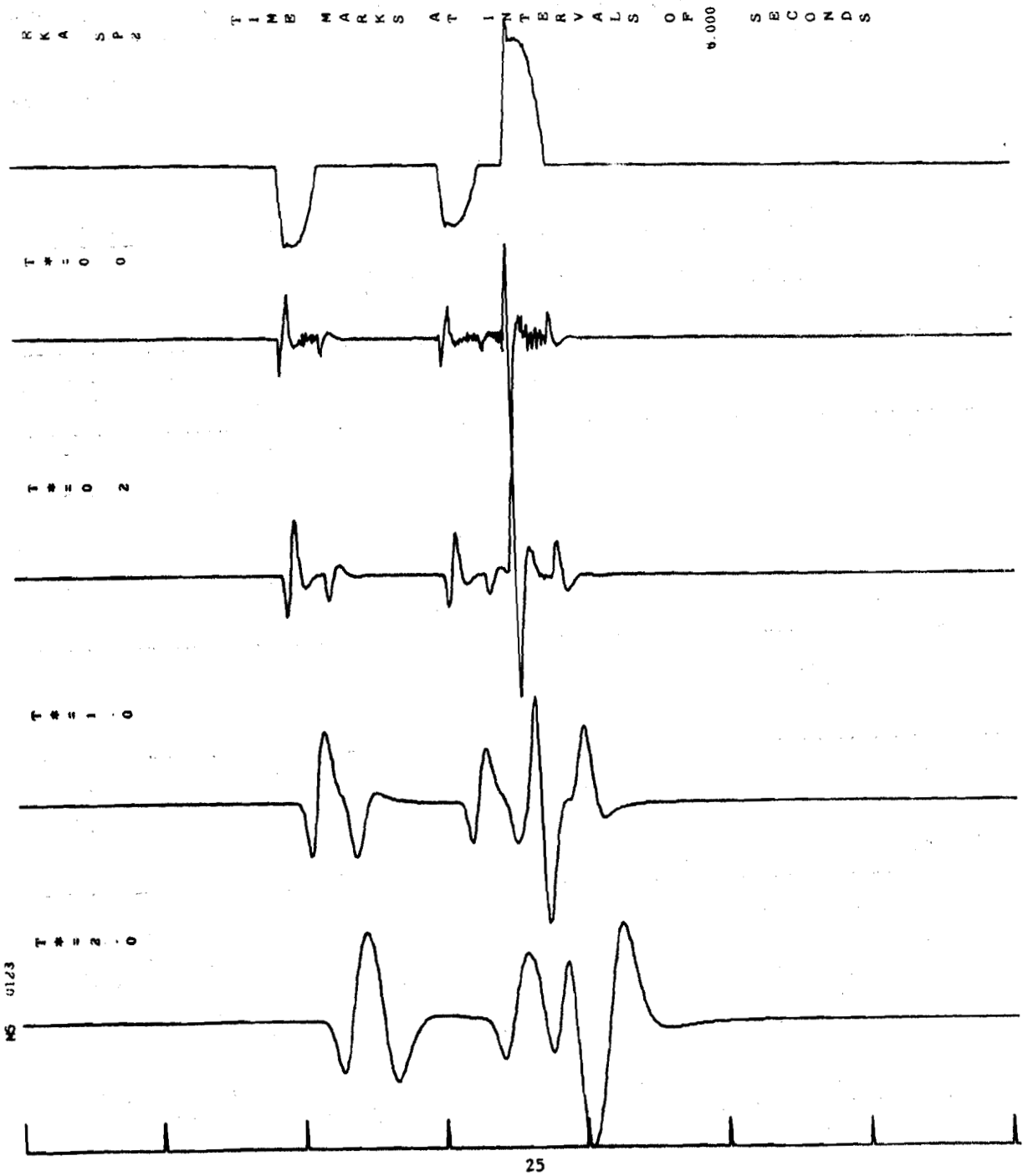
RKA SP2
TIME MARKS AT INTERVALS OF 0.000 SECONDS
T**=0 0
T**=0 2
T**=1 0
T**=2 0
NO 0123

4. INTERPRETING MODELS WITH CRUSTAL LAYERING: M6 TO M27

In computing seismograms with crustal layering, one source crustal model has been used, a standard crust with sediment and one receiver crust, the crustal model for Eskdalemuir, Scotland. The properties of these models are listed in table 3. The receiver layering has no very large impedance contrasts and thus contributes little to the shape of the final seismogram. The impedance contrast that contributes most to the shape of the seismogram (apart from the free surface) is that between the sediment (layer 1) and basement (layer 2) of the source crust.

TABLE 3

Crustal Models Used in the Computation of Seismograms: M6 - M27

1. Standard Continental Crust with Sediment [4]

	P Wave Velocity, km s^{-1}	S Wave Velocity, km s^{-1}	Density, g cm^{-3}	Thickness, km
Layer 1	3.0	1.66	2.35	2.0
Layer 2	6.1	3.50	2.7	9.0
Layer 3	6.4	3.68	2.9	9.0
Layer 4	6.7	3.94	2.9	18.0
Halfspace	8.15	4.75	3.3	∞

2. Eskdalemuir, Scotland [5]

Layer 1	6.14	3.55	2.8	5.3
Layer 2	7.28	4.20	3.2	19.7
Halfspace	8.09	4.67	3.4	∞

Figure 9 shows the ray paths that produce the most prominent arrivals (although not all the seismograms show all these arrivals). These arrivals, A1 to A8, are identified in figure 10 (the seismogram is the displacement at the recording station computed for Model M6). Note that five of these arrivals are due to S to P conversion.

For each model the maximum positive and negative amplitude (in nanometres) for each seismogram is given. The effect of t* and recording system on amplitudes can thus be seen.

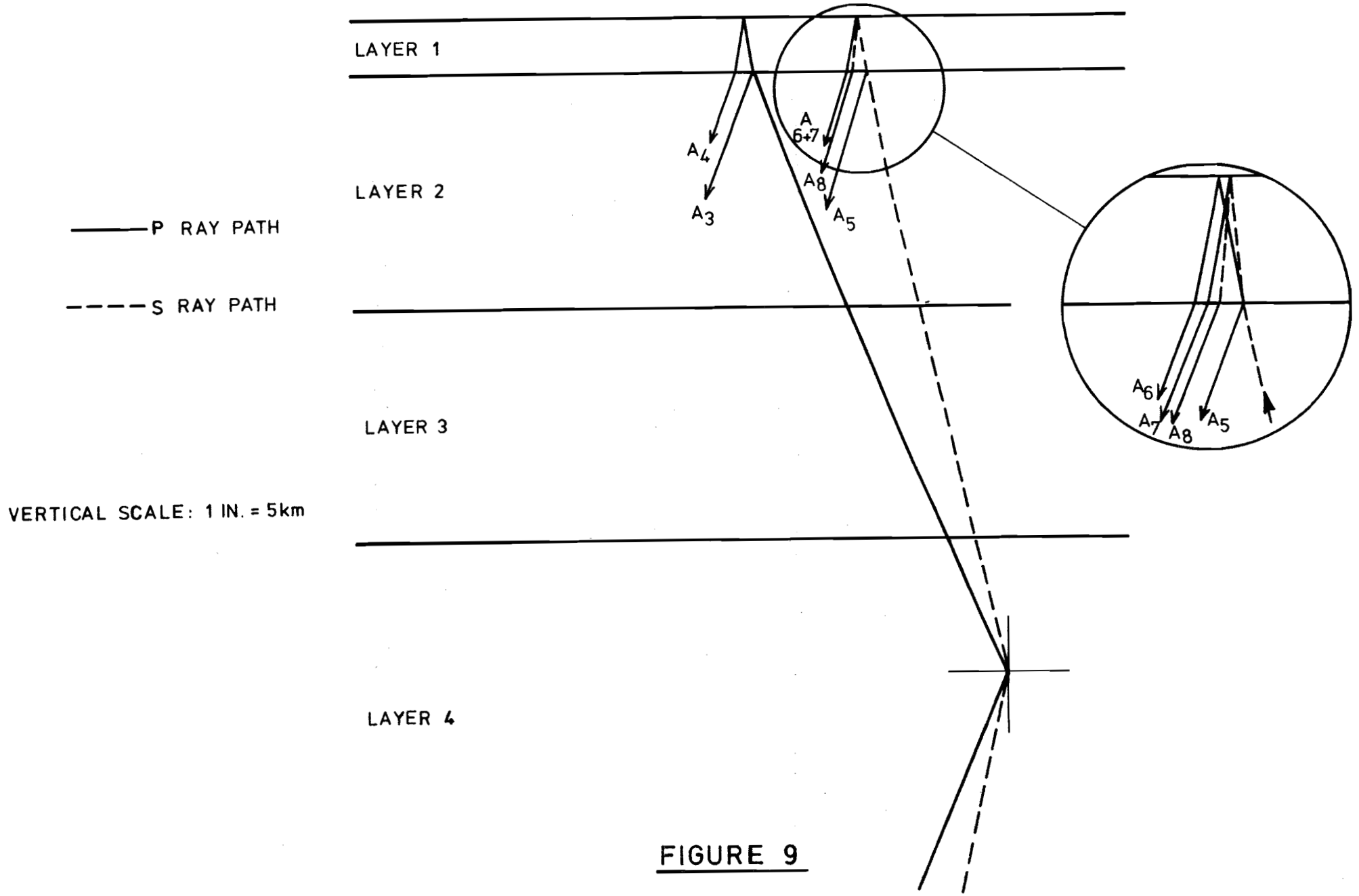
LAYER 1
LAYER 2
LAYER 3
LAYER 4
P RAY PATH
S RAY PATH
VERTICAL SCALE: 1 IN. = 5km
A4
A3
A6+7
A8
A5
A6
A7
A8
A5

FIGURE 9

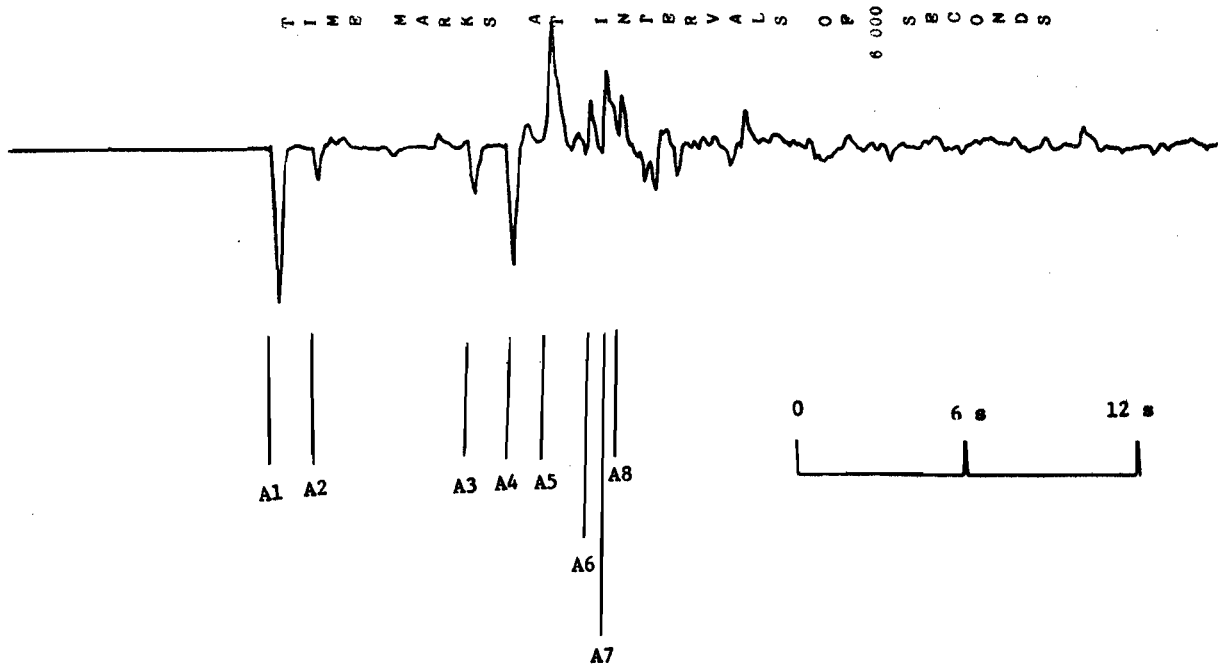

FIGURE 10. ARRIVALS A1 - A8 IDENTIFIED ON SEISMOGRAM FOR MODEL M6

5. VERTICAL DIP SLIP AND VERTICAL STRIKE SLIP MODELS: M6 TO M11

Because the fault planes for these models are vertical there is very little change in shape of the seismogram with azimuth. Seismograms are therefore shown for only one azimuth: 90° to strike of fault for vertical dip slip and 45° to strike of fault for vertical strike slip. Both models show prominent sP arrivals. For the vertical dip slip the vertical through the fault plane is an antinode of S.

Model M6

Dip of fault plane : 90°

Direction of slip on fault plane : vertical

Shape of fault plane : circular

Dimensions of fault plane : 1 km radius

Azimuth : 90° to strike

Amplitudes

	Channel 1	Channel 2	Channel 3	Channel 4	Channel 5
M6K					
Maximum	426.3	407.6	224.4	74.5	30.1
Minimum	-528.5	-478.5	-234.4	-61.0	-32.4
M6SP					
Maximum	426.3	755.3	176.9	10.0	1.1
Minimum	-528.5	-601.3	-125.5	-7.5	-1.1

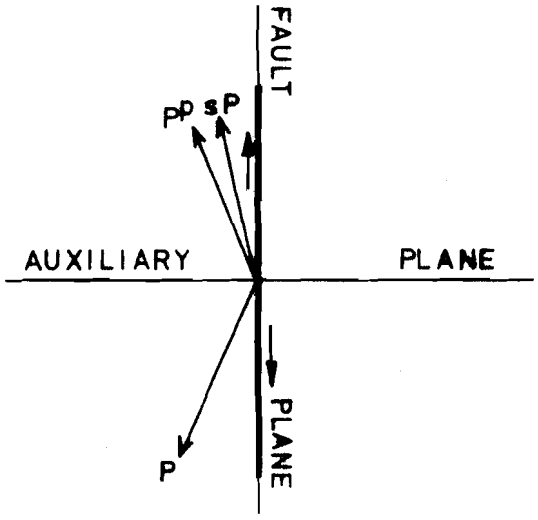

FIGURE 11. CROSS SECTION THROUGH THE SOURCE IN THE PLANE OF THE OBSERVER

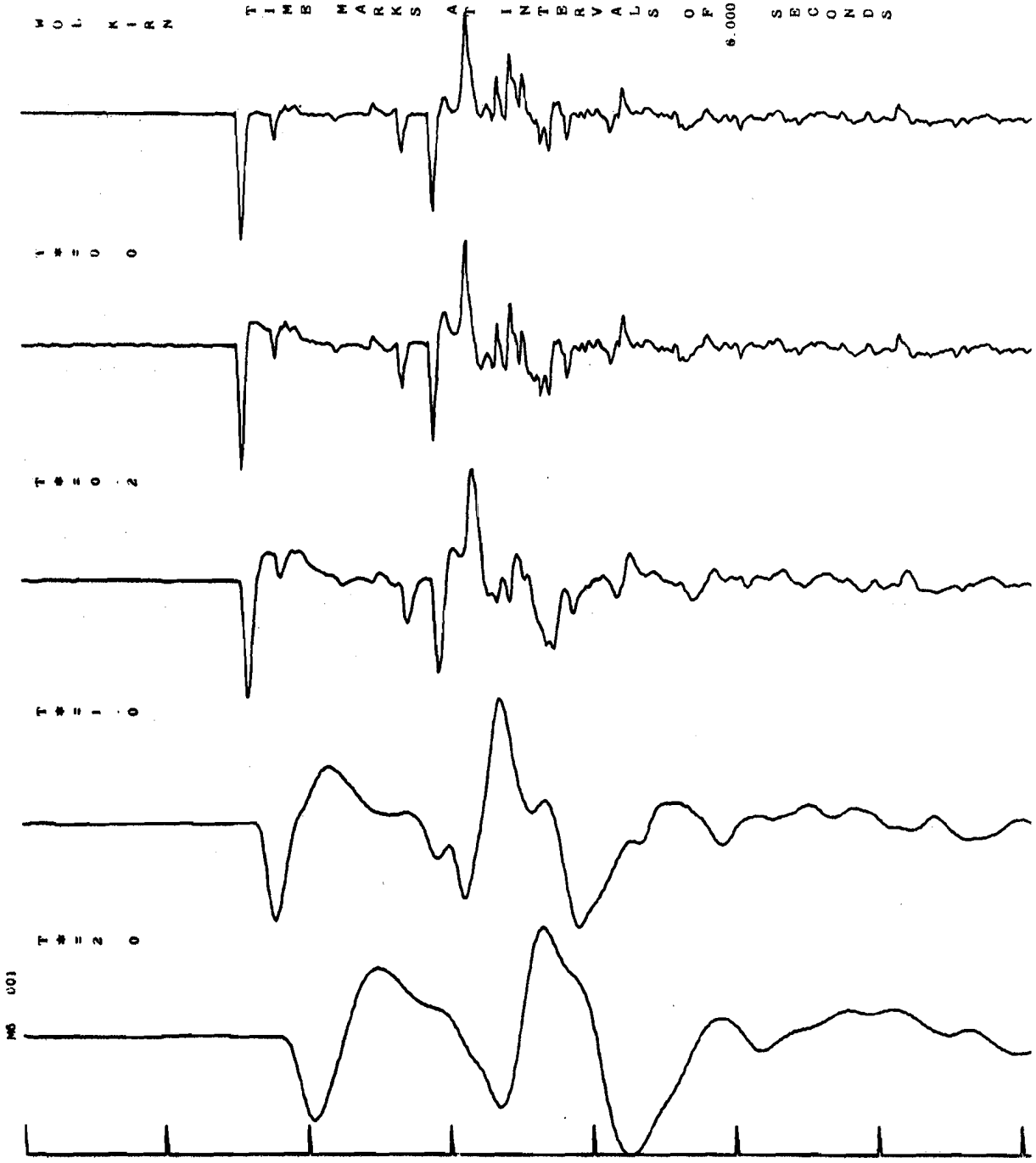
MOL K-RN
TIME MARKS AT INTERVALS OF 6.000 SECONDS
F*=0 0
F*=0 .2
F*=- .0
F*=2 0
100

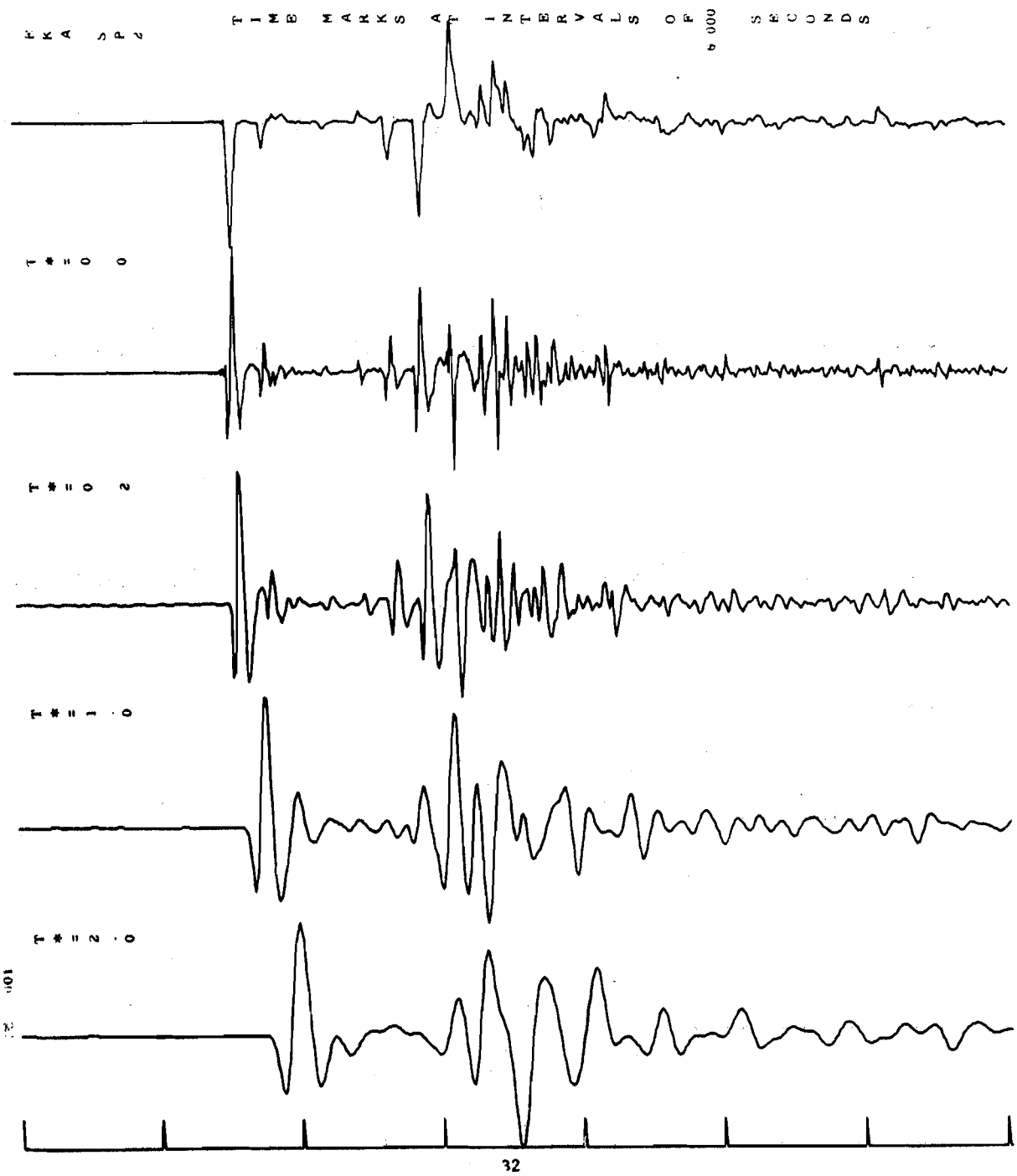
TIME MARKS AT INTERVALS OF 0.000 SECONDS
T*=0.0
T*=0.2
T*=1.0
T*=2.0

Model M7

Dip of fault plane	:	90°
Direction of slip on fault plane	:	vertical
Shape of fault plane	:	circular
Dimensions of fault plane	:	5 km radius
Azimuth	:	90° to strike

Amplitudes

	Channel 1	Channel 2	Channel 3	Channel 4	Channel 5
M7K					
Maximum	12582	13015	10479	5343.1	3134.1
Minimum	-13209	-9781.5	-8220.7	-5515	-3662.1
M7SP					
Maximum	12582	2263.6	690.0	123.3	38.6
Minimum	-13209	-2932.8	-823.6	-206.2	-45.3

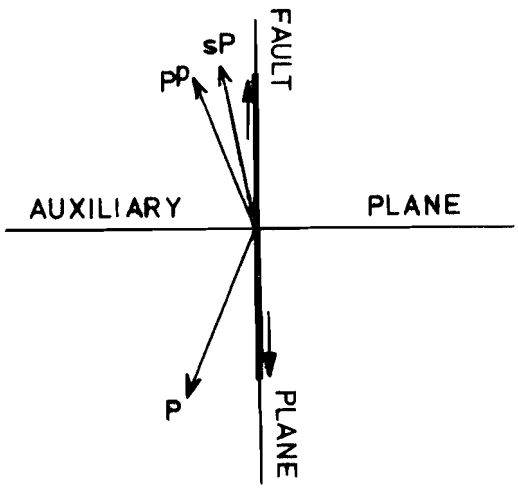

FIGURE 12. CROSS SECTION THROUGH THE SOURCE IN THE PLANE OF THE OBSERVER

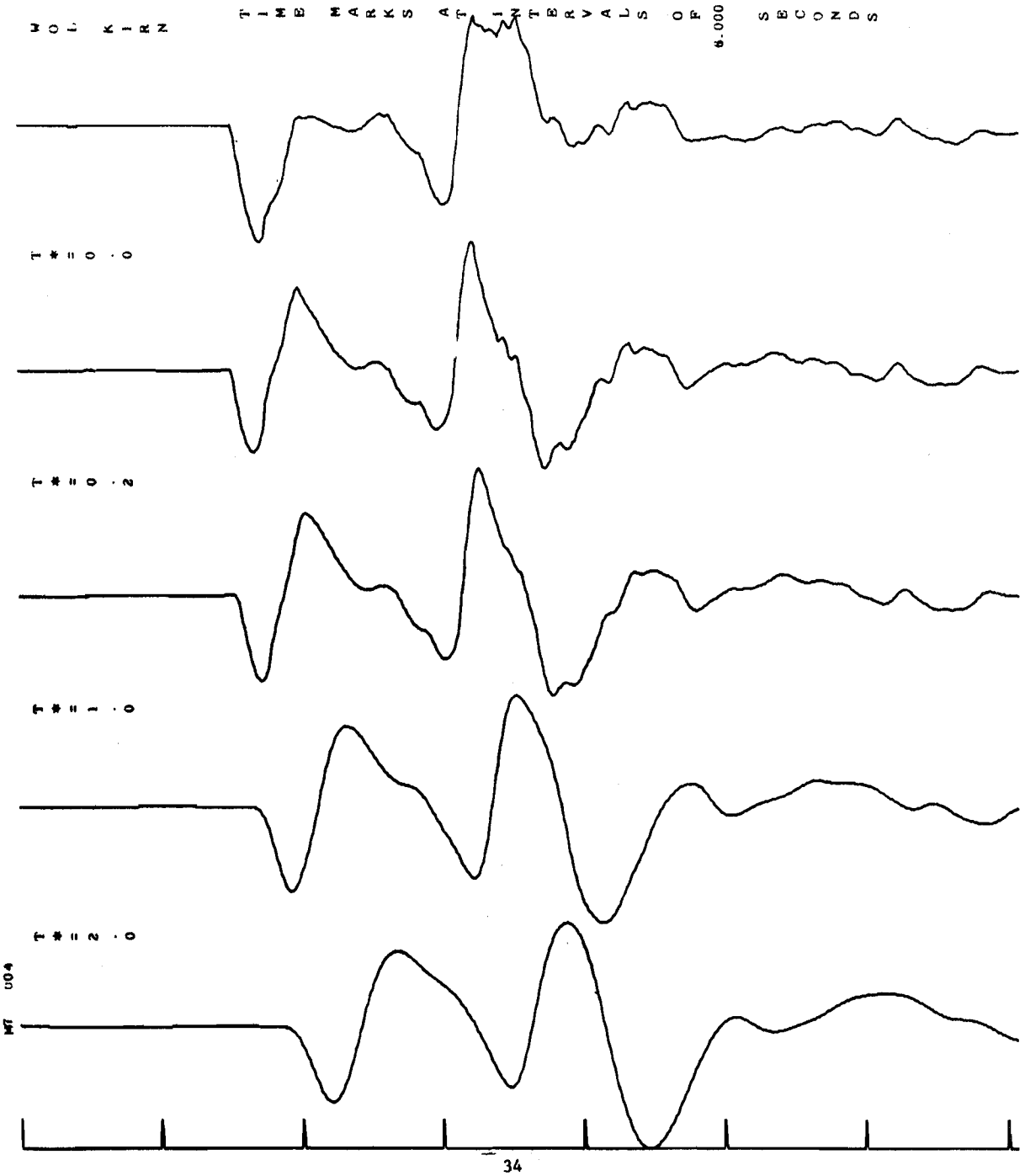
MOL KIRN
TIME MARKS AT INTERVALS OF 0.000 SECONDS
T*=0.0
T*=0.2
T*=1.0
T*=2.0
MT 004

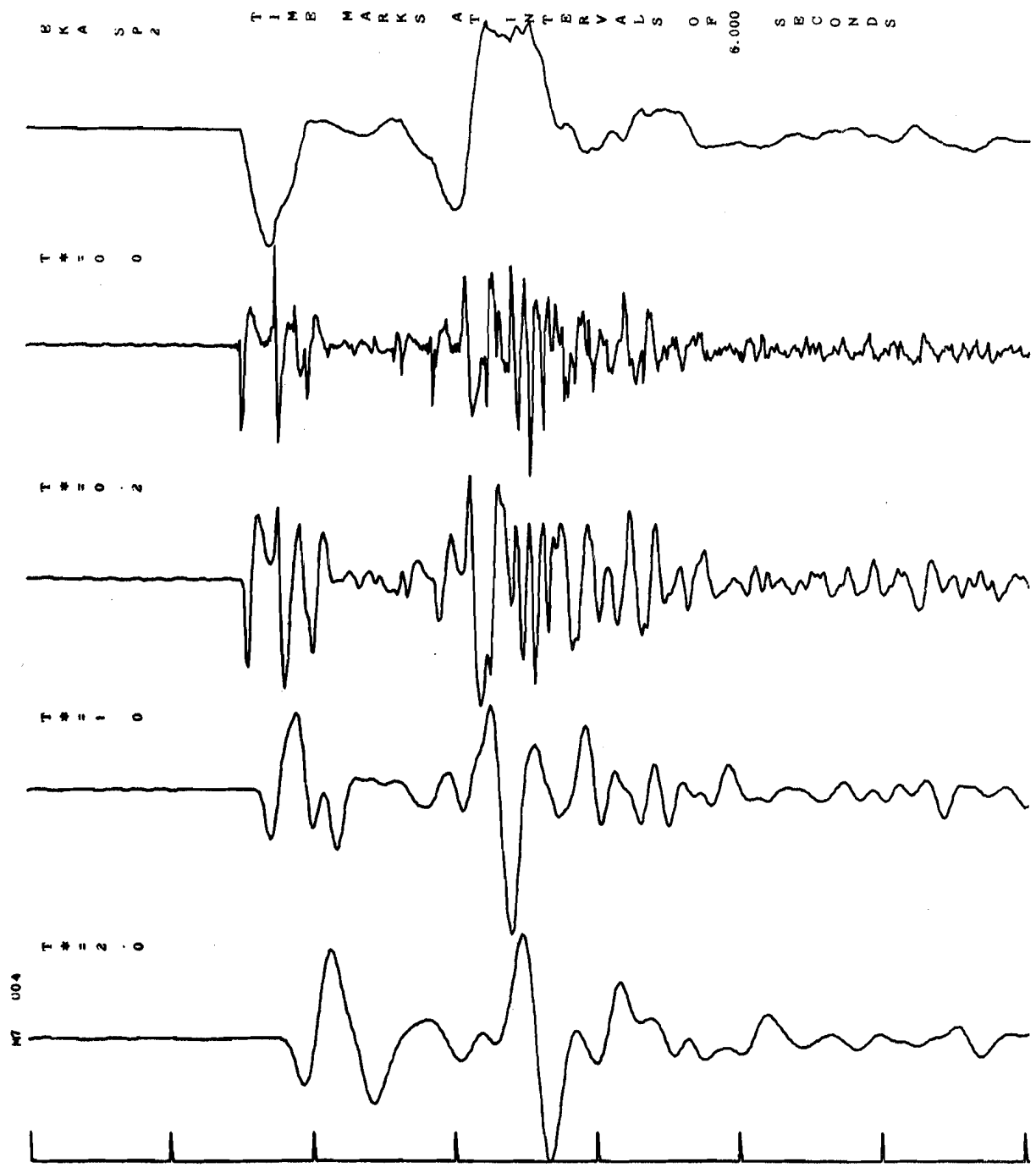
BKA SP 2
TIME MARKS AT INTERVALS OF 6.000 SECONDS
T*=0 0
T*=0 .2
T*=1 0
T*=2 .0
MT U04

Model M8

Dip of fault plane	:	90°
Direction of slip on fault plane	:	vertical
Shape of fault plane	:	ellipse
Dimensions of fault plane	:	2.5 × 2.0 km
Azimuth	:	90° to strike
Orientation of major axis of ellipse	:	vertical
Point of initiation of fracture	:	upper focus

Amplitudes

	Channel 1	Channel 2	Channel 3	Channel 4	Channel 5
M8K					
Maximum	1105.7	974.9	804.4	455.2	251.25
Minimum	-2041.9	-1661.9	-1228.6	-503.3	-243.9
M8SP					
Maximum	1105.7	762.4	280.2	45.3	7.8
Minimum	-2041.9	-987.2	-366.5	-41.4	-3.6

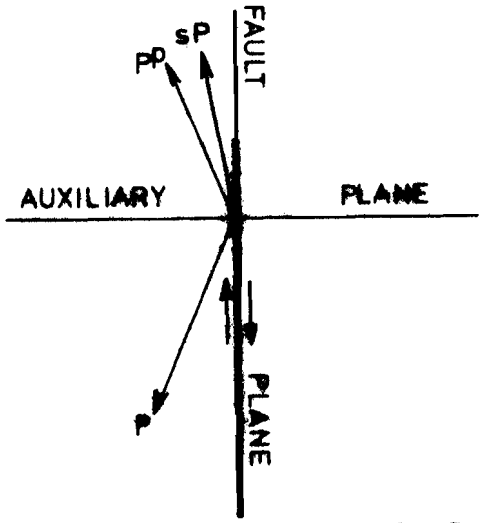

FIGURE 13. CROSS SECTION THROUGH THE SOURCE IN THE PLANE OF THE OBSERVER

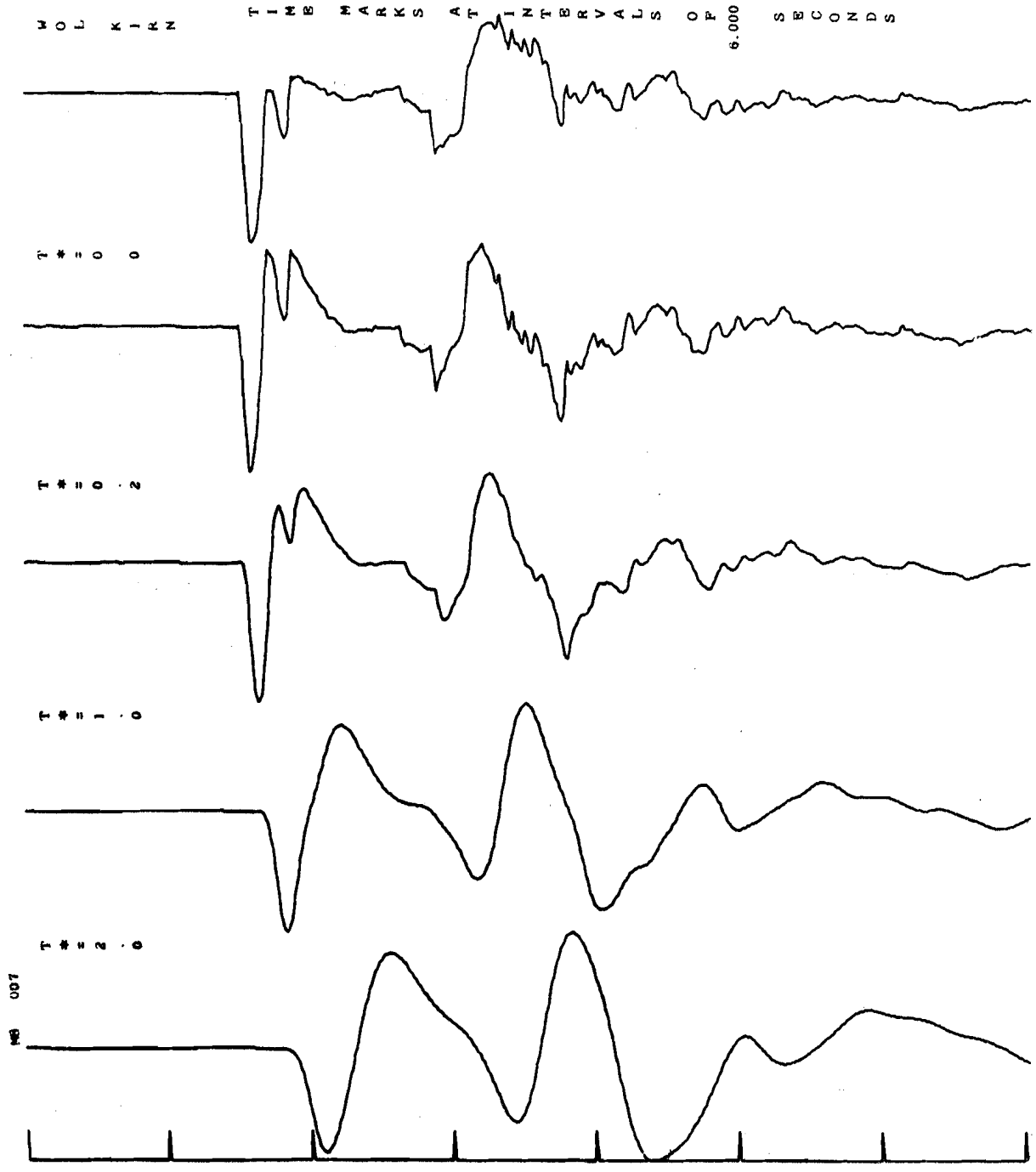
MOL KIRN
TIME MARKS AT INTERVALS OF 6.000 SECONDS
T*=0 0
T*=0 .2
T*=1 .0
T*=2 .0
MS 007

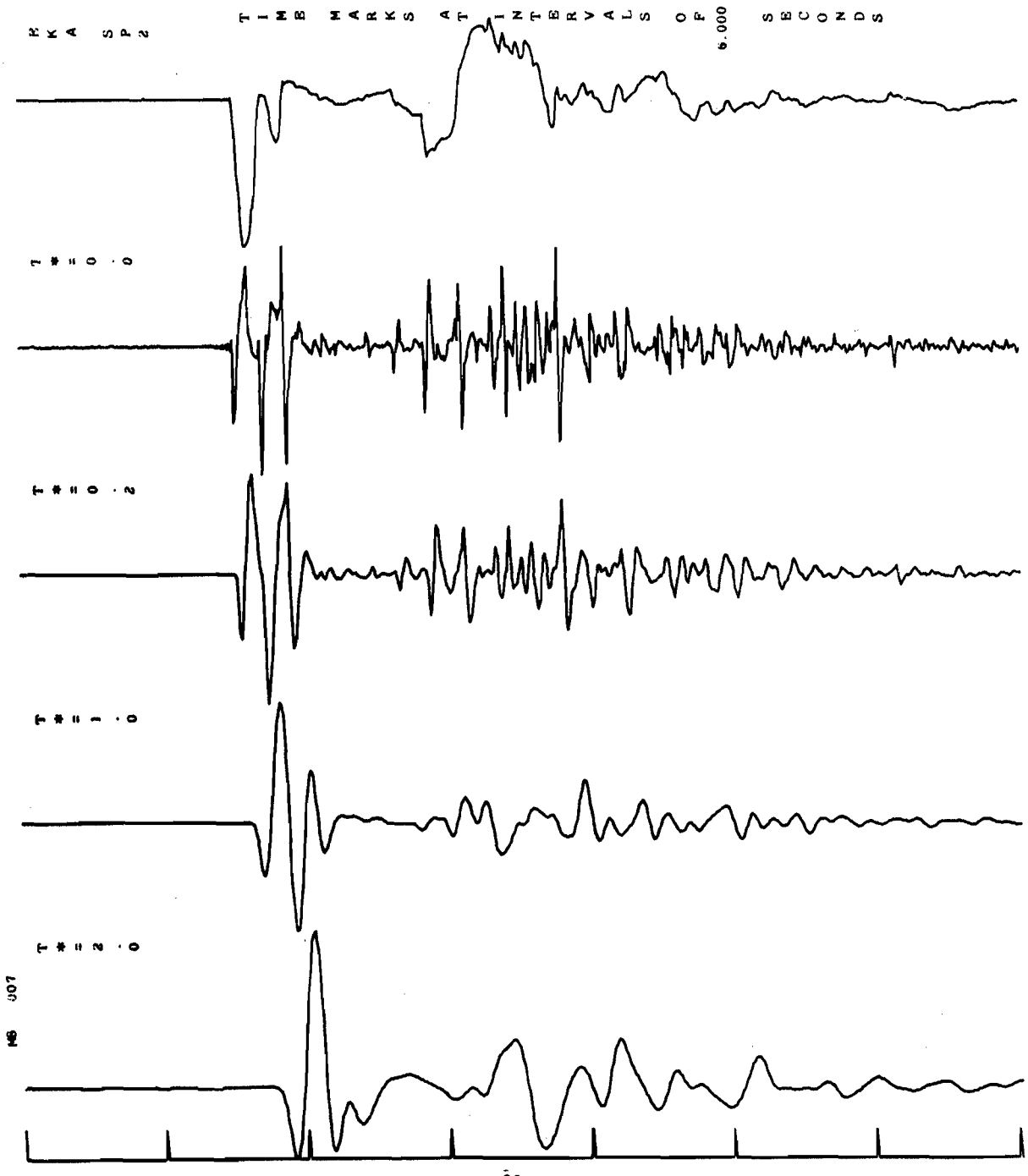
TIME MARKS AT INTERVALS OF 6.000 SECONDS
RKA SP2
T*=0.0
T*=0.2
T*=1.0
T*=2.0

Model M9

Dip of fault plane	:	90°
Direction of slip on fault plane	:	vertical
Shape of fault plane	:	ellipse
Dimensions of fault plane	:	2.5 × 2.0 km
Azimuth	:	90°
Orientation of major axis of ellipse	:	vertical
Point of initiation of fracture	:	lower focus

Amplitudes

	Channel 1	Channel 2	Channel 3	Channel 4	Channel 5
M9K					
Maximum	2981.2	2661.7	2020.4	728.2	299.4
Minimum	-1526.6	-1581.7	-1281.0	-565.4	-349.3
M9SP					
Maximum	2981.2	2605.9	583.1	51.2	6.0
Minimum	-1526.6	-2628.8	-719.9	-64.5	-11.0

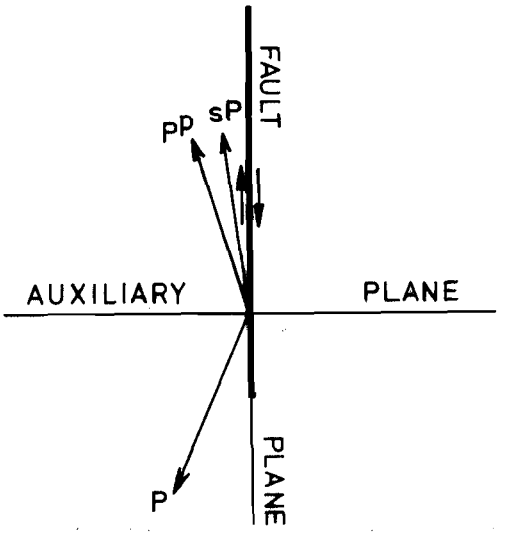

FIGURE 14. CROSS SECTION THROUGH THE SOURCE IN THE PLANE OF THE OBSERVER

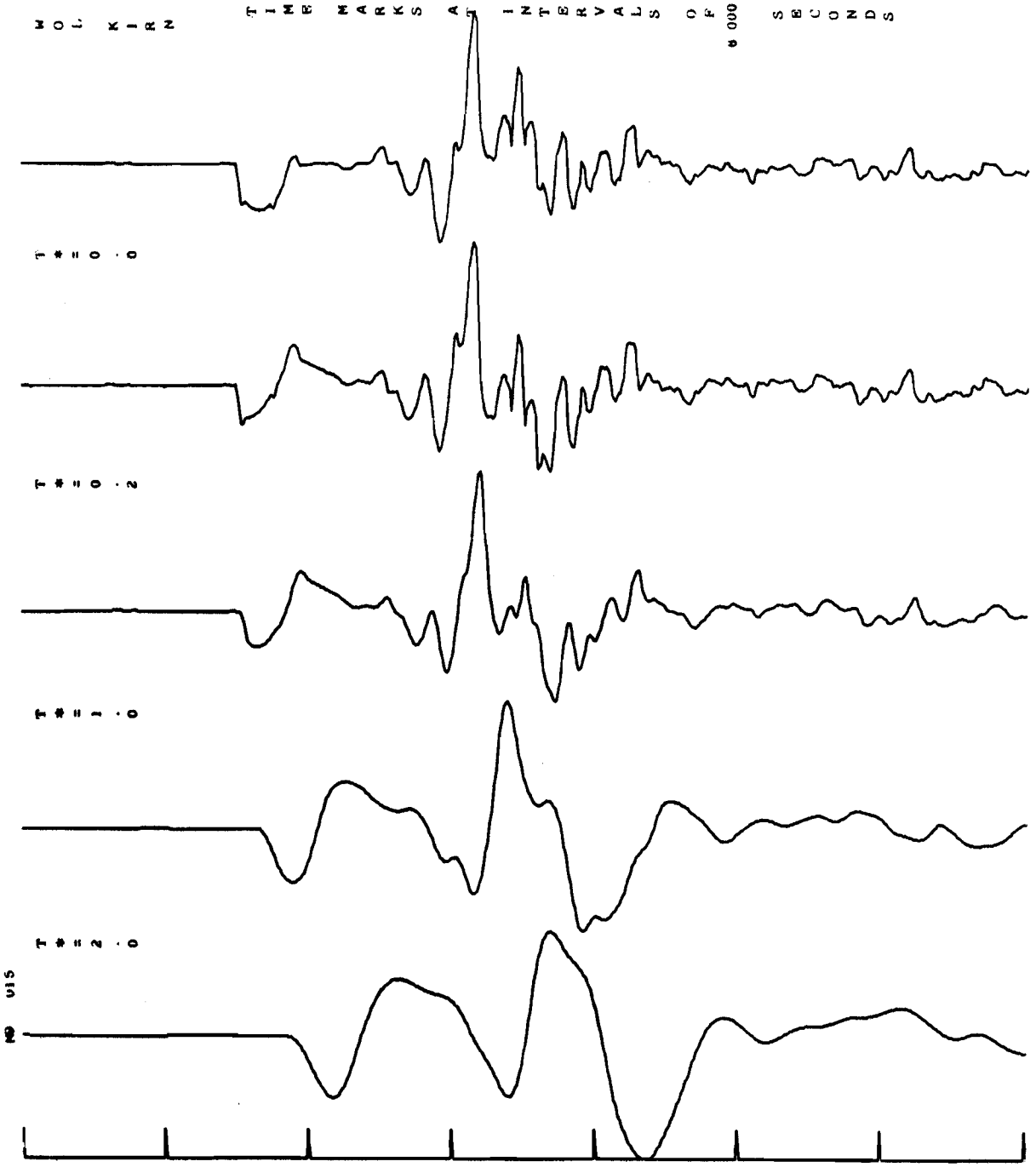
MOL KIRN
TIME MARKS AT INTERVALS OF 0.000 SECONDS
T*=0.0
T*=0.2
T*=1.0
T*=2.0
U15

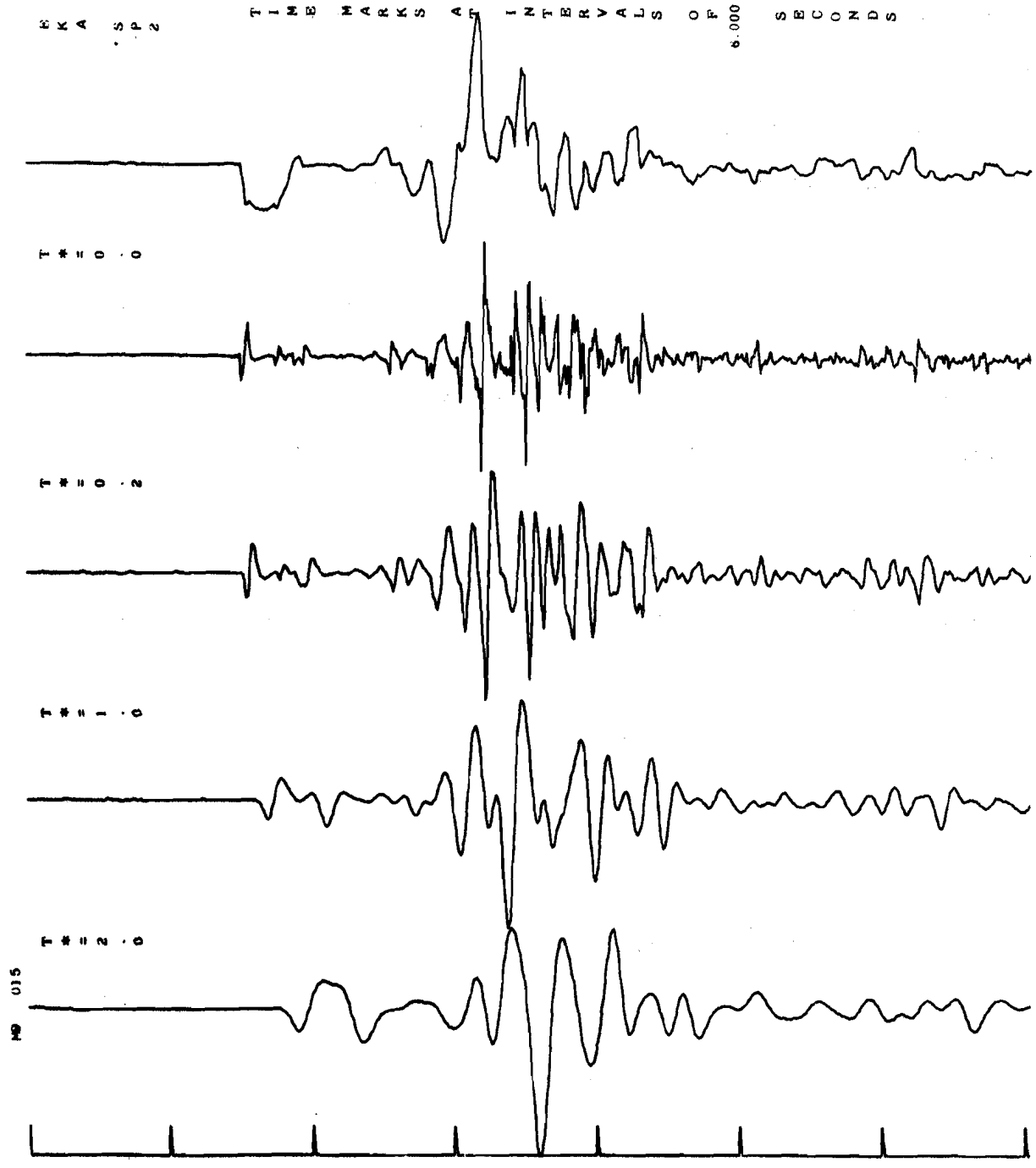
EKA .SP 2
TIME MARKS AT INTERVALS OF 6.000 SECONDS
F*=0.0
F*=0.2
F*=-.6
F*=2.6
015

Model M10

Dip of fault plane	:	90°
Direction of slip on fault plane	:	vertical
Shape of fault plane	:	ellipse
Dimensions of fault plane	:	2.5 × 2.0 km
Azimuth	:	90° to strike
Orientation of major axis	:	horizontal
Point of initiation of fracture	:	a focus

Amplitudes

	Channel 1	Channel 2	Channel 3	Channel 4	Channel 5
M10K					
Maximum	1865.5	2179.1	1582.4	754.8	380.6
Minimum	-1629.8	-1693.8	-1233.8	-737.5	-461.6
M10SP					
Maximum	1865.5	1199.7	314.3	24.8	5.3
Minimum	-1629.8	-1293.9	-384.1	-39.6	-7.6

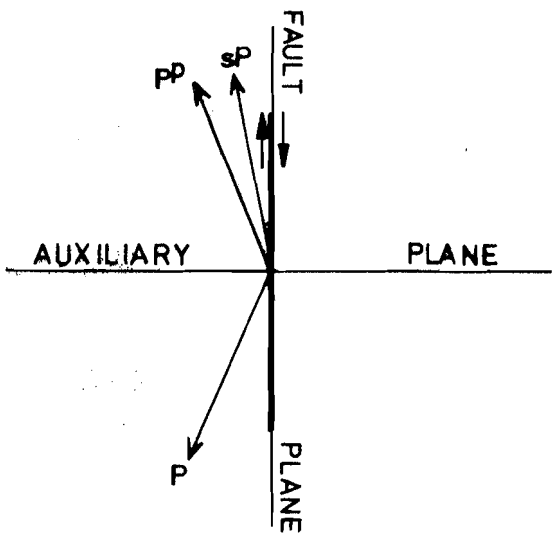

FIGURE 15. CROSS SECTION THROUGH THE SOURCE IN THE PLANE OF THE OBSERVER

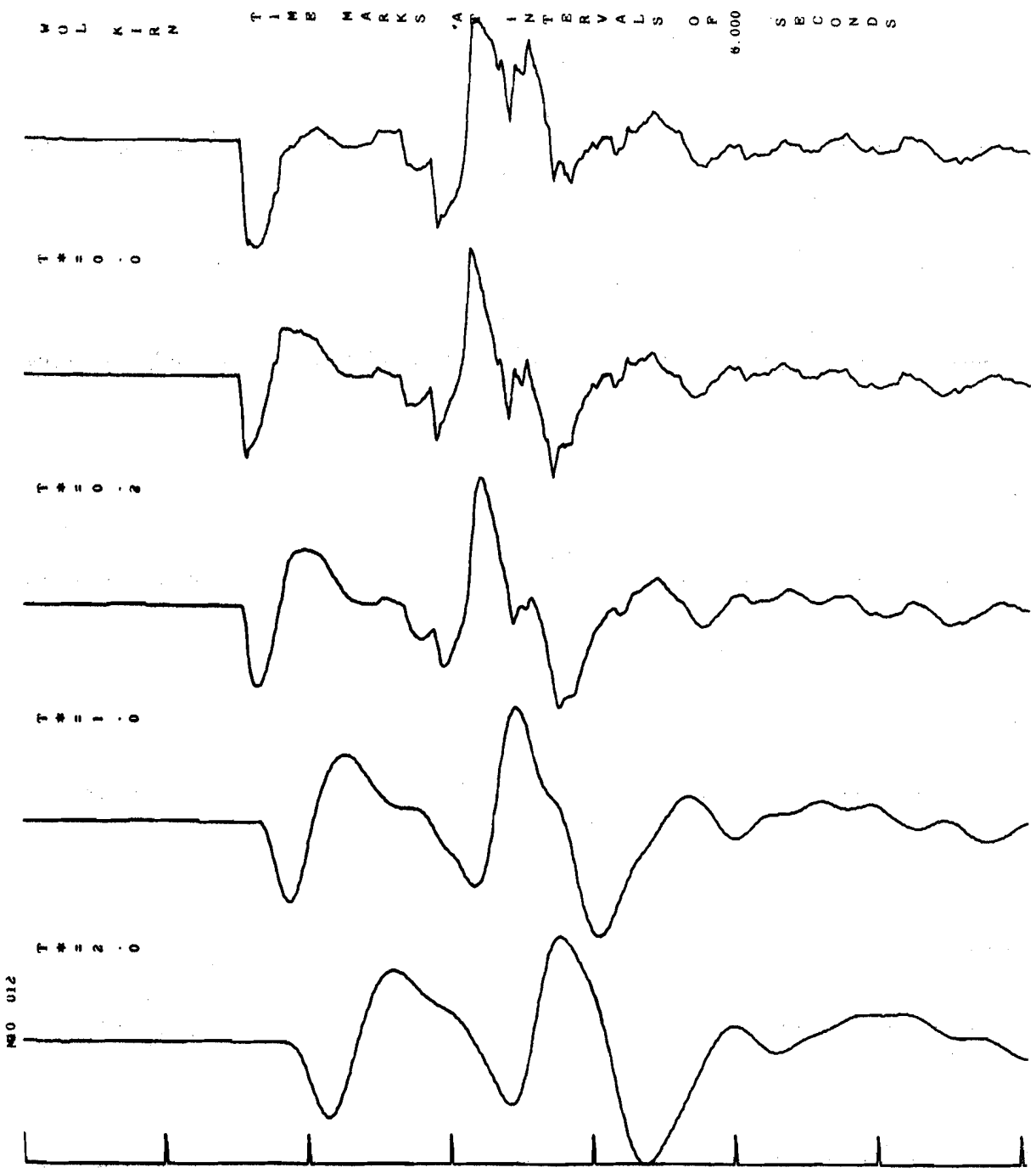
MOL KIRN
TIME MARKS AT INTERVALS OF 6.000 SECONDS
T*=0.0
T*=0.2
T*=1.0
T*=2.0
NO 012

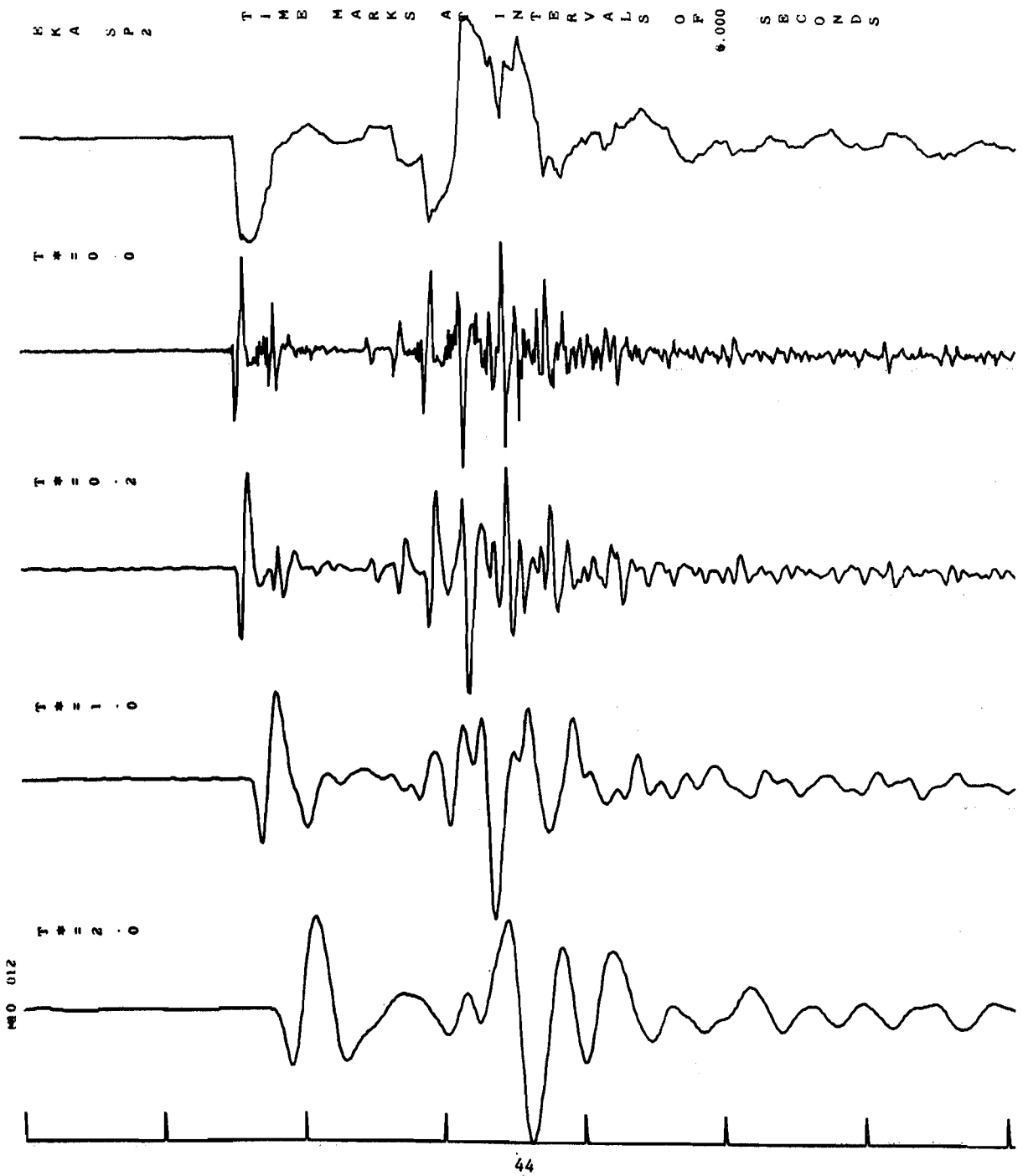
EKA SP2
TIME MARKS AT INTERVALS OF 0.000 SECONDS
T*=0.0
T*=0.2
T*=1.0
T*=2.0
MO 012

Model M11

Dip of fault plane	:	90°
Direction of slip on fault plane	:	horizontal
Shape of fault plane	:	circular
Dimensions of fault plane	:	1.0 km radius
Azimuth	:	45°

Amplitudes

	Channel 1	Channel 2	Channel 3	Channel 4	Channel 5
M11K					
Maximum	84.2	72.0	34.1	11.0	7.0
Minimum	-112.0	-102.6	-54.1	-19.8	-8.9
M11SP					
Maximum	84.2	159.2	37.7	2.1	0.3
Minimum	-112.0	-115.4	-30.1	-1.9	-0.2

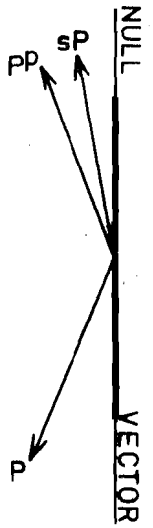

FIGURE 16. CROSS SECTION THROUGH THE SOURCE IN THE PLANE OF THE OBSERVER

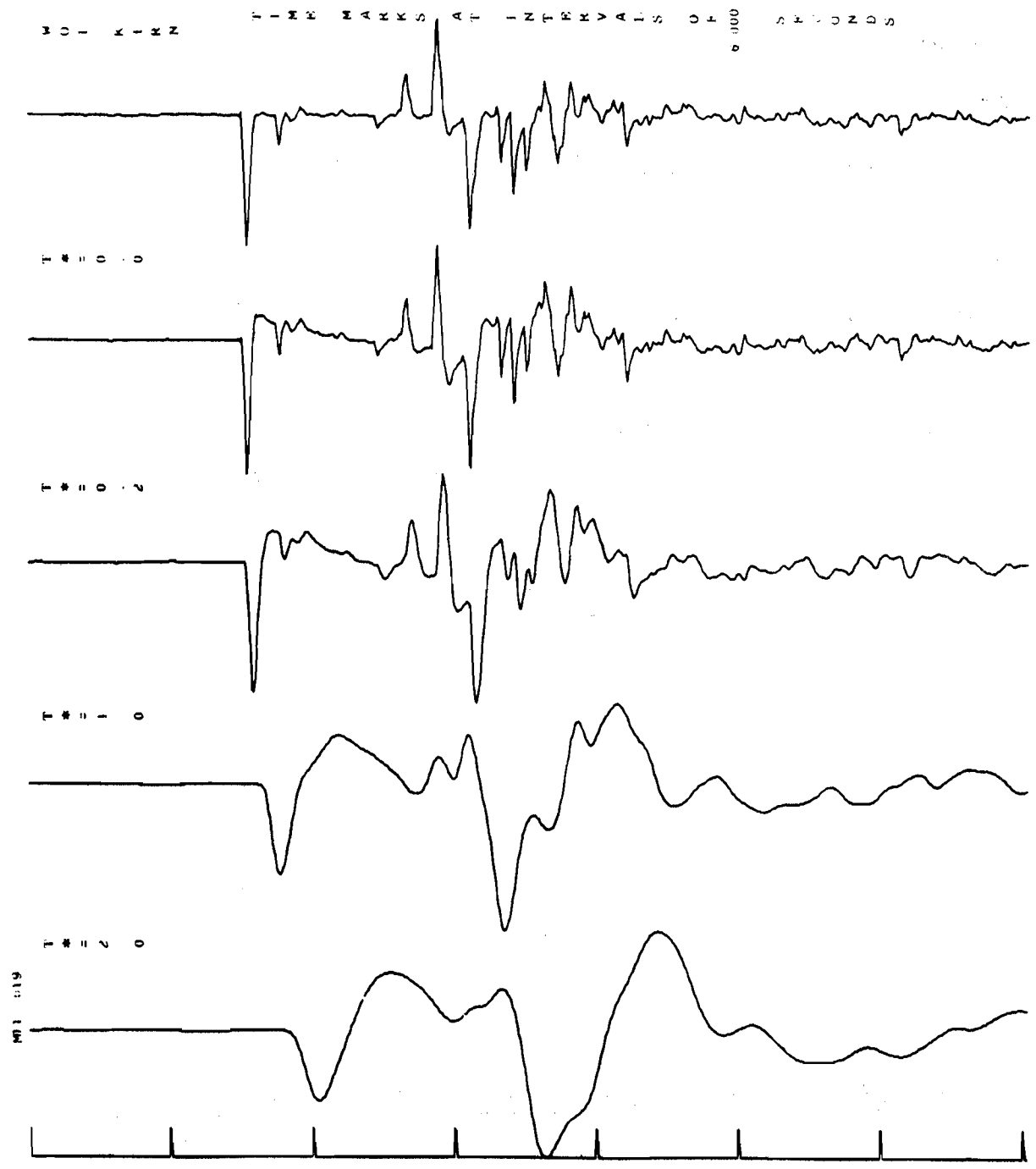

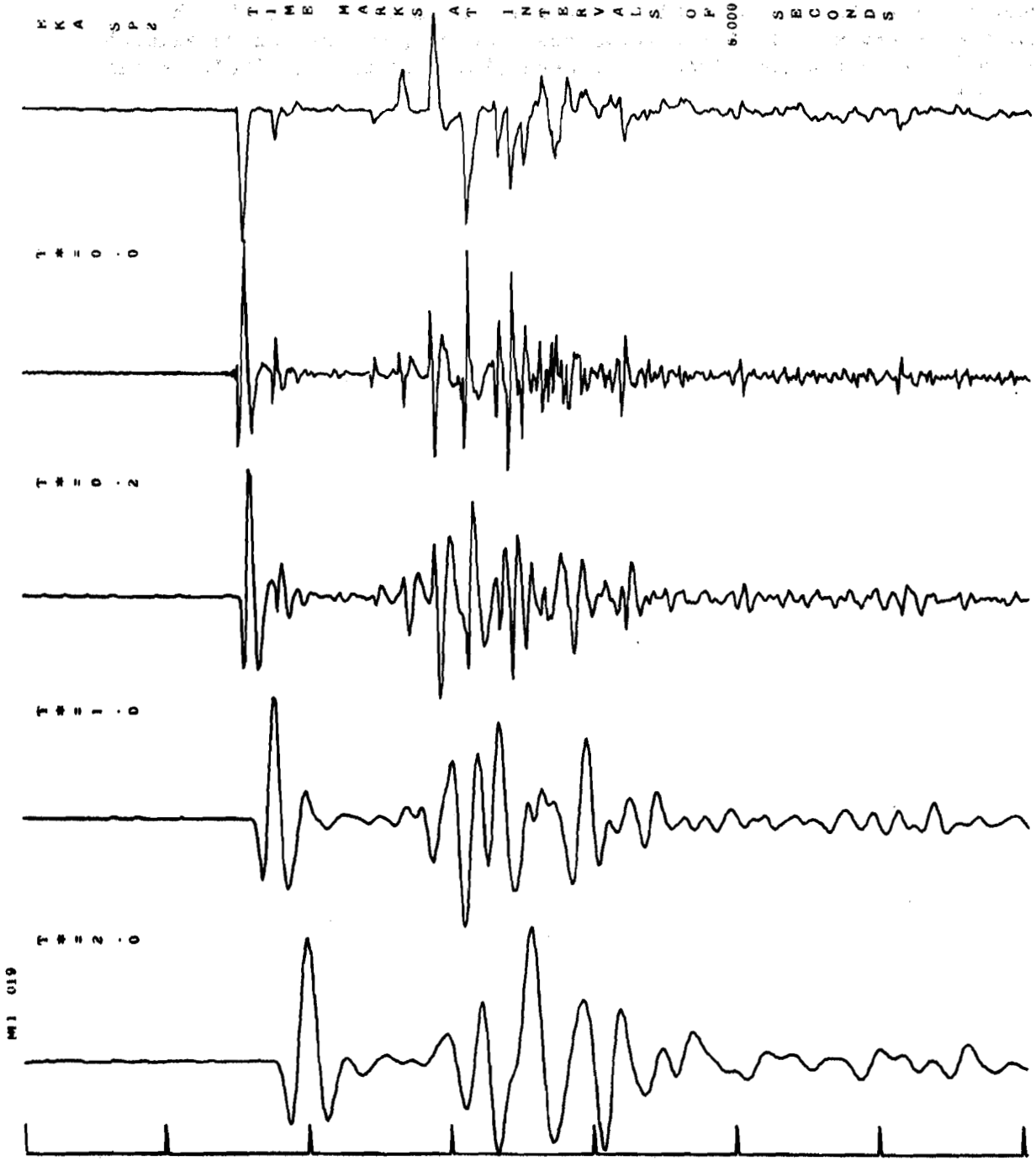
EKA SP2
TIME MARKS AT INTERVALS OF 5.000 SECONDS
T**=0.0
T**=0.2
T**=1.0
T**=2.0
M1 019

6. 45° DIP SLIP MODELS - SLIP DIRECTION 90° TO STRIKE: M12 TO M22

The vertical through a 45° dip slip model is a node of S so that S to P conversions contribute in general less to the seismograms in this section than in section 5. S derived arrivals are particularly small relative to P along azimuths of 0° and 180° (the strike of the fault plane). Observed on an azimuth of 90° direct P has a sharper front than on azimuths of -90°. This is because on an azimuth of 90° the fracture spreads initially towards the observer, whereas on an azimuth of -90° the motion for direct P is essentially across the field of the observer.

Model M12

Dip of fault plane	:	45°
Direction of slip on fault plane	:	90° to strike
Shape of fault plane	:	circular
Dimensions of fault plane	:	1 km radius
Azimuth	:	-90° to strike

Amplitudes

	Channel 1	Channel 2	Channel 3	Channel 4	Channel 5
M12K					
Maximum	524.3	464.1	246.6	54.9	21.7
Minimum	-367.8	-315.6	-143.9	-37.2	-18.4
M12SP					
Maximum	524.3	464.9	133.6	7.7	0.7
Minimum	-367.8	-804.8	-226.1	-10.0	-1.0

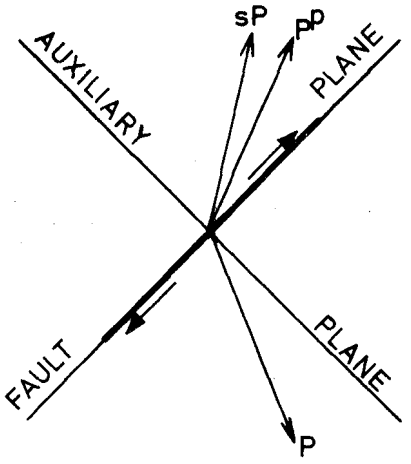

FIGURE 17. CROSS SECTION THROUGH THE SOURCE IN THE PLANE OF THE OBSERVER

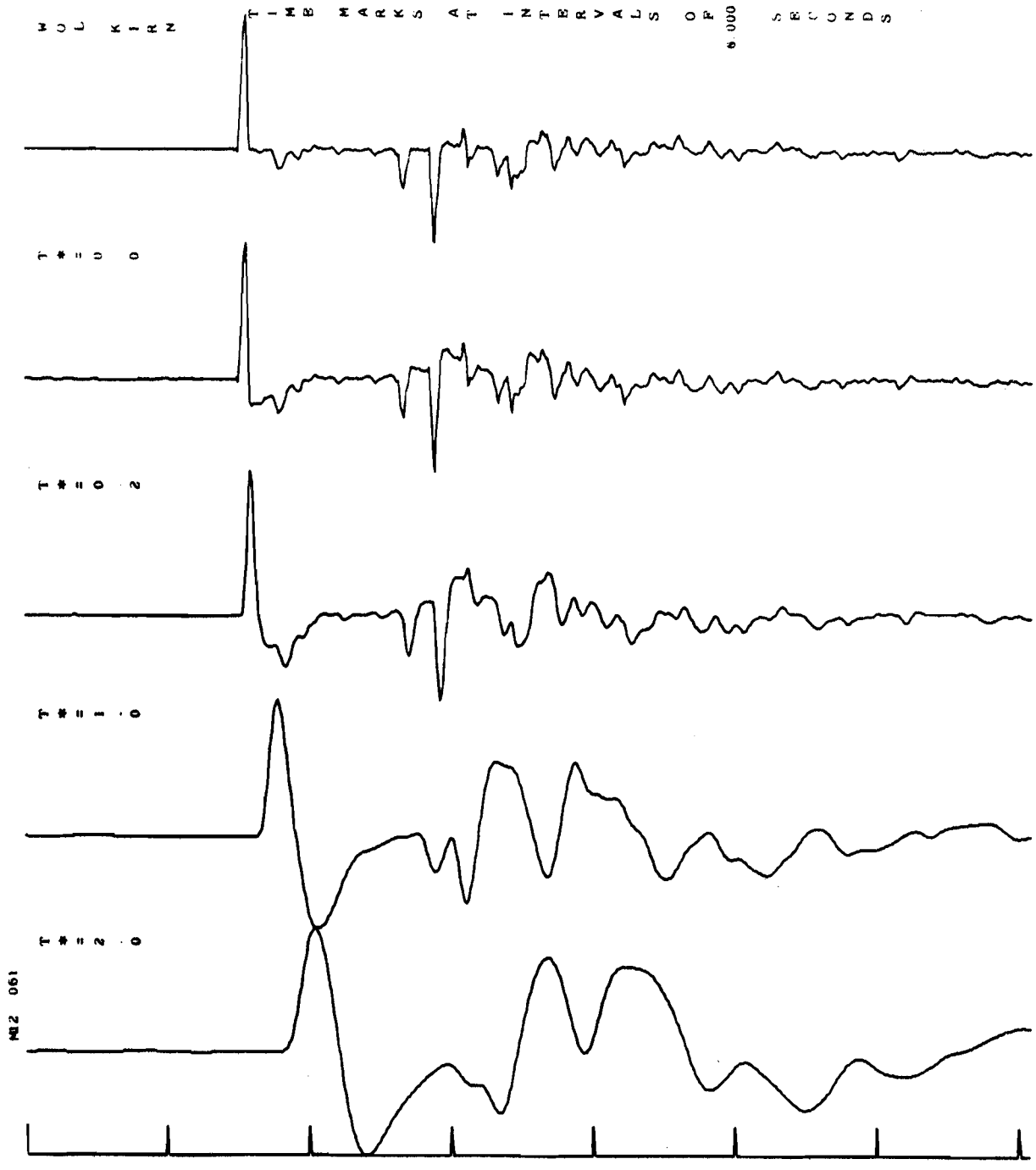
MOL KIRN
TIME MARKS AT INTERVALS OF 6.000 SECONDS
T*=0.0
T*=0.2
T*=1.0
T*=2.0
NN2 061

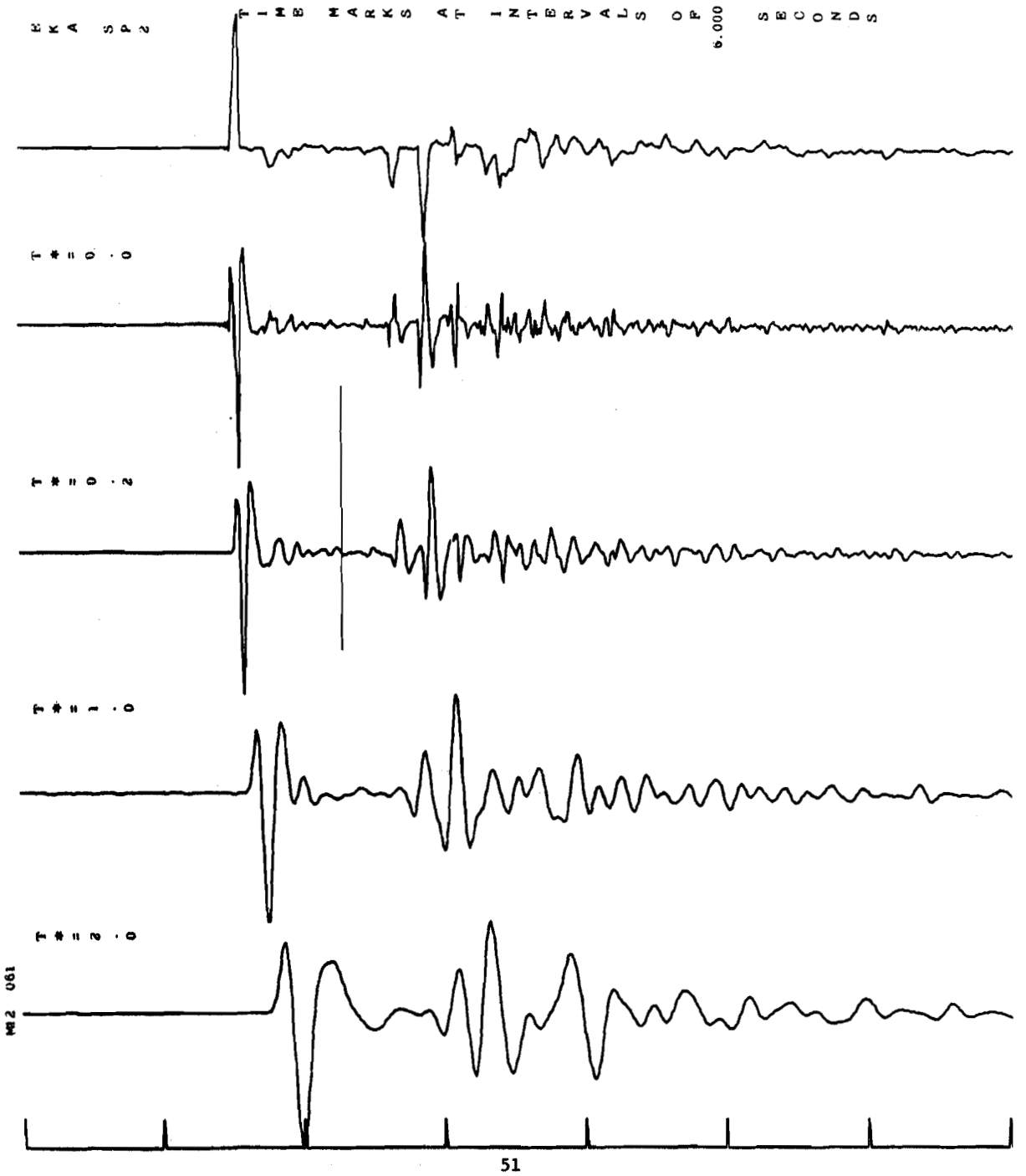
EKA SP2
TIME MARKS AT INTERVALS OF 6.000 SECONDS
T*=0.0
T*=0.2
T*=0.4
T*=0.6
M2 061

Model M13

Dip of fault plane	:	45°
Direction of dip on fault plane	:	90° to strike
Shape of fault plane	:	circular
Dimensions of fault plane	:	1.0 km radius
Azimuth	:	0°

Amplitudes

	Channel 1	Channel 2	Channel 3	Channel 4	Channel 5
M13K					
Maximum	615.2	547.0	282.6	66.8	26.6
Minimum	-479.2	-402.0	-183.0	-41.6	-21.5
M13SP					
Maximum	615.2	675.6	173.9	9.8	0.9
Minimum	-479.2	-849.2	-220.3	-11.9	-1.3

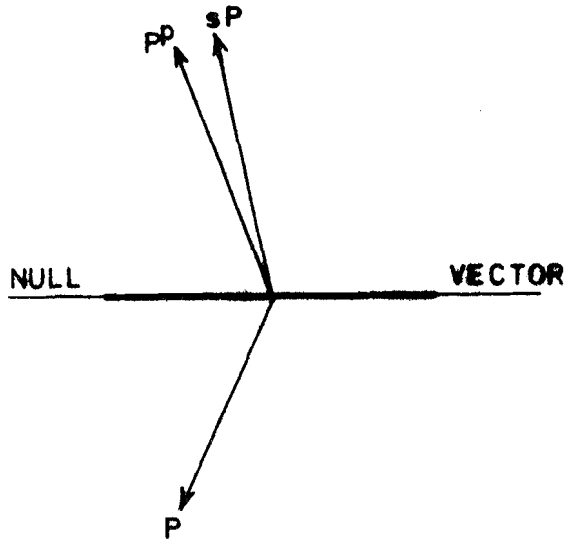

FIGURE 18. CROSS SECTION THROUGH THE SOURCE IN THE PLANE OF THE OBSERVER

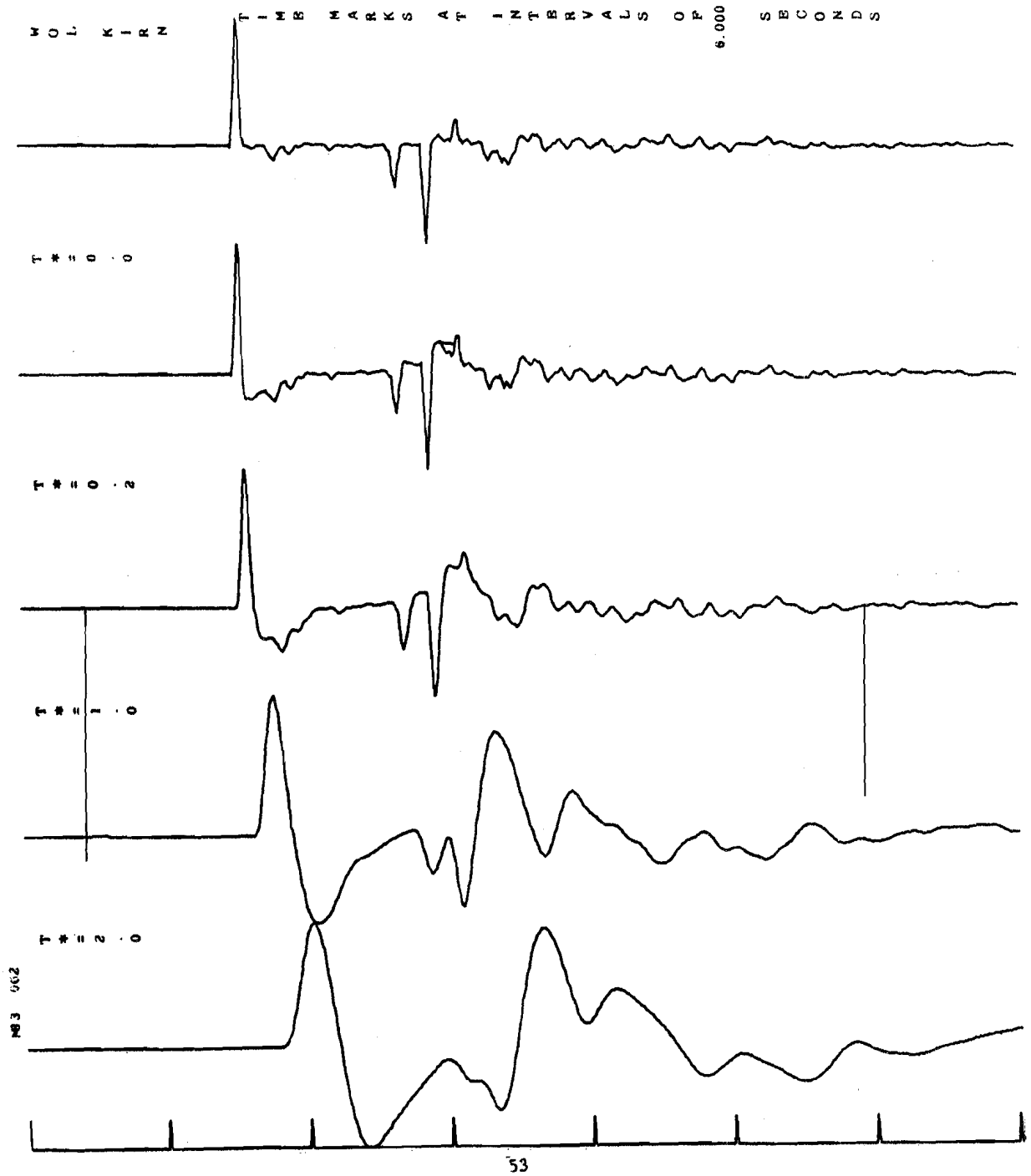
MOL K-RN
T-MR MARKS AT INTERVALS OF 6.000 SECONDS
T**=0.0
T**=0.2
T**=1.0
T**=2.0
NB3 962

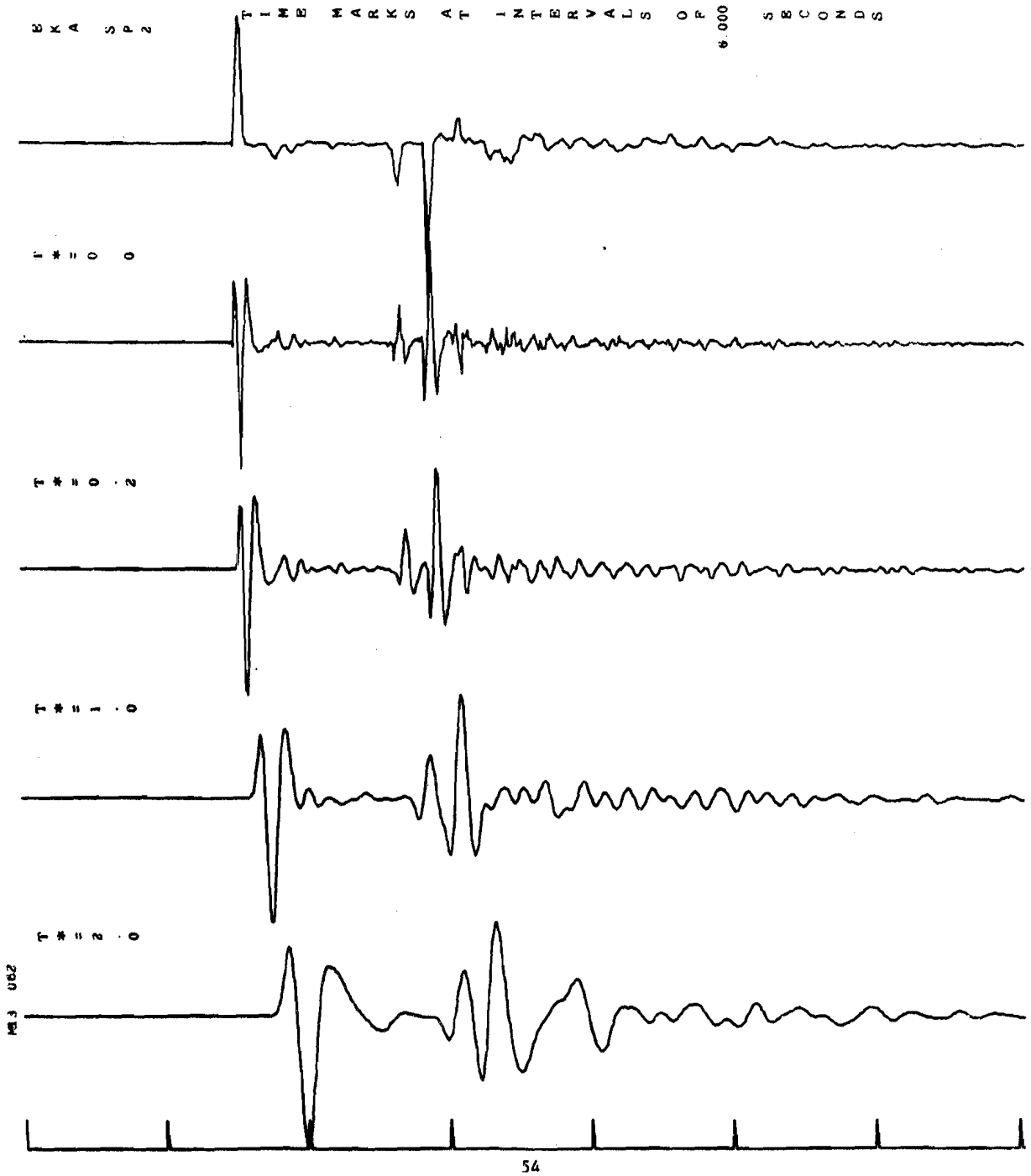
BKA SP2
TIME MARKS AT INTERVALS OF 0.000 SECONDS
T*=0.0
T*=0.2
T*=1.0
T*=2.0
MBJ 062

Model M14

Dip of fault plane	:	45°
Direction of slip on fault plane	:	90° to strike
Shape of fault plane	:	circular
Dimensions of fault plane	:	5.0 km radius
Azimuth	:	-90°

Amplitudes

	Channel 1	Channel 2	Channel 3	Channel 4	Channel 5
M14K					
Maximum	12988.0	7351.7	6440.3	3925.1	2151.4
Minimum	-9420.2	-10185.0	-7924.1	-4139.6	-2218.0
M14SP					
Maximum	12988.0	1961.4	807.6	172.0	37.1
Minimum	-9420.2	-2256.0	-760.3	-111.6	-40.3

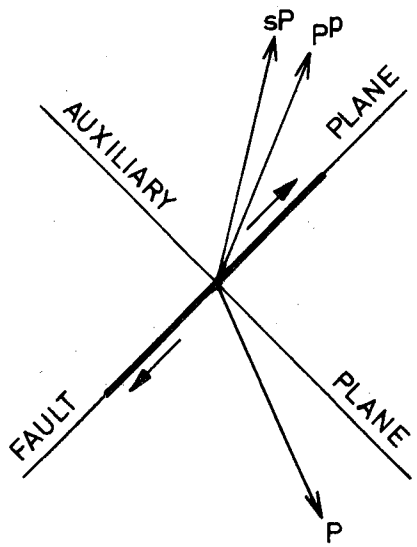

FIGURE 19. CROSS SECTION THROUGH THE SOURCE IN THE PLANE OF THE OBSERVER

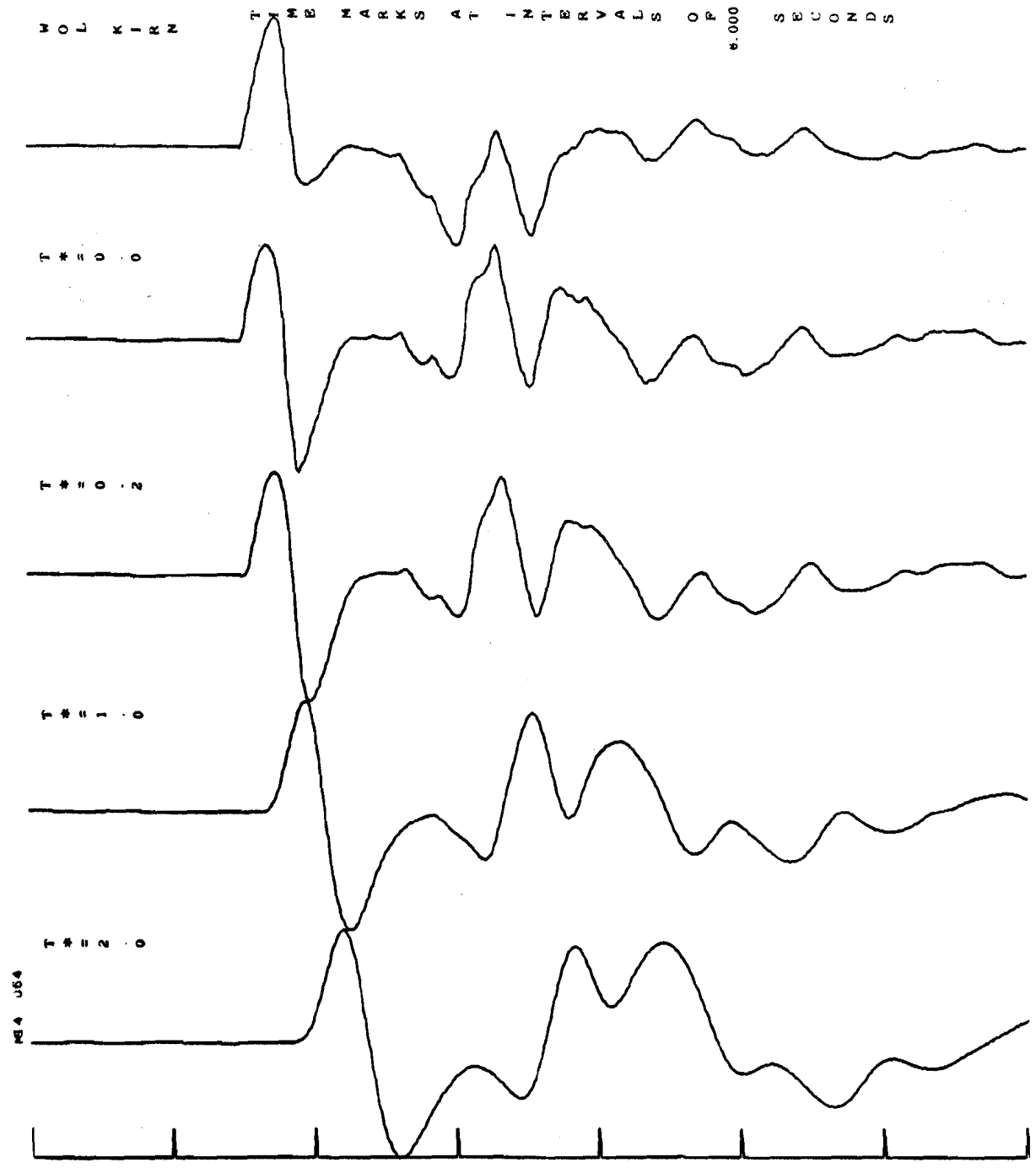
MOL K-RN
TIME MARKS AT -INTERVALS OF 0.000 SECONDS
T*=0.0
T*=0.2
T*=1.0
T*=2.0
MB4 U64

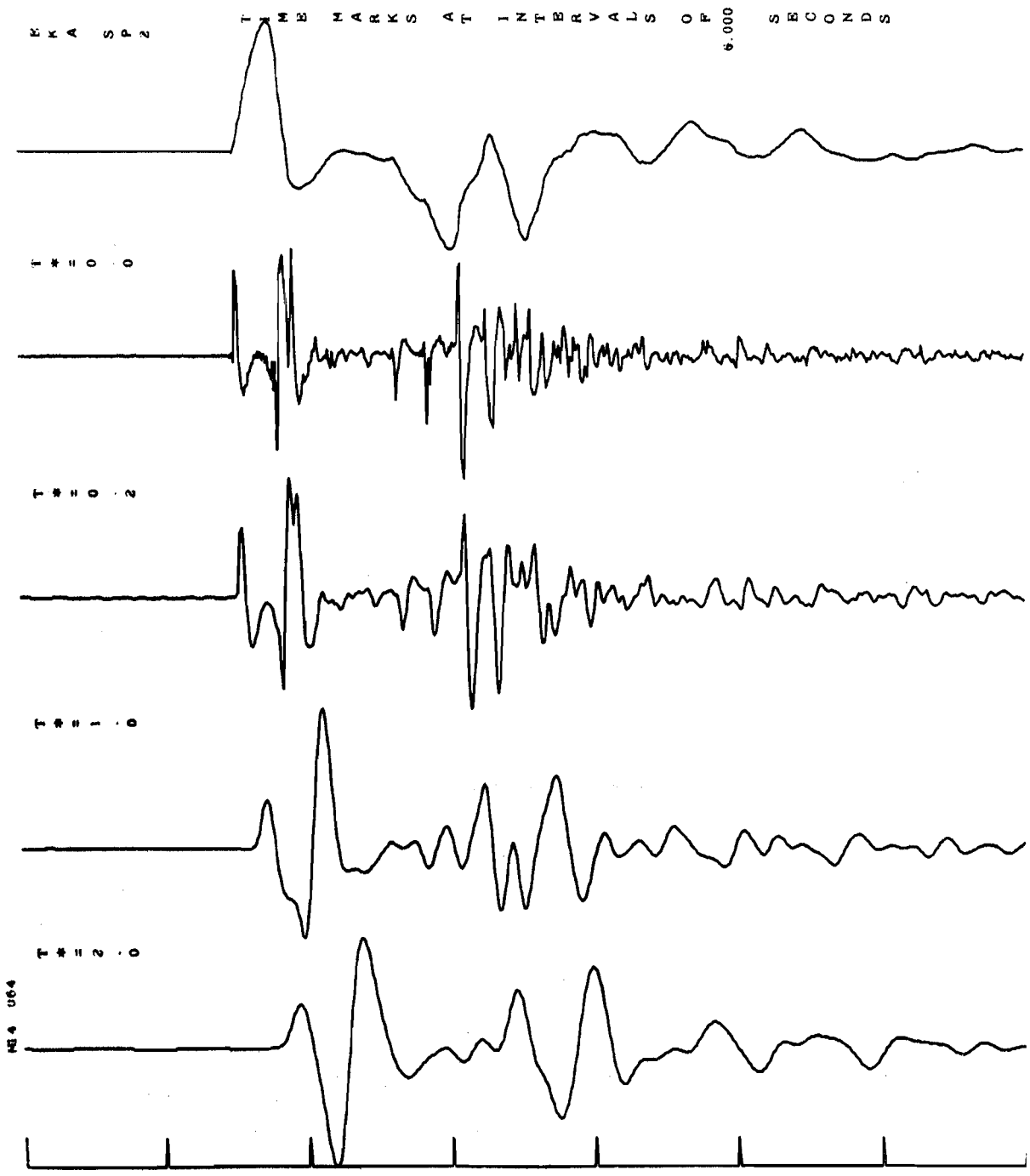
EKA SP2
TIME MARKS AT INTERVALS OF 0.000 SECONDS
T**=0.0
T**=0.2
T**=-.0
T**=2.0
NS4 U64

Model M15

Dip of fault plane	:	45°
Direction of slip in fault plane	:	90° to strike
Shape of fault plane	:	circular
Dimensions of fault plane	:	5.0 km radius
Azimuth	:	0°

Amplitudes

	Channel 1	Channel 2	Channel 3	Channel 4	Channel 5
M15K					
Maximum	15499.0	10342.0	9069.4	5287.4	2906.8
Minimum	-11127.0	-10406.0	-8466.3	-4651.2	-2596.7
M15SP					
Maximum	15499.0	2110.6	845.7	97.8	33.3
Minimum	-11127.0	-2775.3	-654.4	-131.7	-44.2

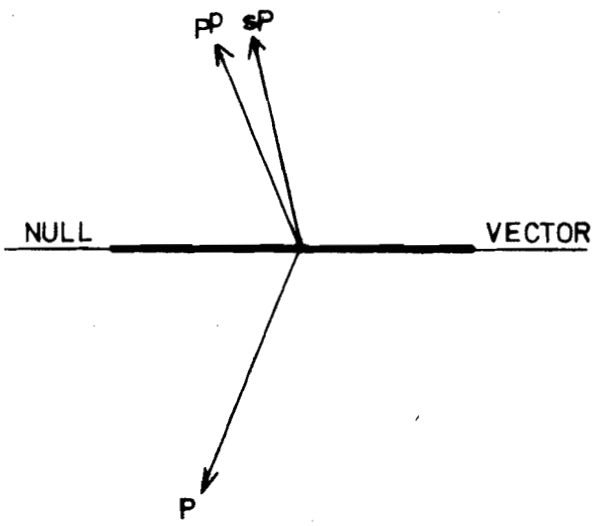

FIGURE 20. CROSS SECTION THROUGH THE SOURCE IN THE PLANE OF THE OBSERVER

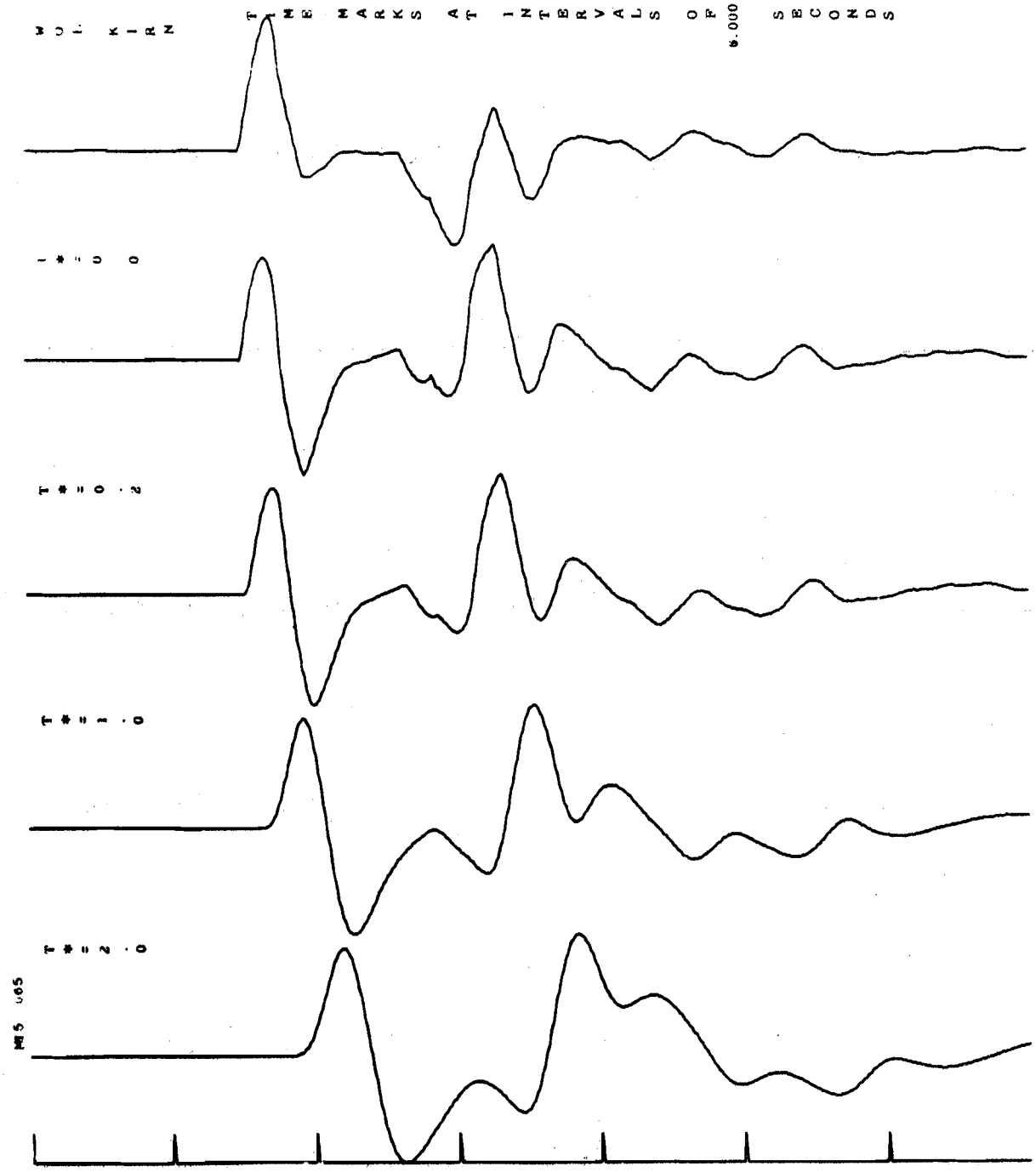
TIME MARKS AT INTERVALS OF 6.000 SECONDS

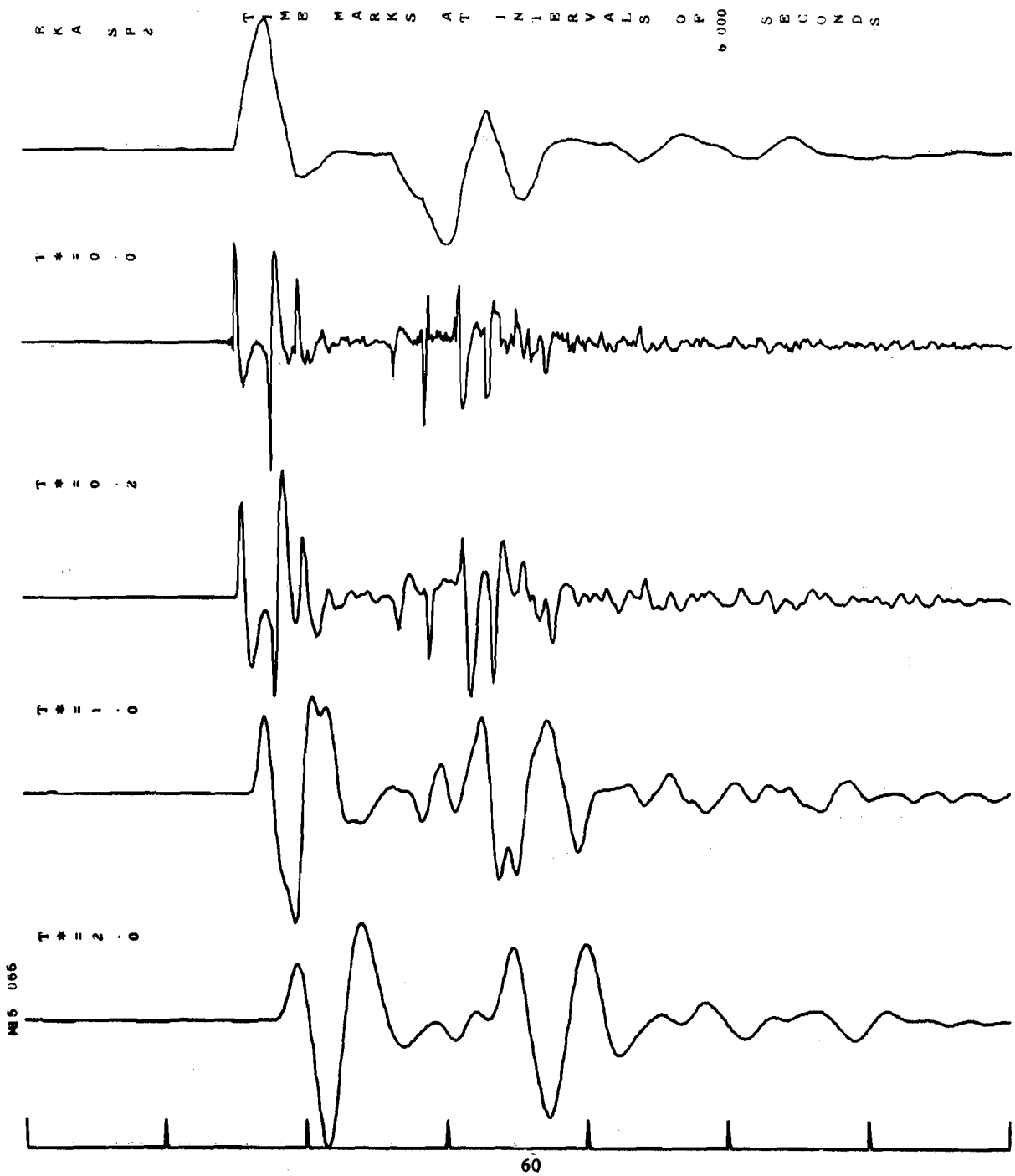
RKA SP 2
TIME MARKS AT INTERVALS OF 6 000 SECONDS
T*=0·0
T*=0·2
T*=1·0
T*=2·0
MS 066
60

Model M16

Dip of fault plane	:	45°
Direction of slip on fault plane	:	90° to strike
Shape of fault plane	:	circular
Dimensions of fault plane	:	5.0 km radius
Azimuth	:	90° to strike

Amplitudes

	Channel 1	Channel 2	Channel 3	Channel 4	Channel 5
M16K					
Maximum	12683.0	8611.1	6822.8	3792.5	2017.1
Minimum	-8542.8	-8137.7	-6841.5	-3812.0	-2107.0
M16SP					
Maximum	12683.0	2041.8	661.6	82.4	28.8
Minimum	-8542.8	-2270.7	-582.6	-118.8	-36.9

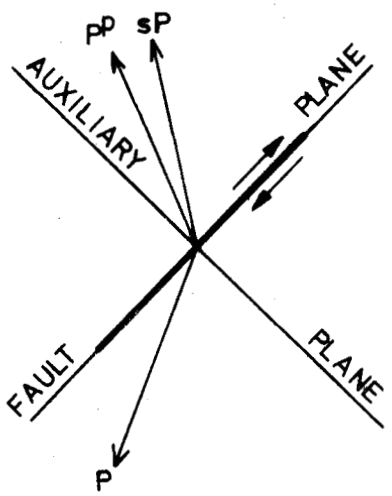

FIGURE 21. CROSS SECTION THROUGH THE SOURCE IN THE PLANE OF THE OBSERVER

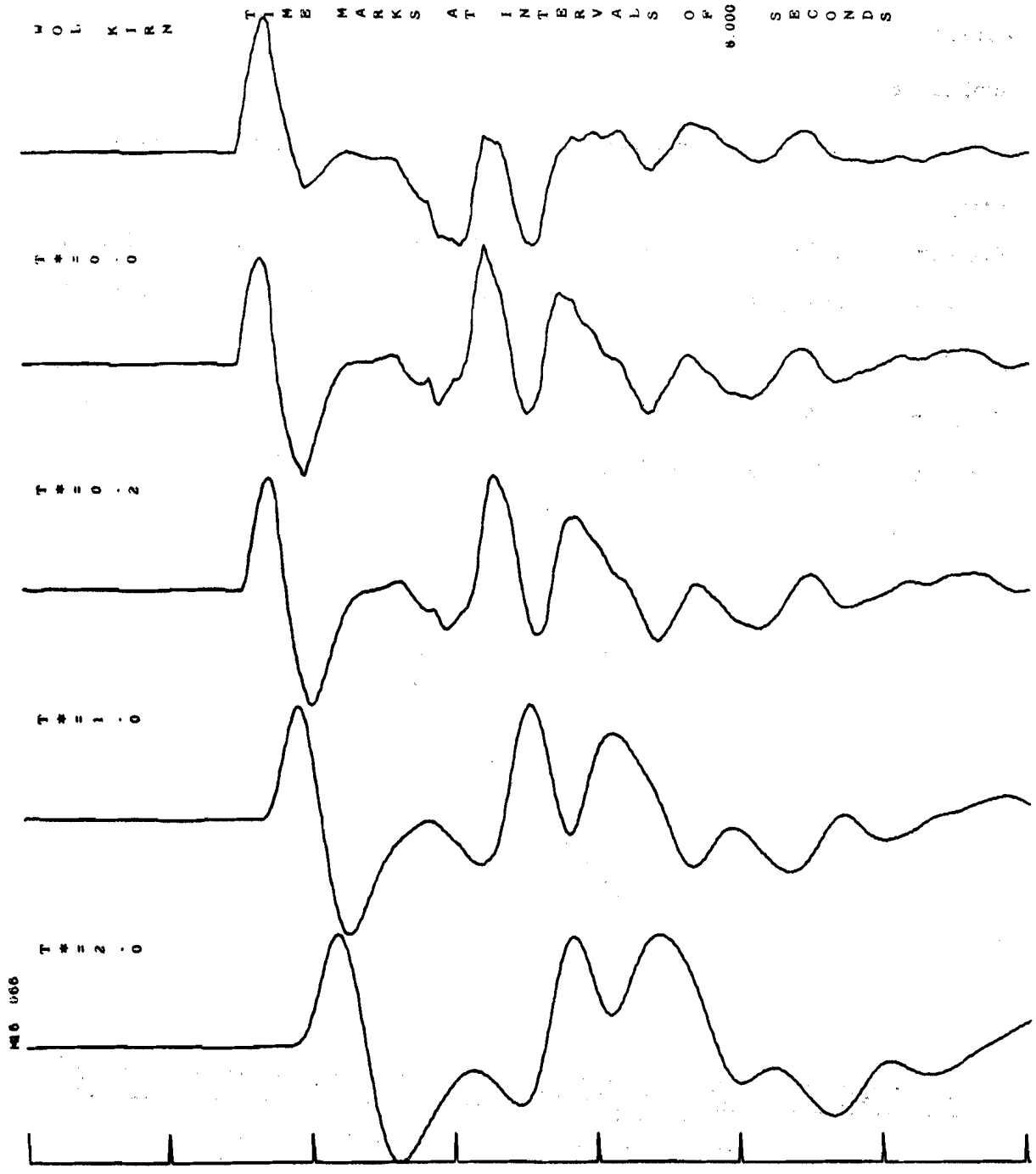
MOL KIRN
TIME MARKS AT INTERVALS OF 0.000 SECONDS
T*=0.0
T*=0.2
T*=1.0
T*=2.0
MS 066

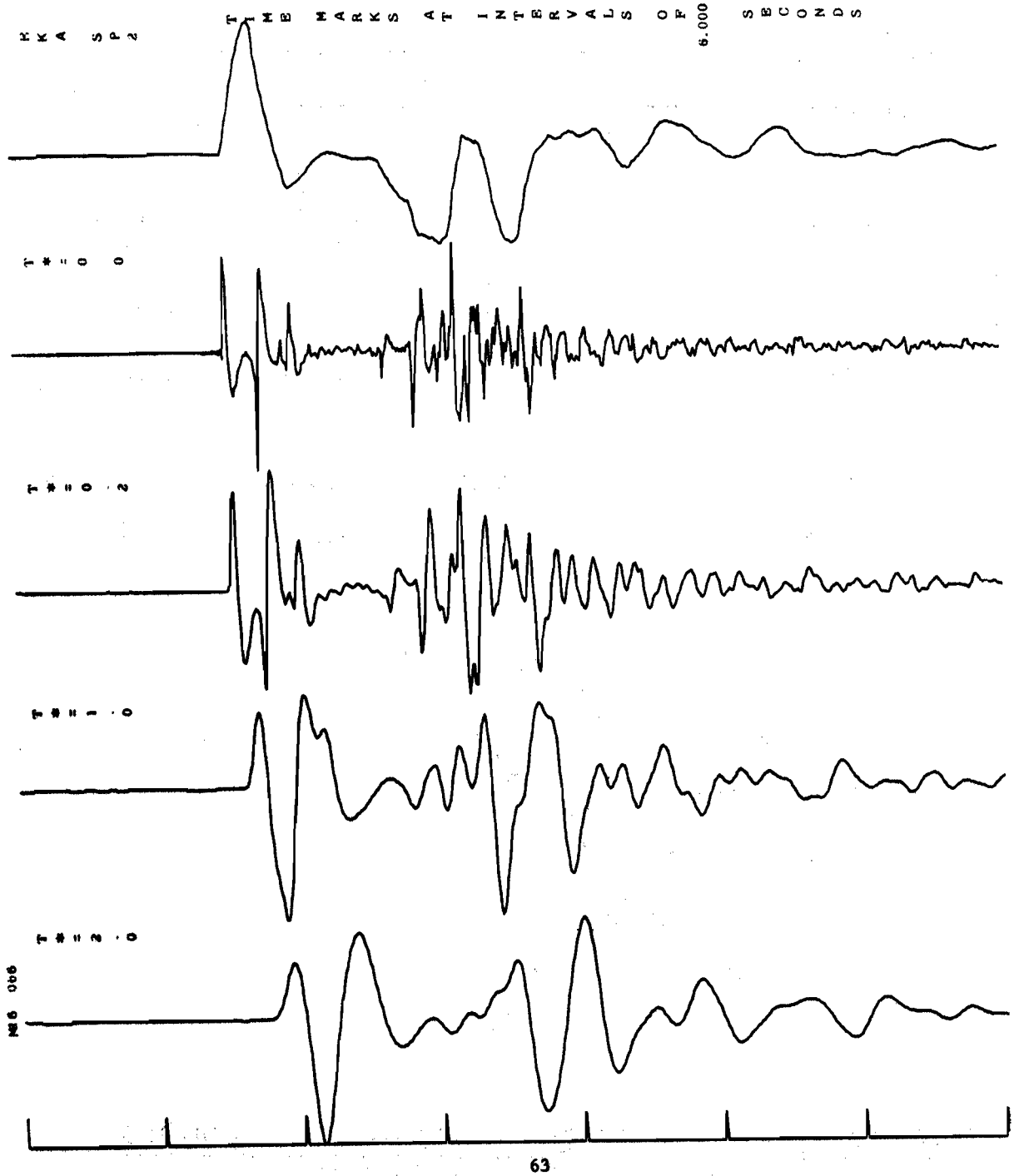
KKA SP2
TIME MARKS AT INTERVALS OF 6.000 SECONDS
f*=0 0
f*=0 .2
f*=- .0
f*=2 .0
M6 006

Model M17

Dip of fault plant	:	45°
Direction of slip on fault plane	:	90° to strike
Shape of fault plane	:	elliptical
Dimensions of fault plane	:	2.5 × 2.0 km
Azimuth	:	-90°
Orientation of major axis of ellipse	:	along line of dip
Point of initiation of fracture	:	lower focus

Amplitudes

	Channel 1	Channel 2	Channel 3	Channel 4	Channel 5
M17K					
Maximum	1032.7	1015.0	756.7	331.1	176.0
Minimum	-1455.5	-908.1	-634.4	-332.9	-173.9
M17SP					
Maximum	1032.7	460.8	230.5	34.4	5.1
Minimum	-1455.5	-851.9	-262.8	-31.1	-4.0

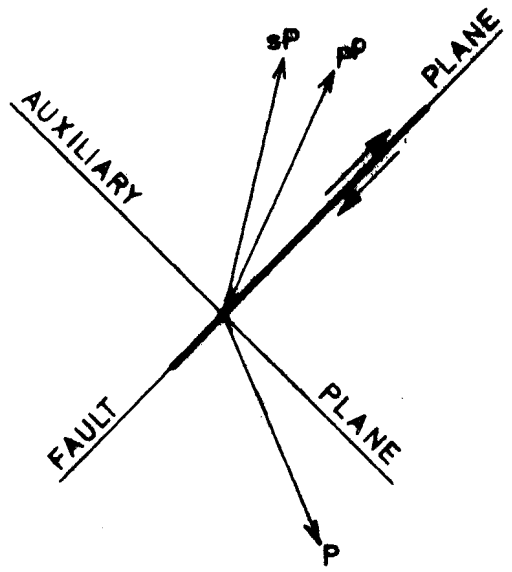

FIGURE 22. CROSS SECTION THROUGH THE SOURCE IN THE PLANE OF THE OBSERVER

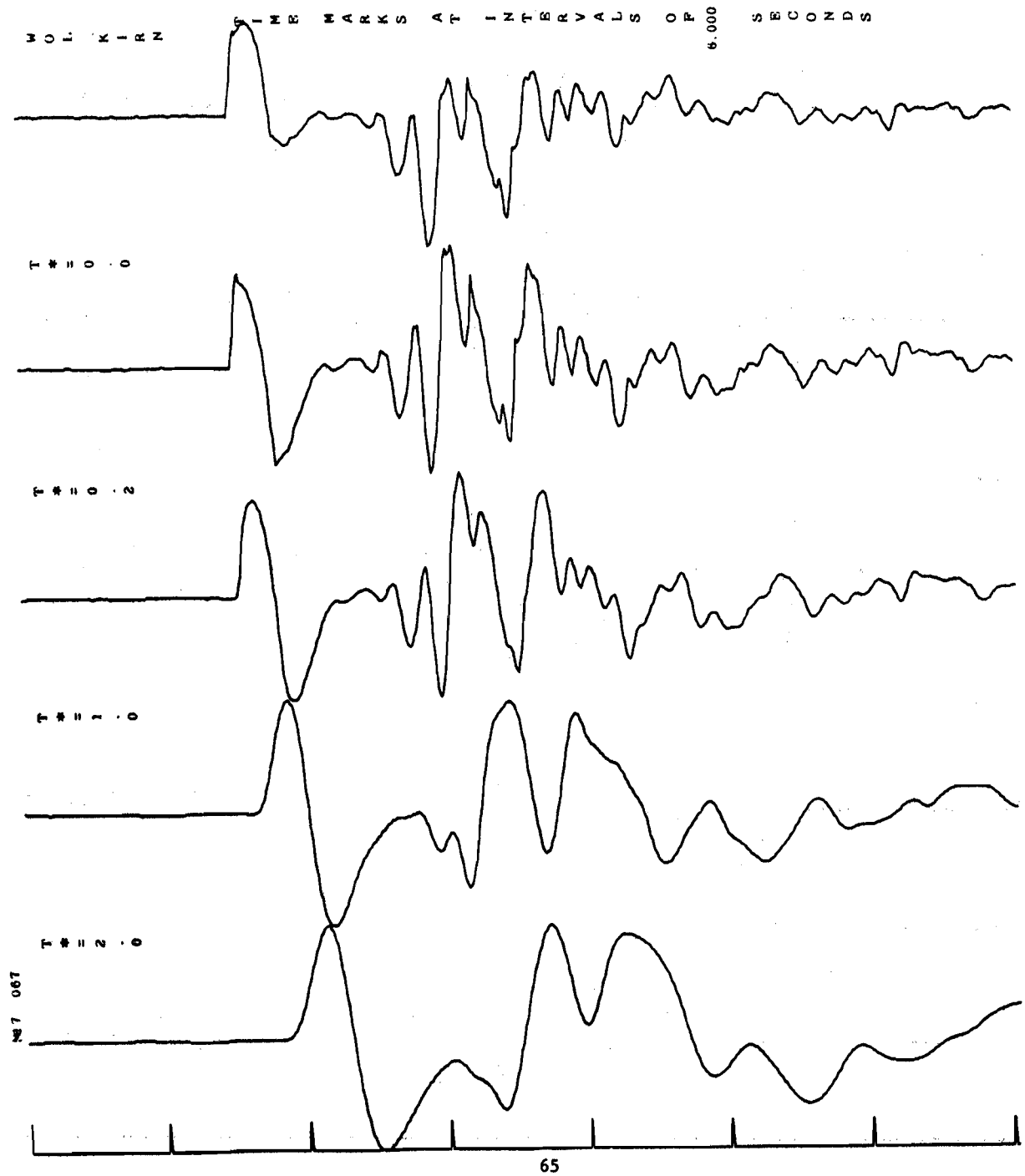
MOL. K-RN
TIME MARKS AT INTERVALS OF 6.000 SECONDS
T*=0.0
T*=0.2
T*=1.0
T*=2.0
NO7 067

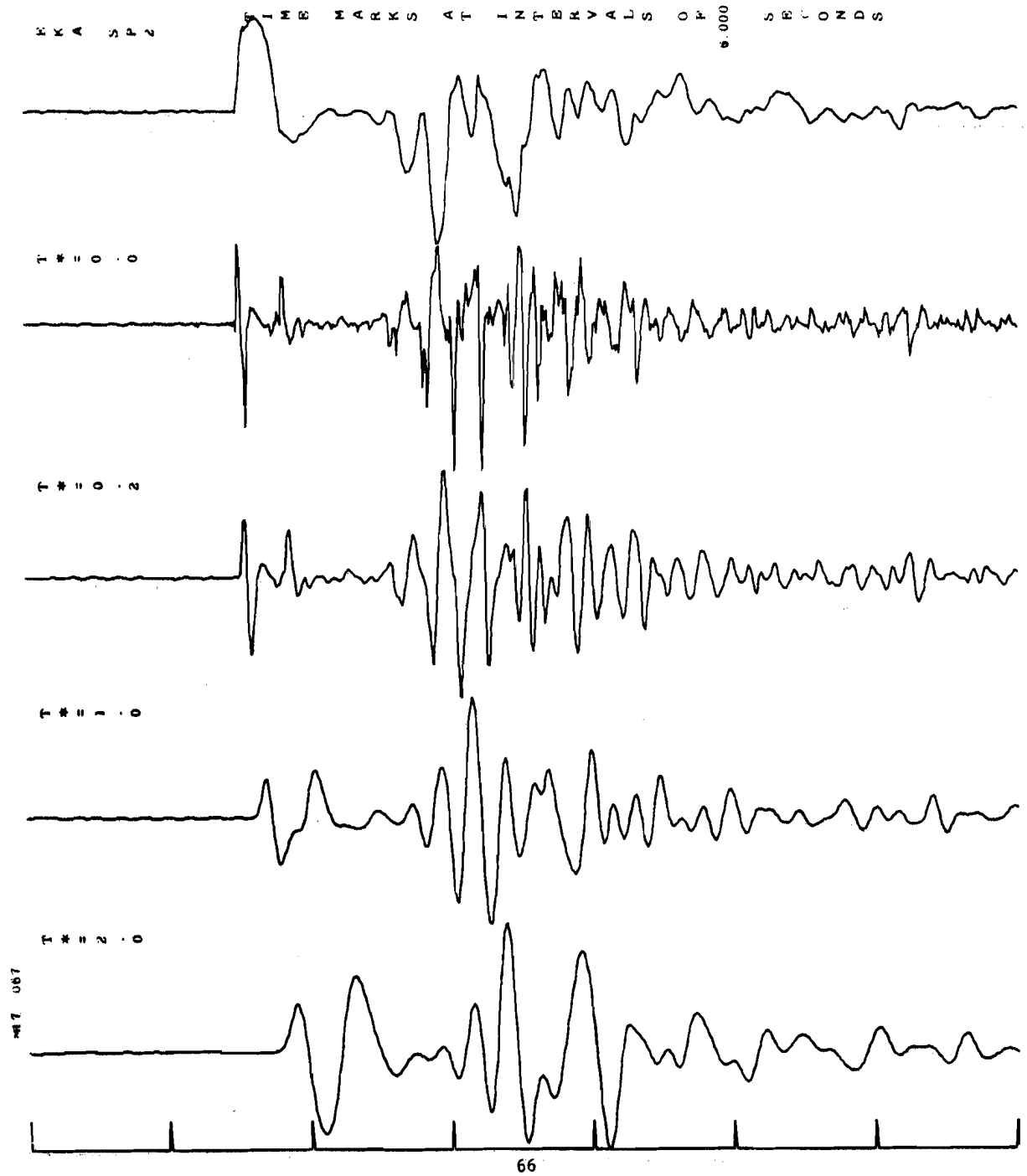
EKA SP2
TIME MARKS AT INTERVALS OF 0.000 SECONDS
T**=0.0
T**=0.2
T**=1.0
T**=2.0
MAT 067

Model M18

Dip of fault plane	:	45°
Direction of slip on fault plane	:	90° to strike
Shape of fault plane	:	elliptical
Dimensions of fault plane	:	2.5 × 2.0 km
Azimuth	:	0°
Orientation of major axis of ellipse	:	along line of dip
Point of initiation of fracture	:	lower focus

Amplitudes

	Channel 1	Channel 2	Channel 3	Channel 4	Channel 5
M18K					
Maximum	1131.5	1248.2	964.2	490.1	257.9
Minimum	-1472.0	-898.5	-696.6	-371.3	-202.9
M18SP					
Maximum	1131.5	605.9	253.0	27.9	5.3
Minimum	-1472.0	-840.5	-226.2	-26.8	-4.3

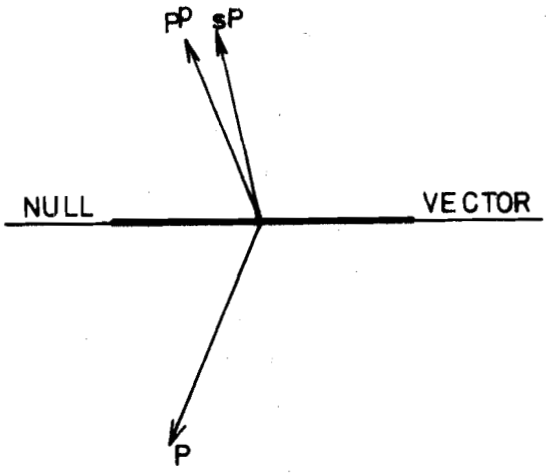

FIGURE 23. CROSS SECTION THROUGH THE SOURCE IN THE PLANE OF THE OBSERVER

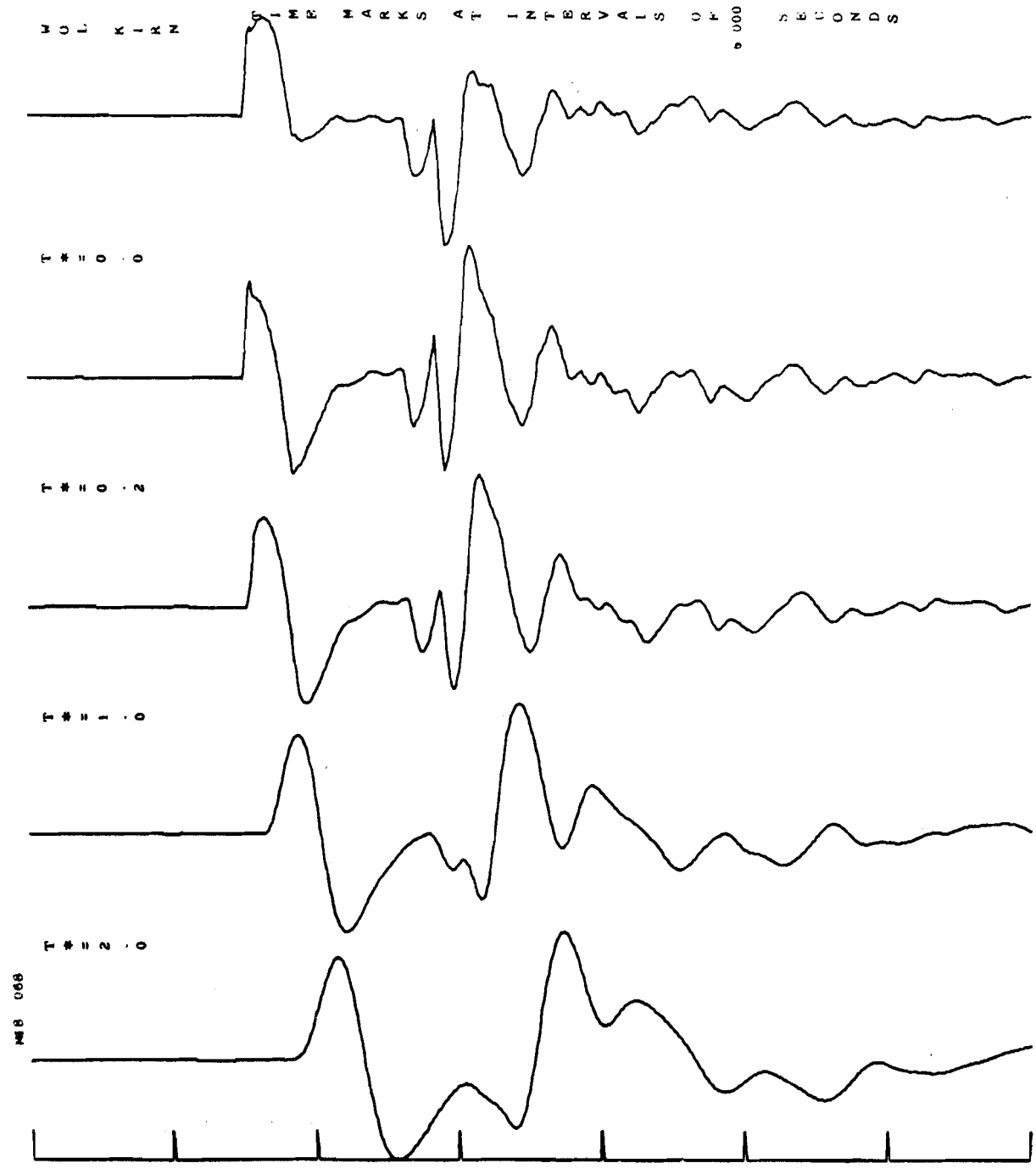
MOL K-KN
TIME MARKS AT INTERVALS OF .000 SECONDS
T*=0.0
T*=0.2
T*=1.0
T*=2.0
NB 068

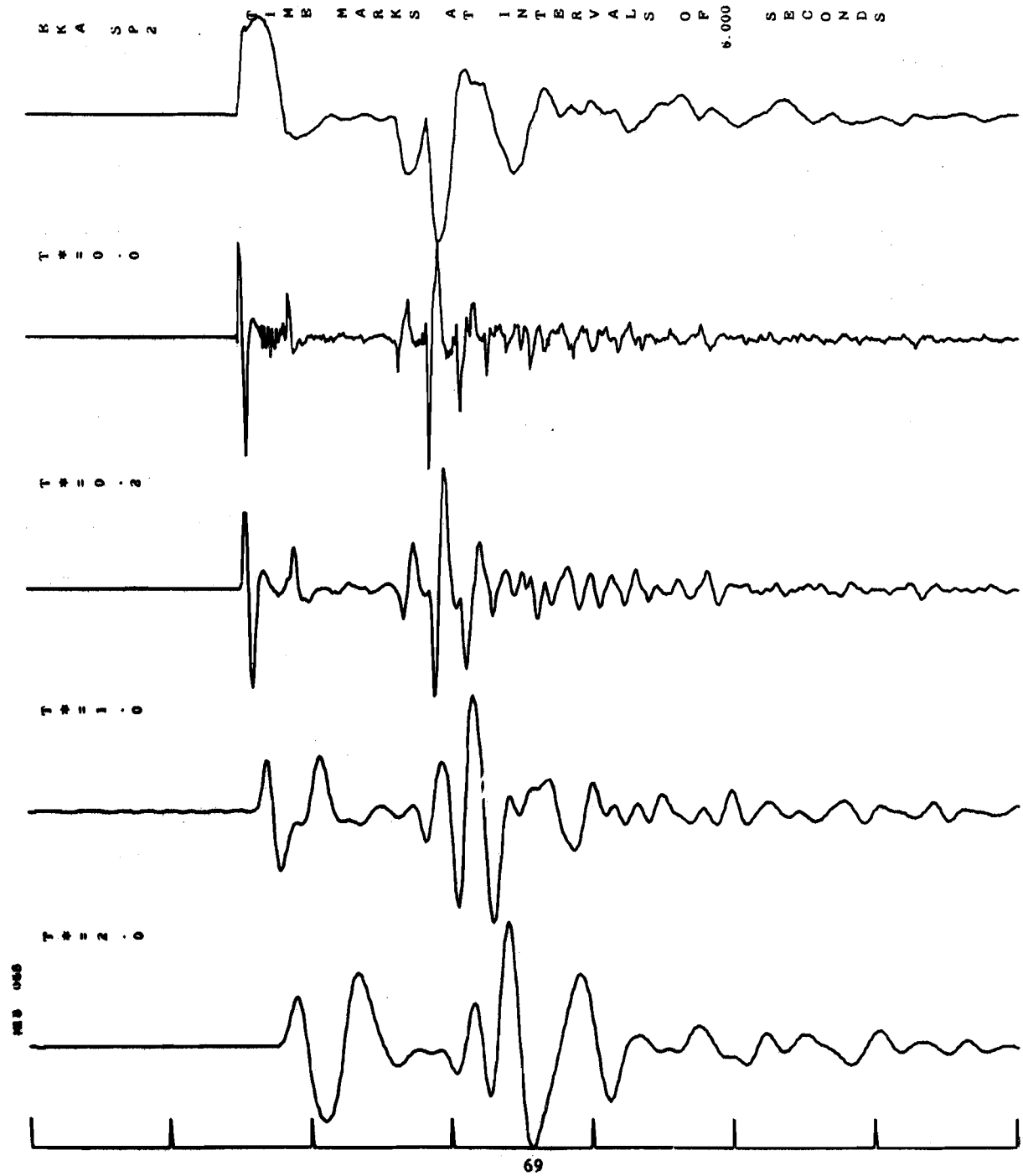
KKA SP2
TIME MARKS AT INTERVALS OF 6.000 SECONDS
T*=0.0
T*=0.2
T*=1.0
T*=2.0

Model M19

Dip of fault plant	:	45°
Direction of slip in fault plane	:	90° to strike
Shape of fault plane	:	elliptical
Dimensions of fault plane	:	2.5 × 2.0 km
Azimuth	:	90.0°
Orientation of major axis of fault plane	:	line of dip
Point of initiation of fracture	:	lower focus

Amplitudes

	Channel 1	Channel 2	Channel 3	Channel 4	Channel 5
M19K					
Maximum	859.8	1010.1	665.7	312.7	167.3
Minimum	-1011.3	-737.1	-594.6	-309.8	-166.4
M19SP					
Maximum	859.8	533.6	151.5	15.2	3.7
Minimum	-1011.3	-724.6	-178.2	-22.1	-3.3

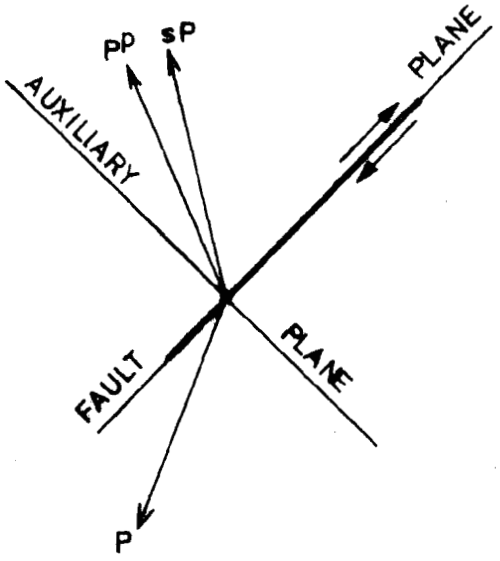

FIGURE 24. CROSS SECTION THROUGH THE SOURCE IN THE PLANE OF THE OBSERVER

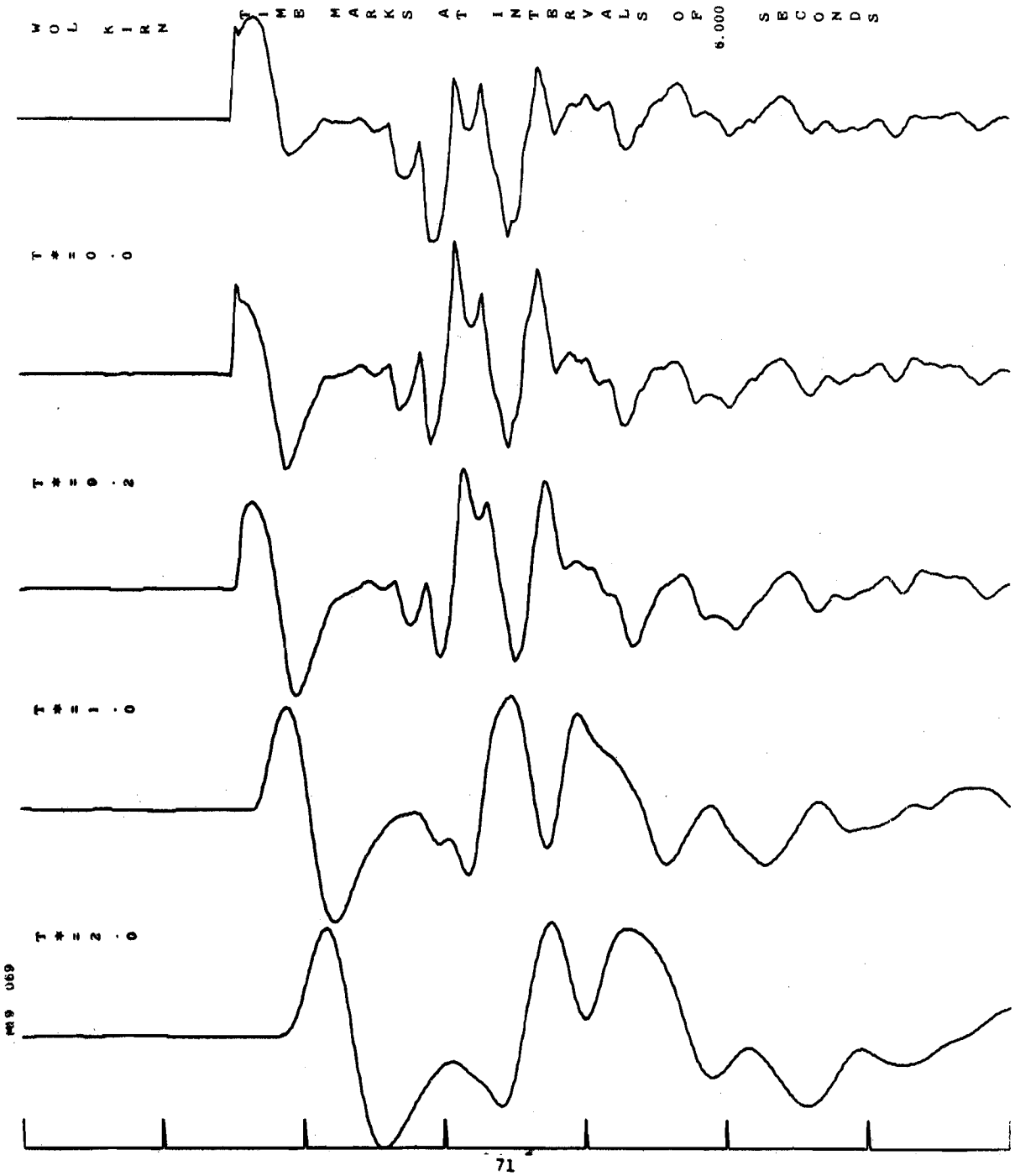
MOL K-RN
TIMB MARKS AT INTERVALS OF 6.000 SECONDS
T**=0.0
T**=0.2
T**=-.0
T**=2.0
M9 069

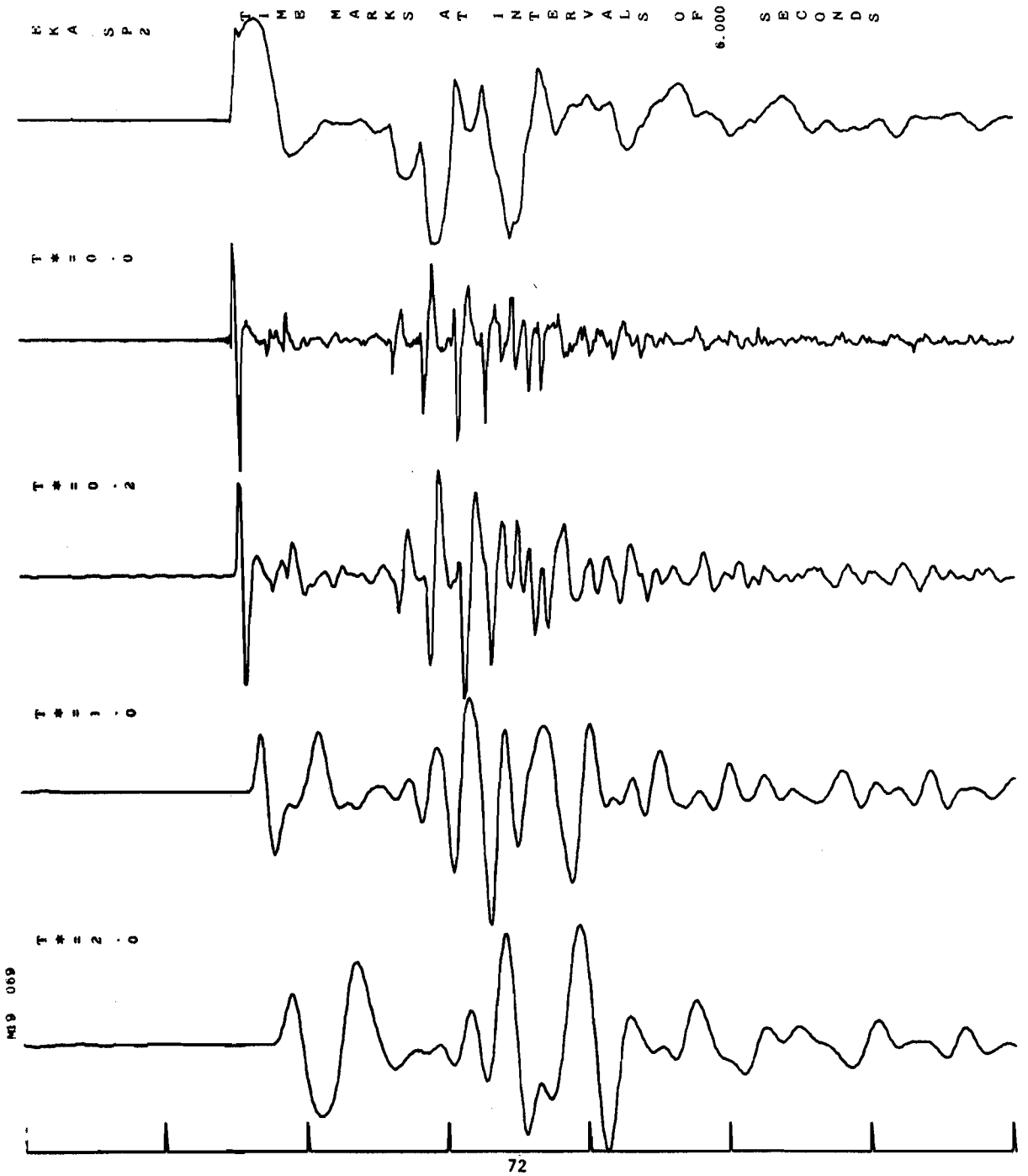
EKA SP2
TIMB MARKS AT INTERVALS OF 6.000 SECONDS
T*=0.0
T*=0.2
T*=1.0
T*=2.0
M19 069

Model M20

Dip of fault plane	:	45°
Direction of slip on fault plane	:	90° to strike
Shape of fault plane	:	elliptical
Dimensions of fault plane	:	2.5 × 2.0 km
Azimuth	:	-90° to strike
Orientation of major axis of ellipse	:	line of dip
Point of initiation of fracture	:	upper focus

Amplitudes

	Channel 1	Channel 2	Channel 3	Channel 4	Channel 5
M20K					
Maximum	1409.4	1130.5	852.5	412.5	198.3
Minimum	-786.4	-878.0	-716.4	-348.7	-179.0
M20SP					
Maximum	1409.4	482.1	140.7	19.0	3.9
Minimum	-786.4	-493.8	-199.9	-23.0	-5.6

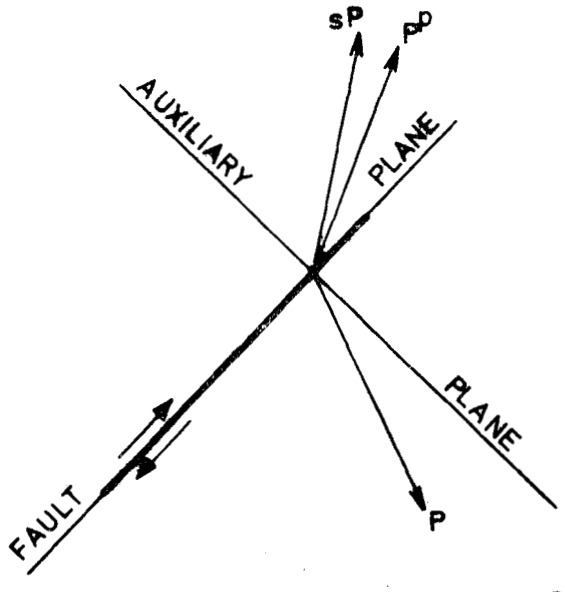

FIGURE 25. CROSS SECTION THROUGH THE SOURCE IN THE PLANE OF THE OBSERVER

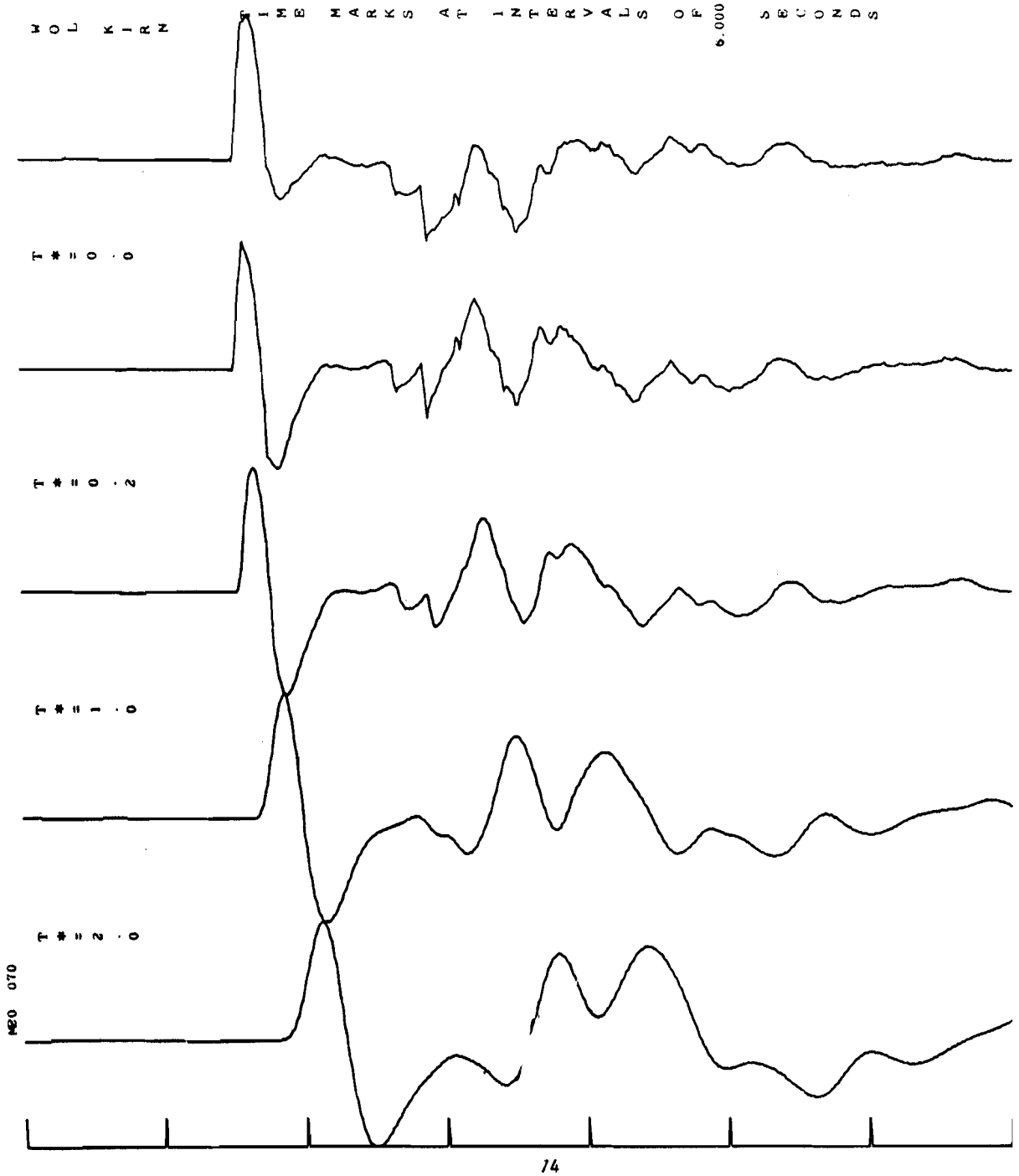
WOLF KIRN
TIME MARKS AT INTERVALS OF 6.000 SECONDS
T*=0.0
T*=0.2
T*=1.0
T*=2.0
NEO 070

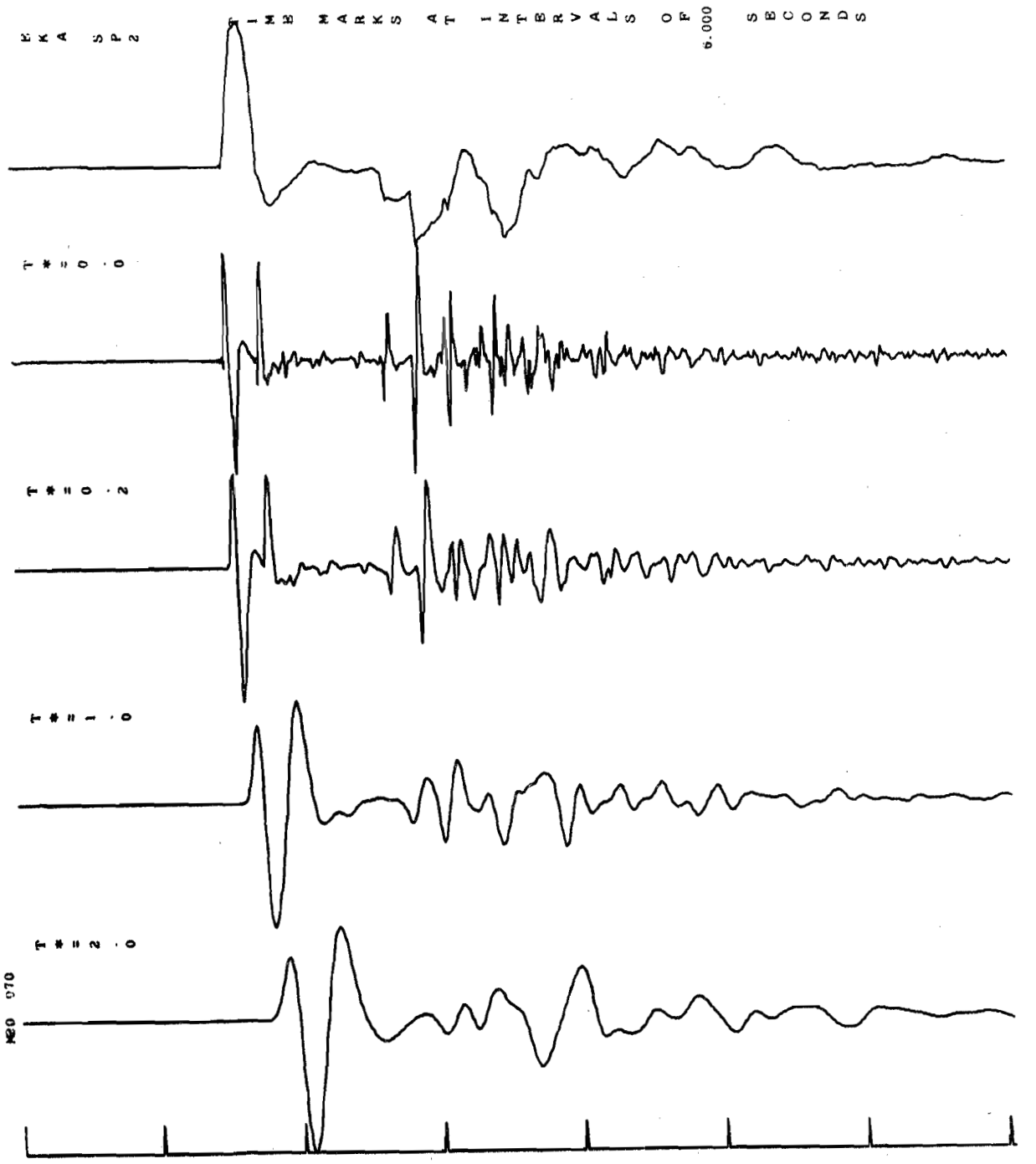
EKA SP2
TIME MARKS AT INTERVALS OF 0.000 SECONDS
T**=0.0
T**=0.2
T**=1.0
T**=2.0
M20 070

Model M21

Dip of fault plane	:	45°
Direction of slip of fault plane	:	90° to strike
Shape of fault plane	:	elliptical
Dimensions of fault plane	:	2.5 × 2.0 km
Azimuth	:	0°
Orientation of major axis of ellipse	:	line of dip
Point of initiation of fracture	:	upper focus

Amplitudes

	Channel 1	Channel 2	Channel 3	Channel 4	Channel 5
M21K					
Maximum	1968.0	1617.7	1203.9	542.7	252.3
Minimum	-1005.5	-979.0	-794.8	-411.4	-217.5
M21SP					
Maximum	1968.0	822.4	250.4	28.9	4.4
Minimum	-1005.5	-732.0	-288.7	-37.1	-7.9

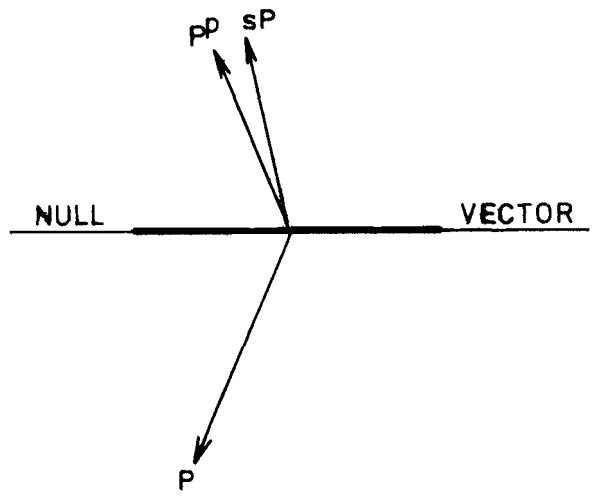

FIGURE 26. CROSS SECTION THROUGH THE SOURCE IN THE PLANE OF THE OBSERVER

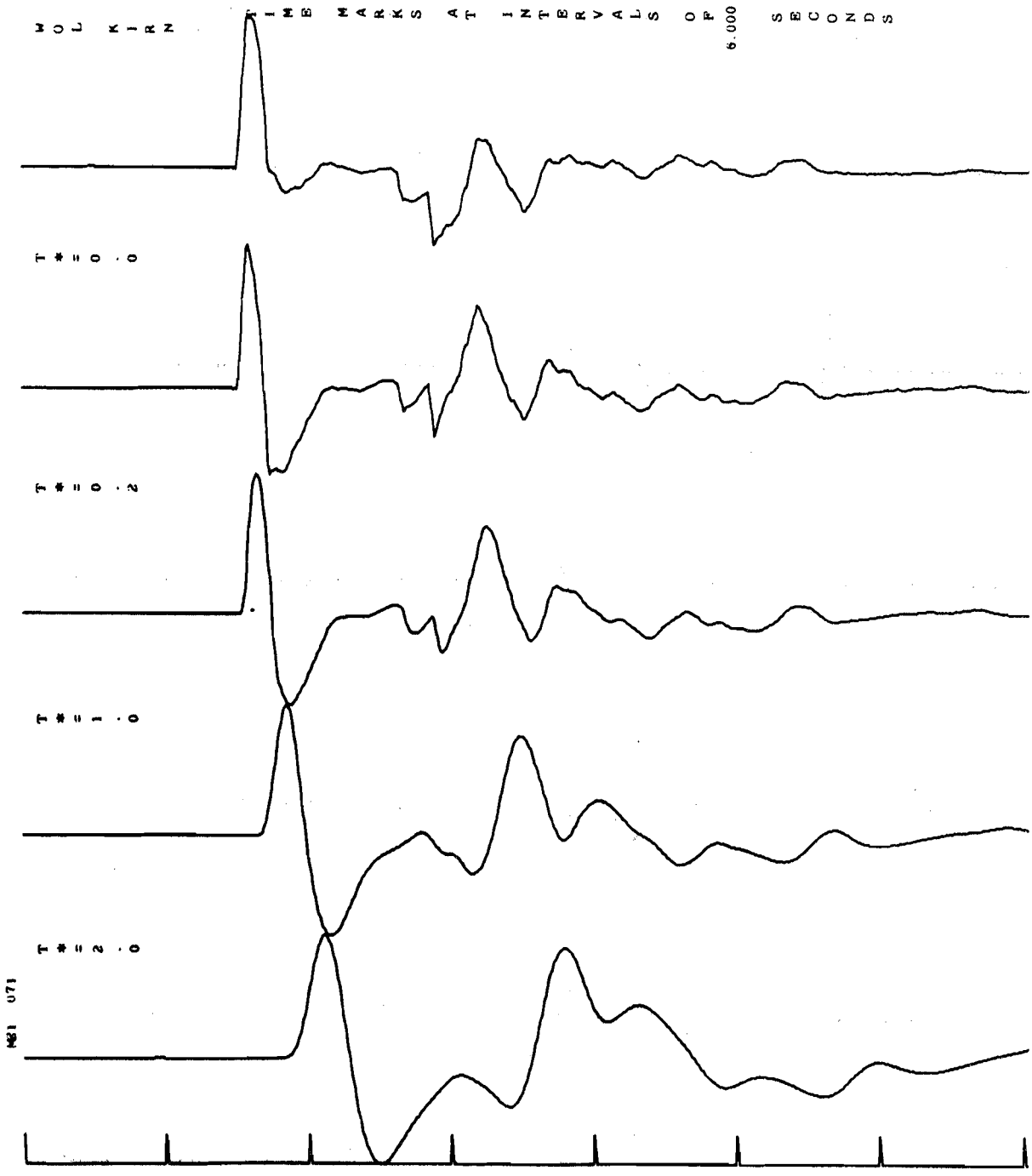
MOJ K-IRN
TIME MARKS AT INTERVALS OF 6.000 SECONDS
T*=0.0
T*=0.2
T*=1.0
T*=2.0
MAY 071

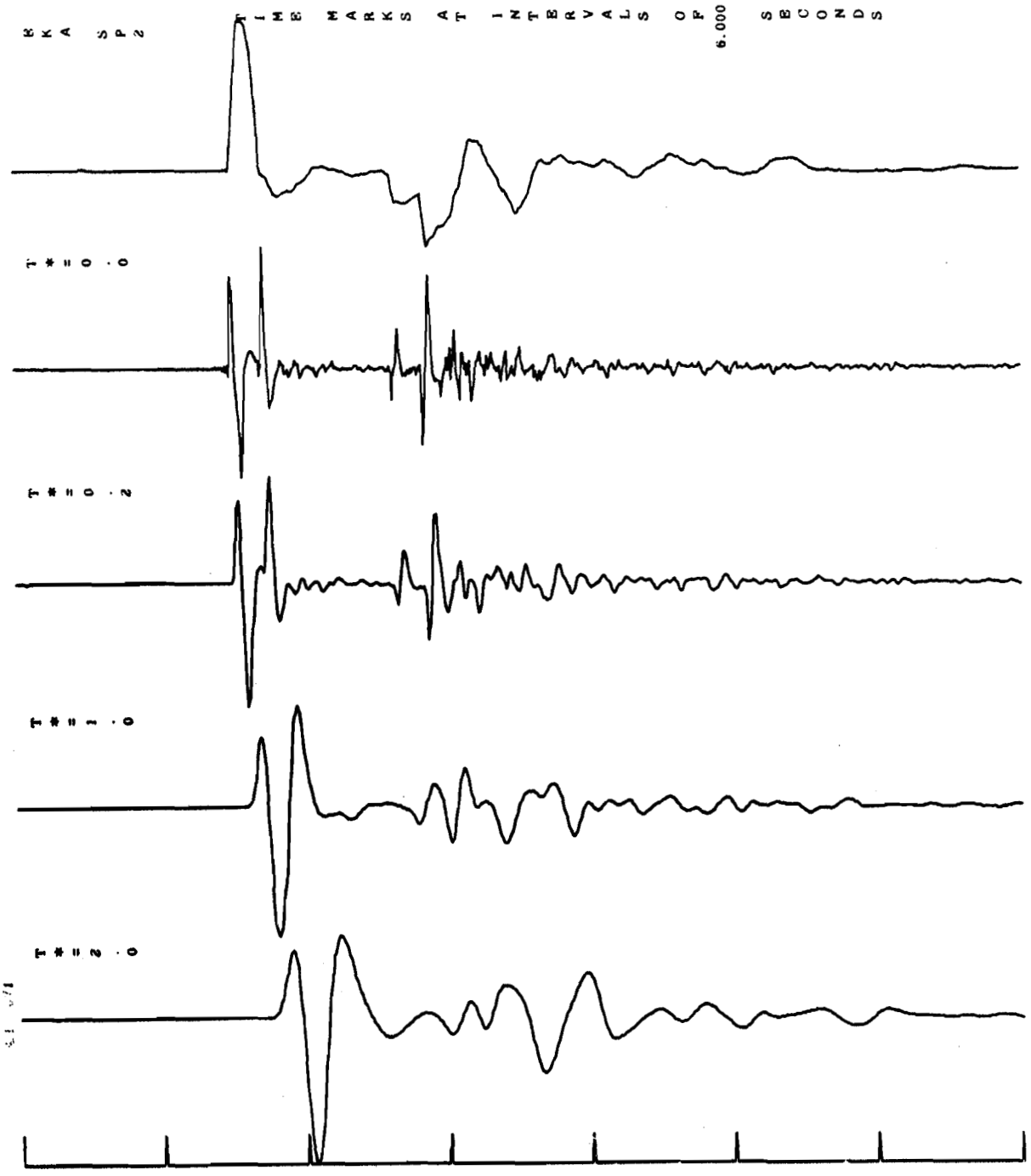
EKA SP2
TIME MARKS AT INTERVALS OF 6.000 SECONDS
T**=0.0
T**=0.2
T**=1.0
T**=2.0

Model M22

Dip of fault plane	:	45°
Direction of slip of fault plane	:	90° to strike
Shape of fault plane	:	elliptical
Dimensions of fault plane	:	2.5 × 2.0 km
Azimuth	:	90.0°
Orientation of major axis of ellipse	:	line of dip
Point of initiation of fracture	:	upper focus

Amplitudes

	Channel 1	Channel 2	Channel 3	Channel 4	Channel 5
M22K					
Maximum	1961.5	1587.4	1173.5	479.2	212.2
Minimum	-879.5	-930.6	-776.3	-360.5	-184.0
M22SP					
Maximum	1961.5	1013.7	352.8	30.1	4.3
Minimum	-879.5	-590.0	-267.2	-43.5	-7.7

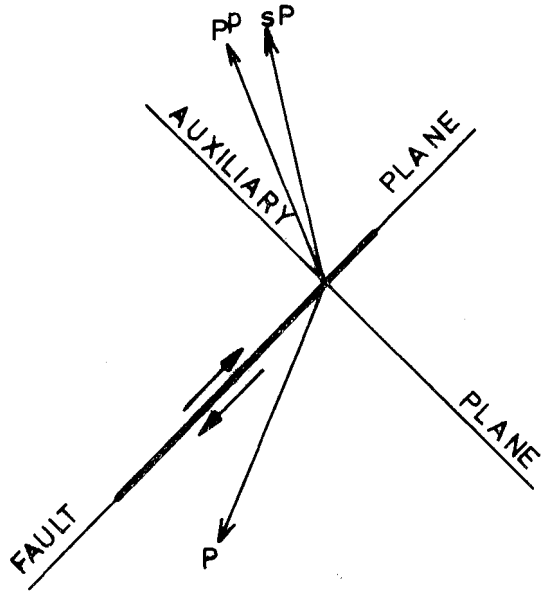

FIGURE 27. CROSS SECTION THROUGH THE SOURCE IN THE PLANE OF THE OBSERVER

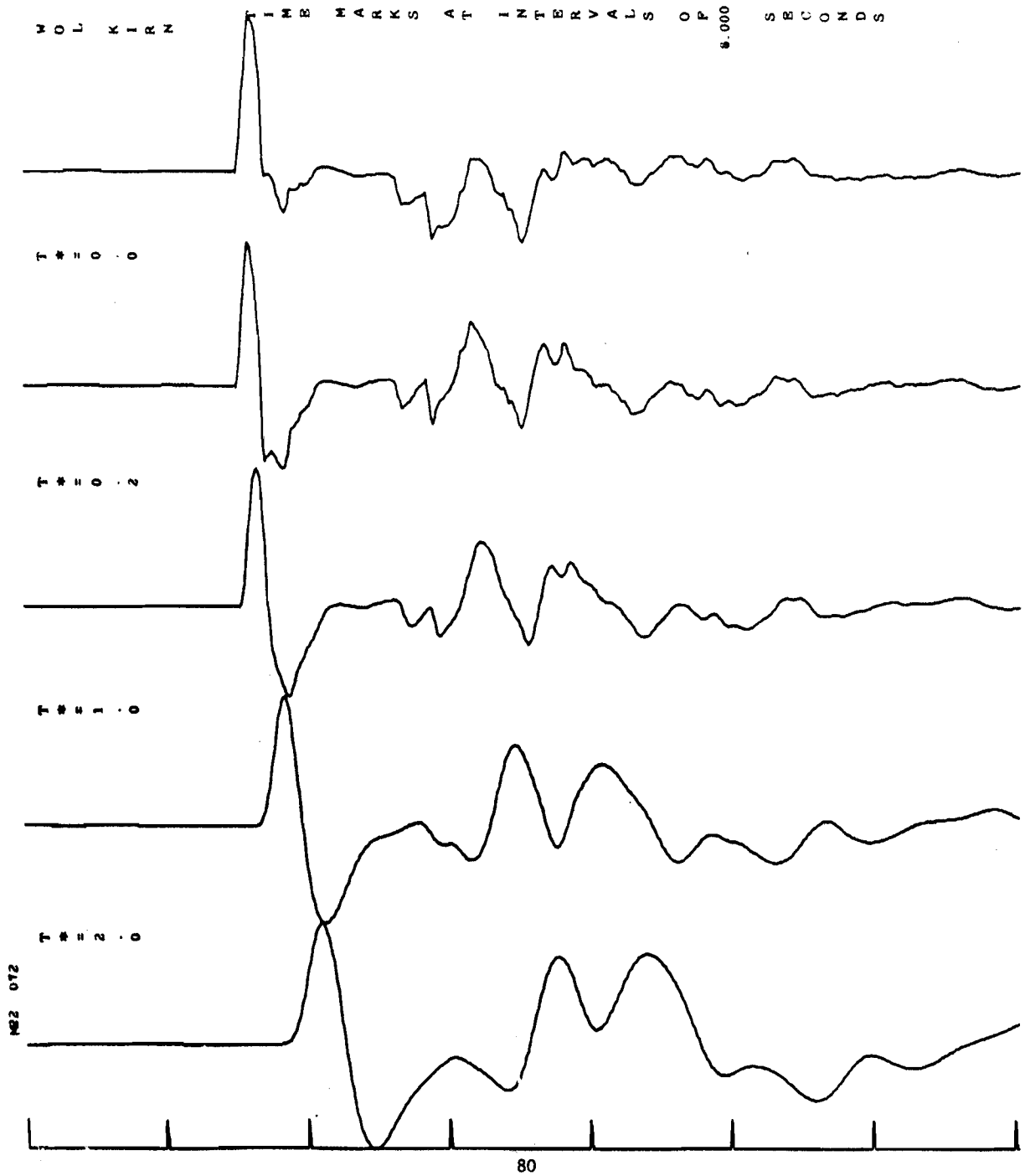
MOL KIRN
TIME MARKS AT INTERVALS OF 5.000 SECONDS
T**=0.0
T**=0.2
T**=1.0
T**=2.0
M82 072
80

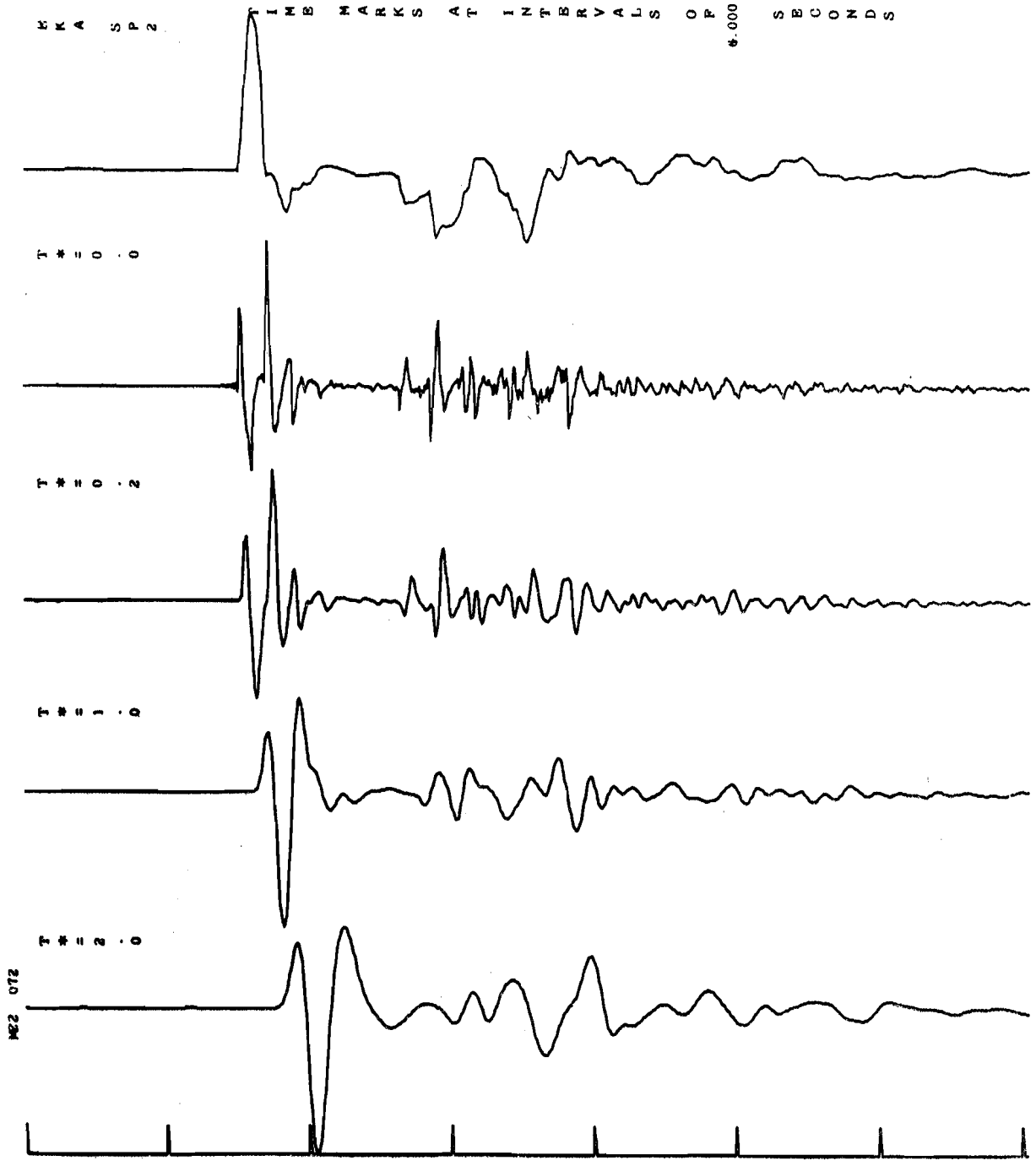
EKA SP2
TIME MARKS AT INTERVALS OF 0.000 SECONDS
T**=0.0
T**=0.2
T**=1.0
T**=2.0
M22 072

7. MODEL WITH SLIP ON PLANES DIPPING AT 45° OR 67.5°, SLIP DIRECTION -45° TO STRIKE: M23 TO M27

In all the models shown in the previous sections the motion on the fault plane is either parallel to, or at right angles to, the strike of the fault. In this section the slip direction makes an angle of -45° with the strike. These models show widely different seismograms for the same model when observed in different azimuths. In particular, for azimuths where the null vector of the focal sphere lies close to the paths followed by pP and sP as they leave the source, the seismogram is very simple consisting principally of a large P pulse.

Model M23

Dip of fault plane	:	67.5°
Direction of slip on fault plane	:	-45° to strike
Shape of fault plane	:	circular
Dimensions of fault plane	:	1.0 km radius
Azimuth	:	90°

Amplitudes

	Channel 1	Channel 2	Channel 3	Channel 4	Channel 5
M23K					
Maximum	205.2	214.4	137.7	52.4	23.3
Minimum	-407.4	-351.6	-167.3	-35.6	-15.0
M23SP					
Maximum	205.2	578.0	150.7	8.5	0.8
Minimum	-407.4	-313.5	-83.1	-4.9	-0.6

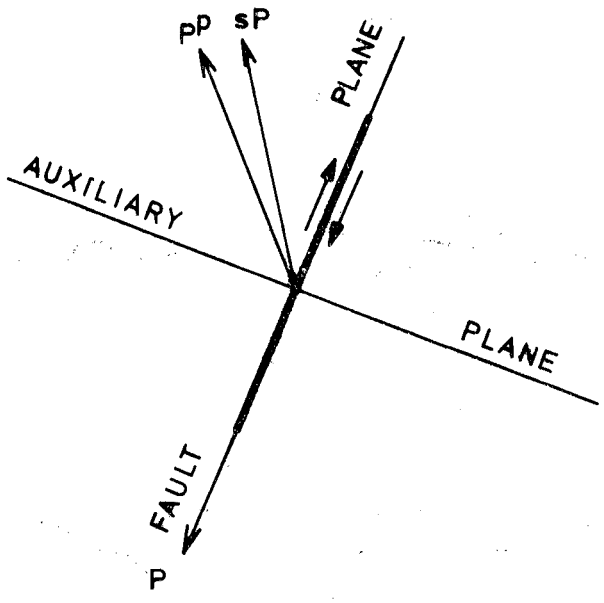

FIGURE 28. CROSS SECTION THROUGH THE SOURCE IN THE PLANE OF THE OBSERVER

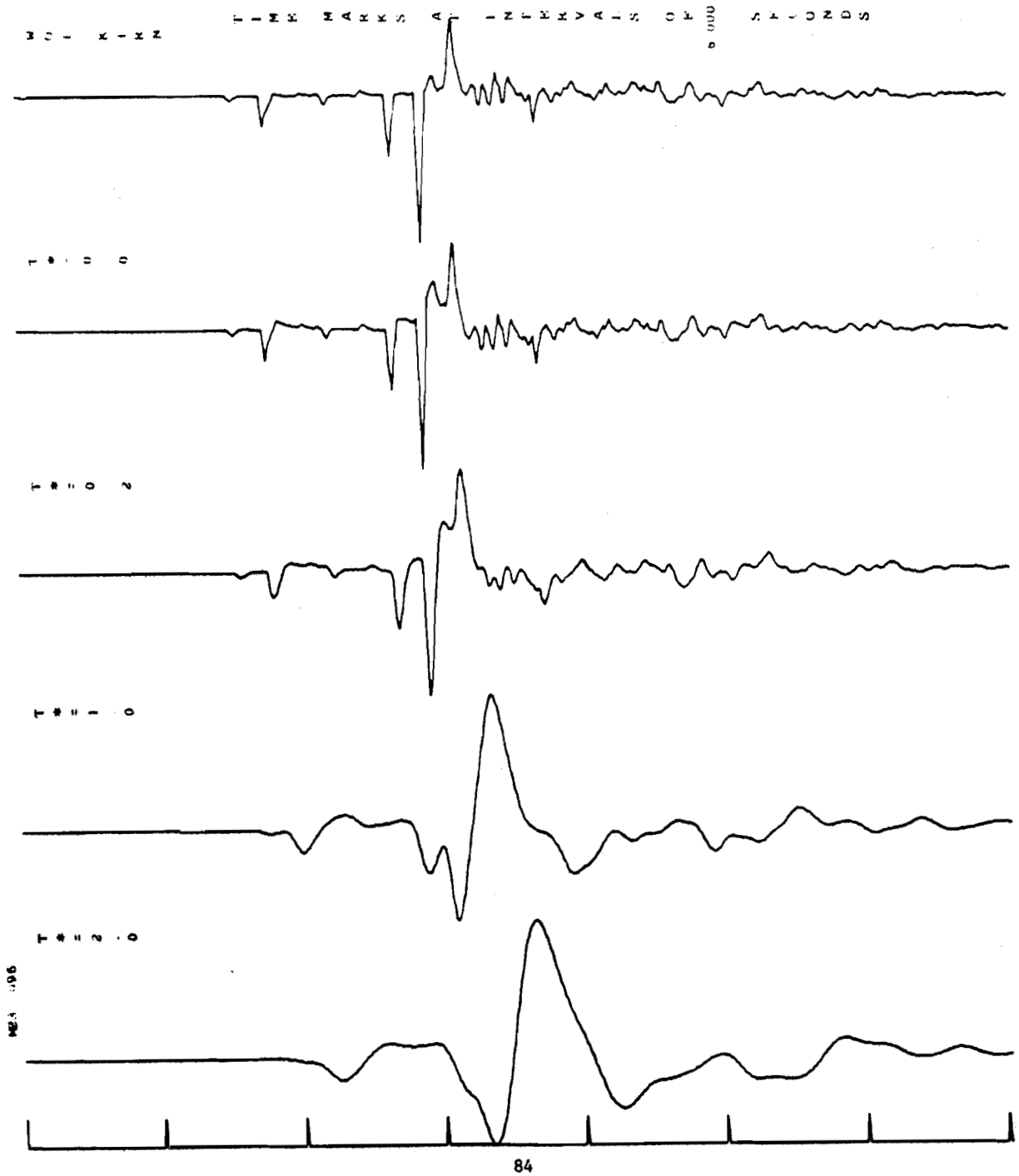

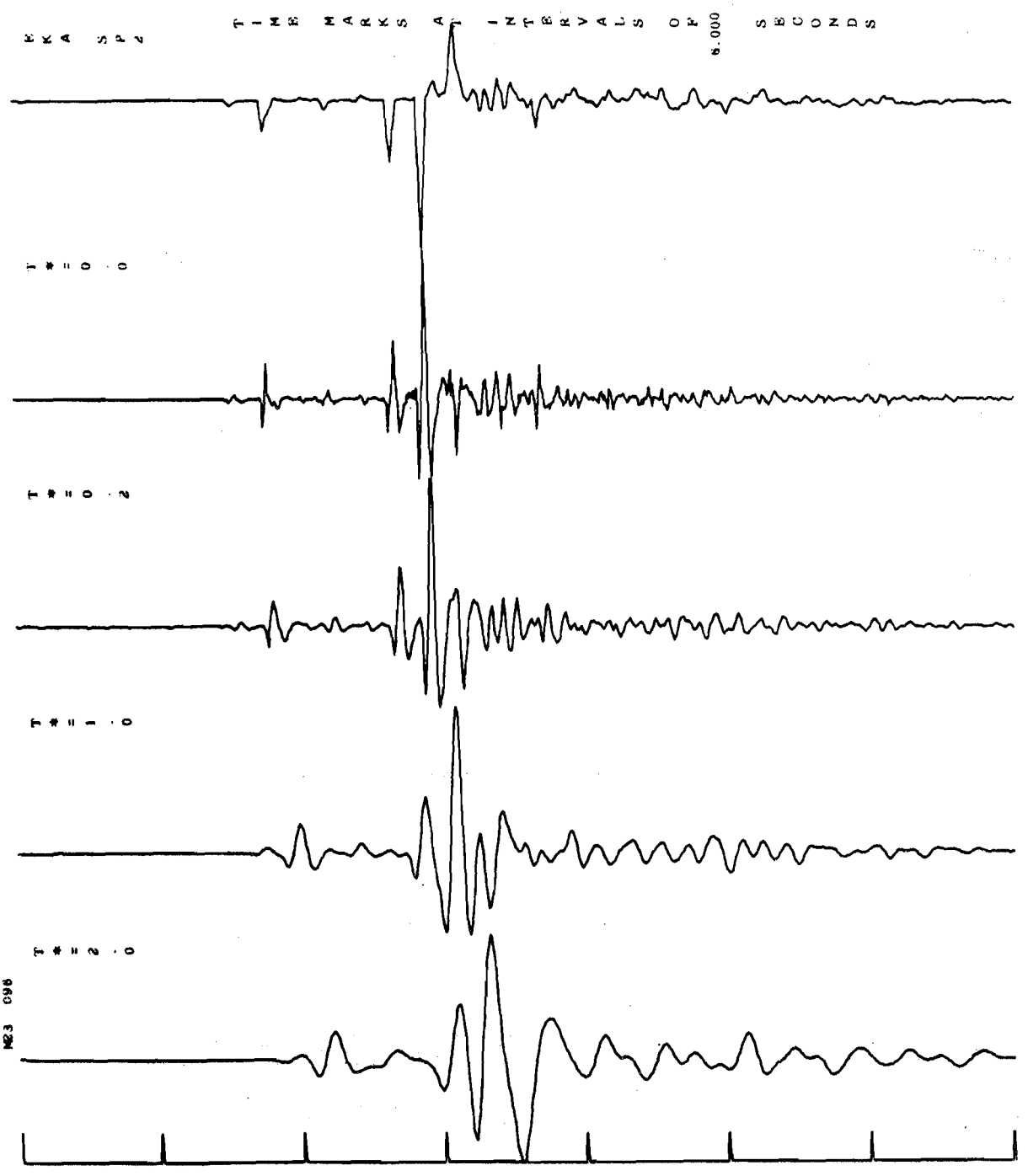
EKA SP2
TIME MARKS AT INTERVALS OF 6.000 SECONDS
T*=0.0
T*=0.2
T*=-.0
T*=2.0
M23 096

Model M24

Dip of fault plane	:	67.5°
Direction of slip on fault plane	:	-45°
Shape of fault plane	:	circular
Dimensions of fault plane	:	1.0 km radius
Azimuth	:	0°

Amplitudes

	Channel 1	Channel 2	Channel 3	Channel 4	Channel 5
M24K					
Maximum	449.5	407.7	198.8	48.7	19.5
Minimum	-118.4	-95.1	-54.7	-29.2	-15.6
M24SP					
Maximum	449.5	339.0	87.5	4.8	0.5
Minimum	-118.4	-639.6	-150.3	-8.5	-0.9

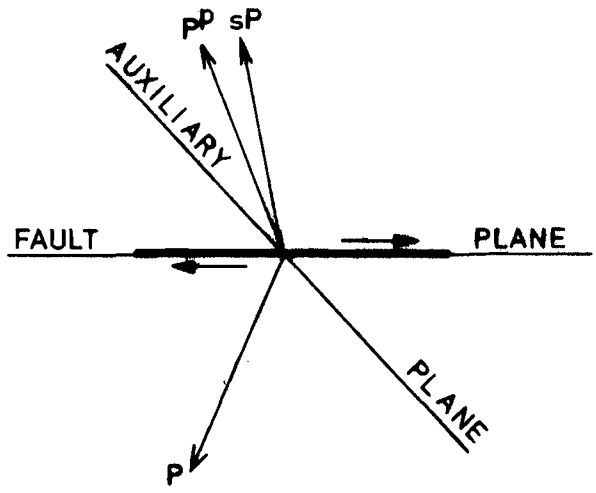

FIGURE 29. CROSS SECTION THROUGH THE SOURCE IN THE PLANE OF THE OBSERVER

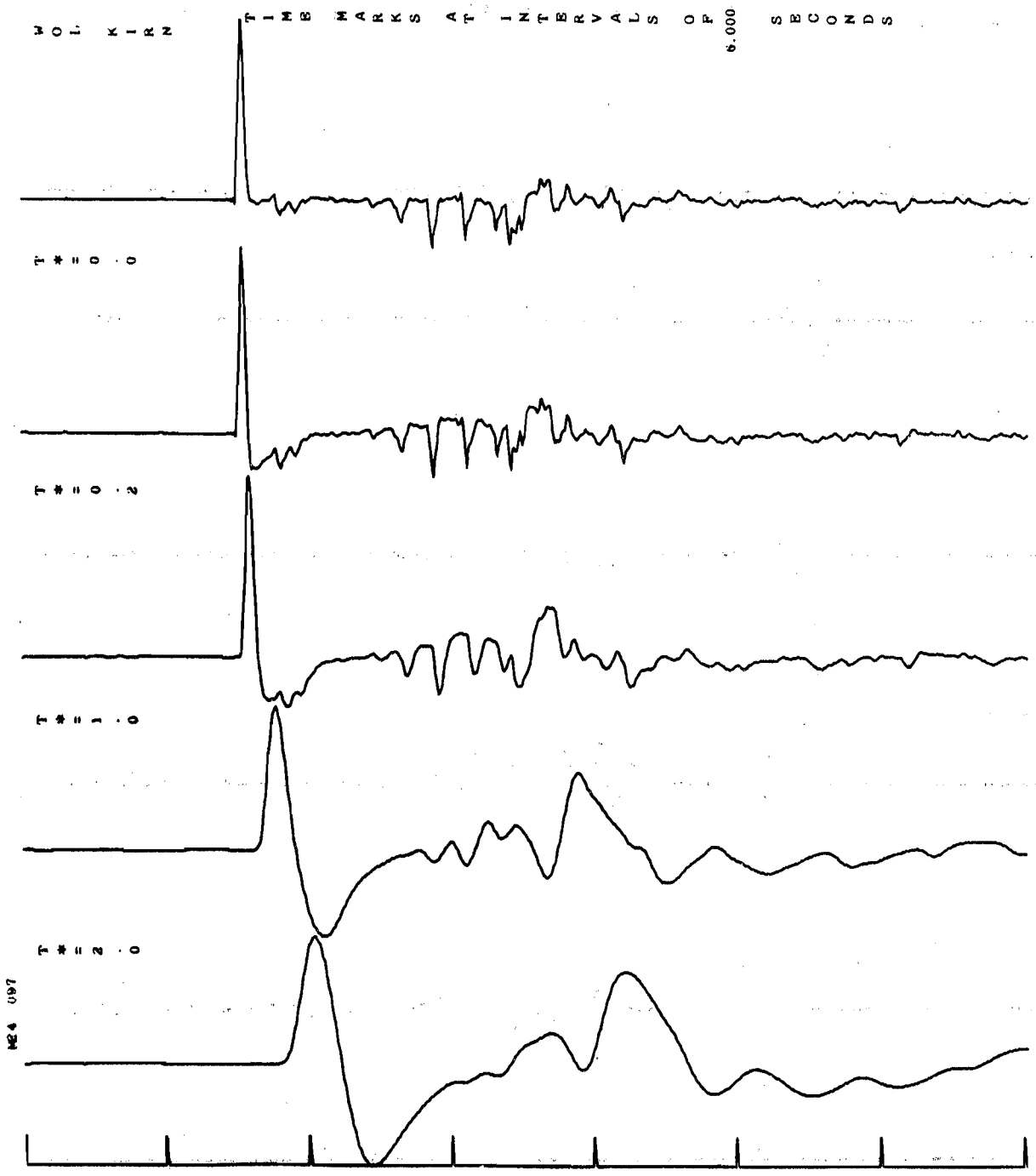
MOL. KIRN
TIME MARKS AT INTERVALS OF 6.000 SECONDS
T*=0.0
T*=0.2
T*=1.0
T*=2.0
ME4 097

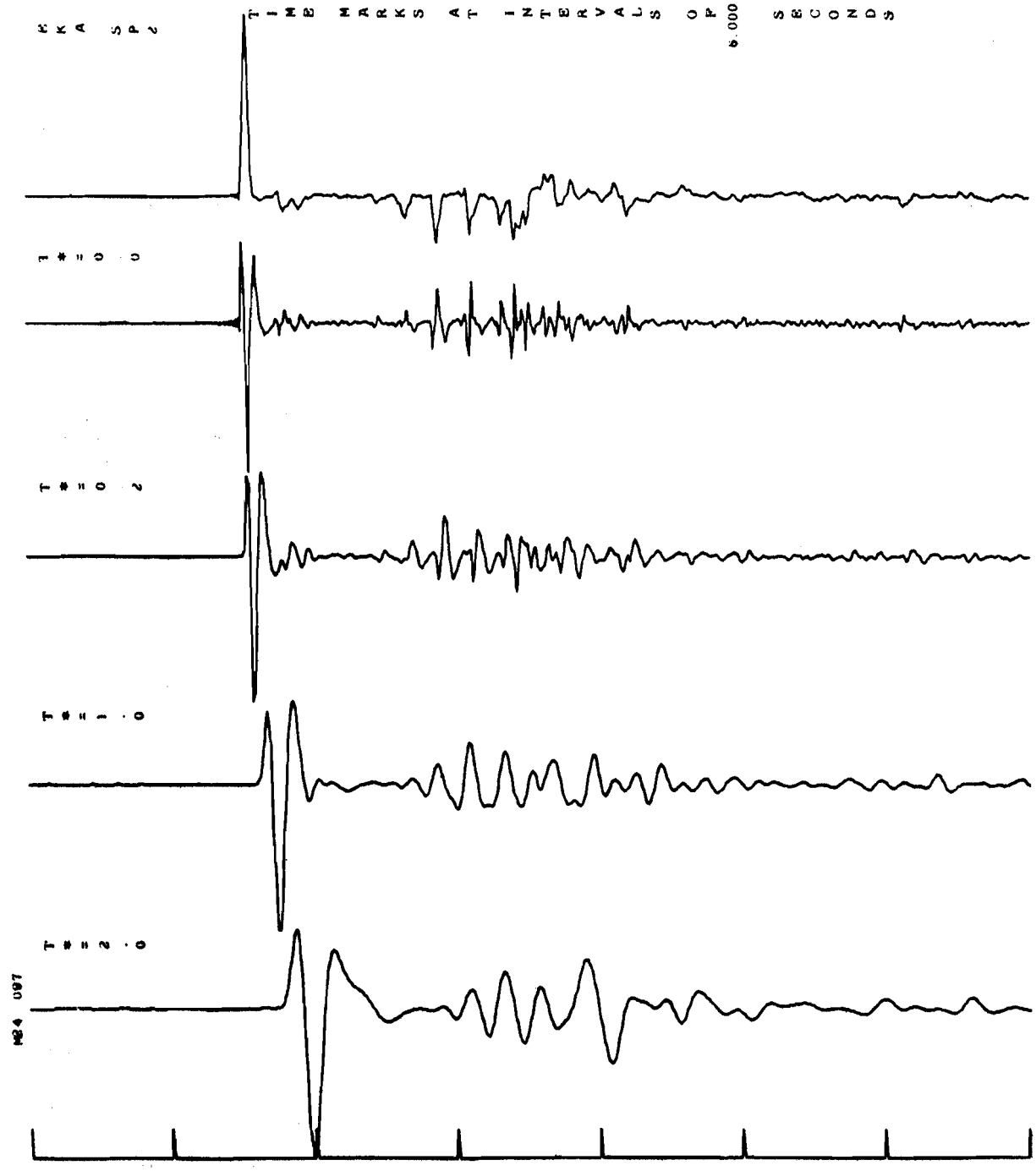
EKA SP2
TIME MARKS AT INTERVALS OF 0.000 SECONDS
T##0.0
T##0.2
T##-.0
T##2.0
M24 U87

Model M25

Dip of fault plane	:	45°
Direction of slip on fault plane	:	-45°
Shape of fault plane	:	circular
Dimensions of fault plane	:	1.0 km radius
Azimuth	:	90.0°

Amplitudes

	Channel 1	Channel 2	Channel 3	Channel 4	Channel 5
M25K					
Maximum	354.7	320.8	156.8	38.3	15.3
Minimum	-272.2	-227.8	-114.0	-26.2	-13.0
M25SP					
Maximum	354.7	449.8	121.2	5.8	0.5
Minimum	-272.2	-505.6	-118.4	-6.7	-0.7

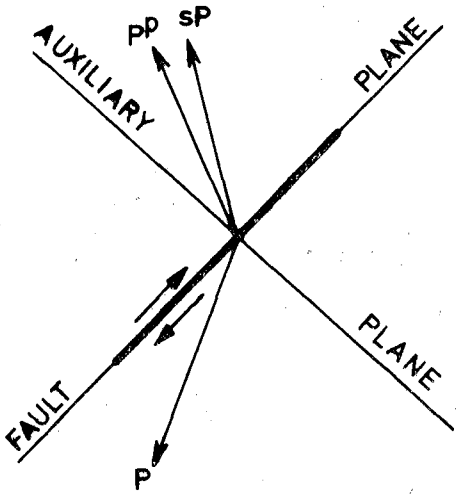

FIGURE 30. CROSS SECTION THROUGH THE SOURCE IN THE PLANE OF THE OBSERVER

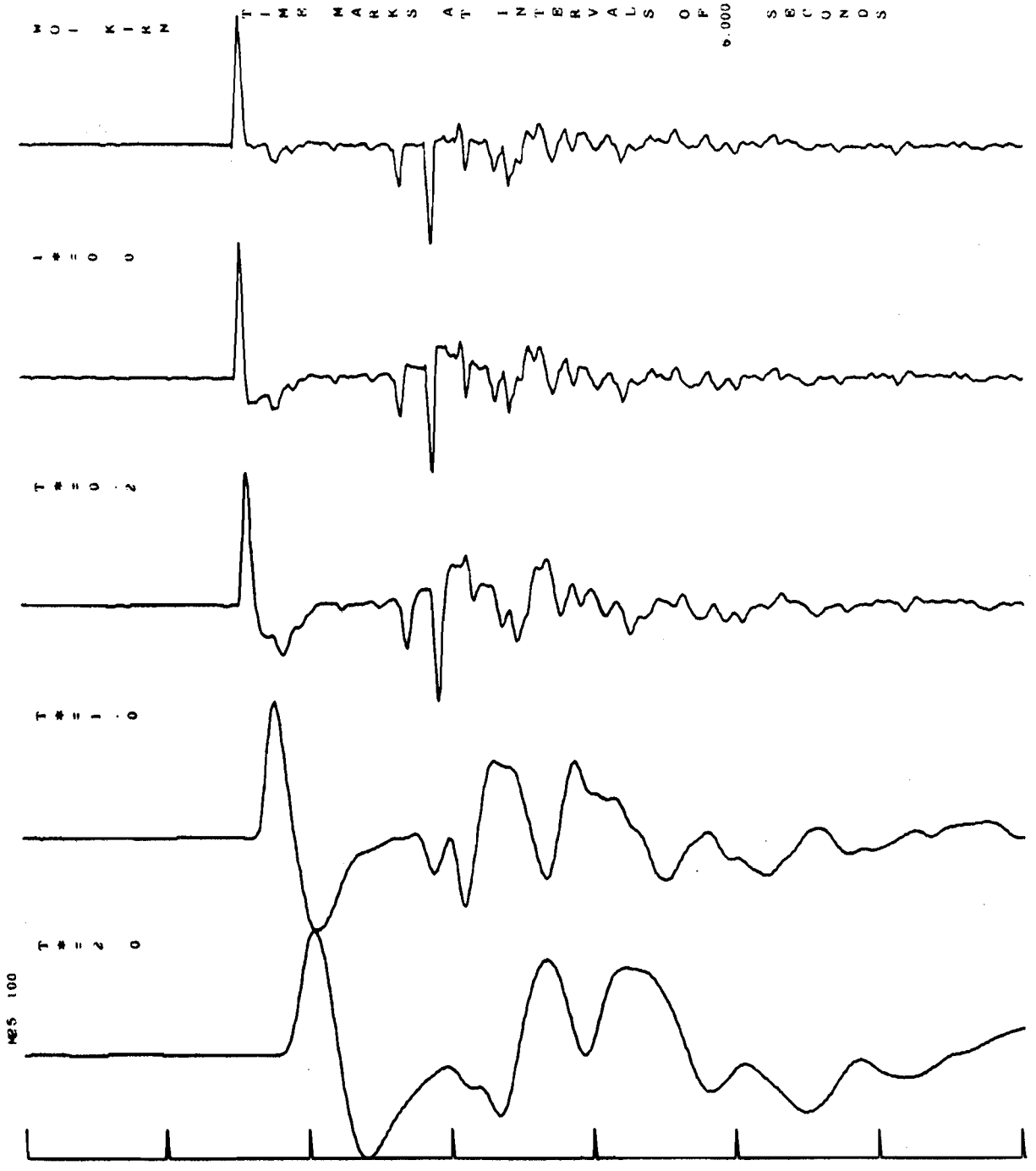
TIME MARKS AT INTERVALS OF 6.000 SECONDS
M25 100

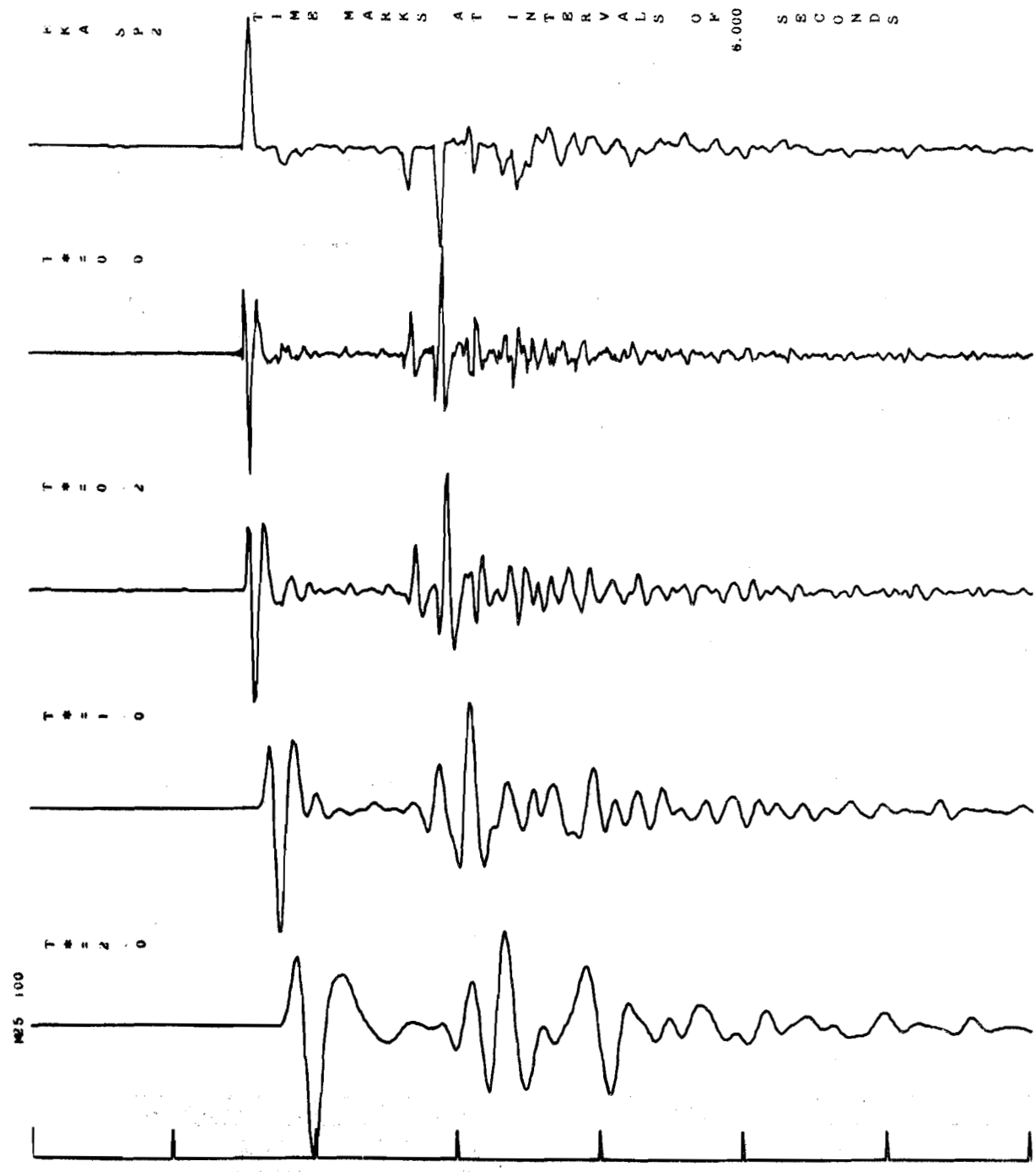
TIME MARKS AT INTERVALS OF 6.000 SECONDS
M25 100

Model M26

Dip of fault plane	:	45°
Direction of slip on fault plane	:	-45°
Shape of fault plane	:	circular
Dimensions of fault plane	:	1.0 km radius
Azimuth	:	0.0°

Amplitudes

	Channel 1	Channel 2	Channel 3	Channel 4	Channel 5
M26K					
Maximum	699.5	622.1	321.4	75.9	30.3
Minimum	-200.1	-147.2	-83.7	-45.2	-24.2
M26SP					
Maximum	699.5	491.3	143.6	7.6	0.7
Minimum	-200.1	-965.2	-250.6	-13.5	-1.4

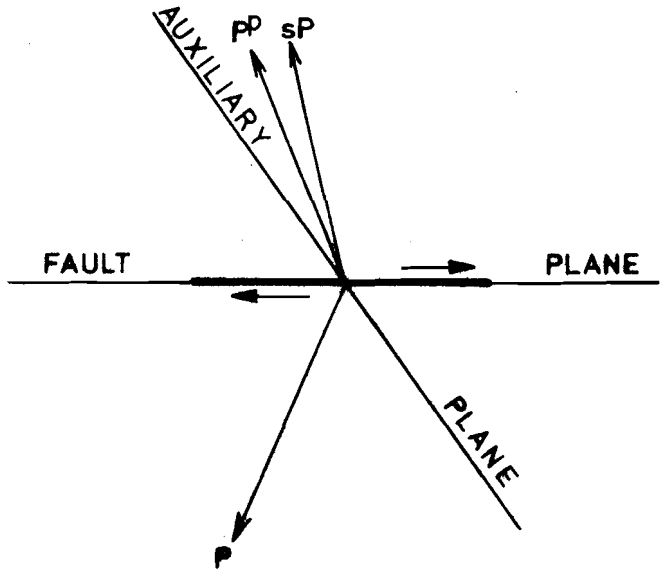

FIGURE 31. CROSS SECTION THROUGH THE SOURCE IN THE PLANE OF THE OBSERVER

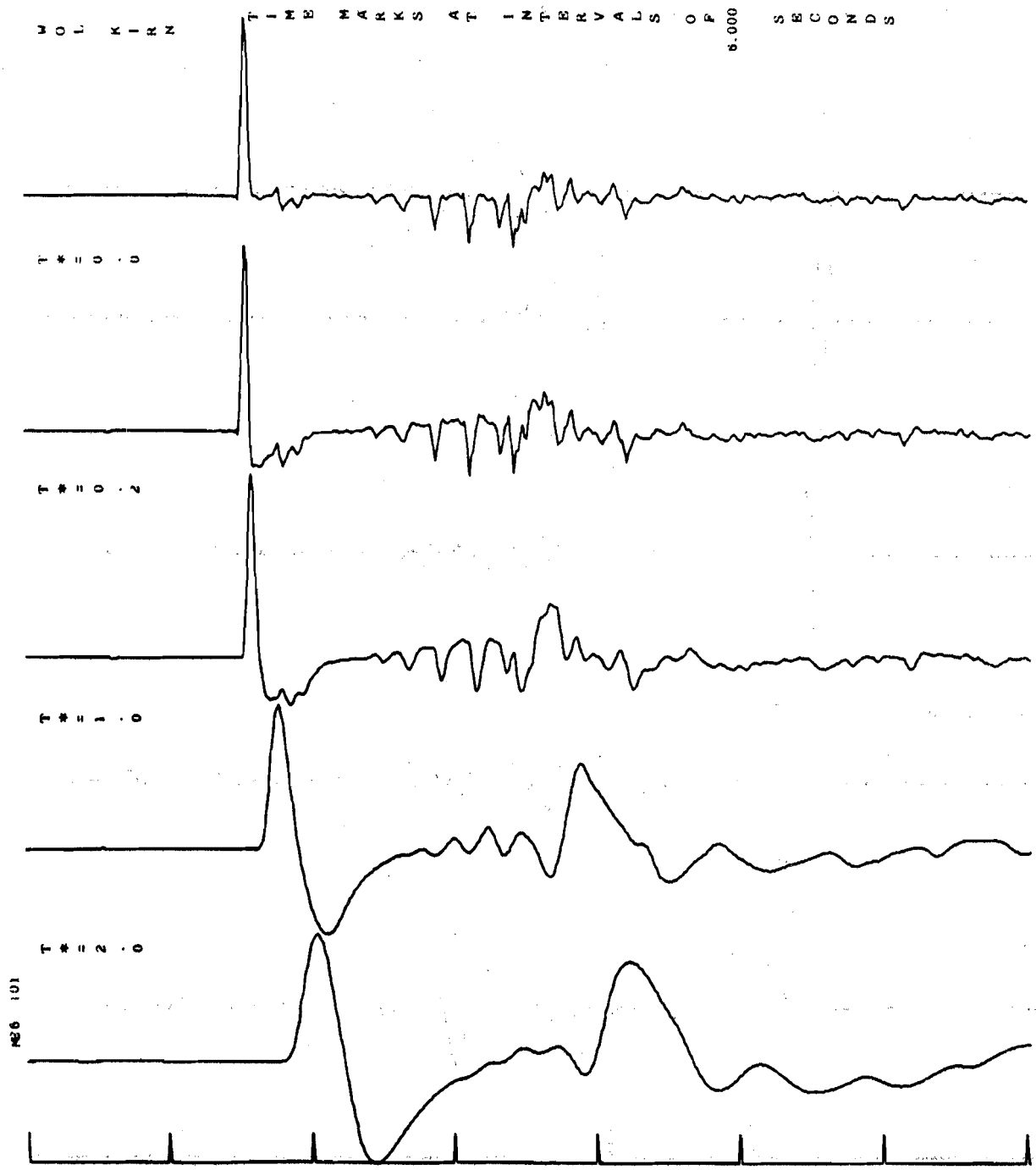
MOL K-RN
TIME MARKS AT INTERVALS OF 6.000 SECONDS
T*=0.0
T*=0.2
T*=1.0
T*=2.0
M26 101

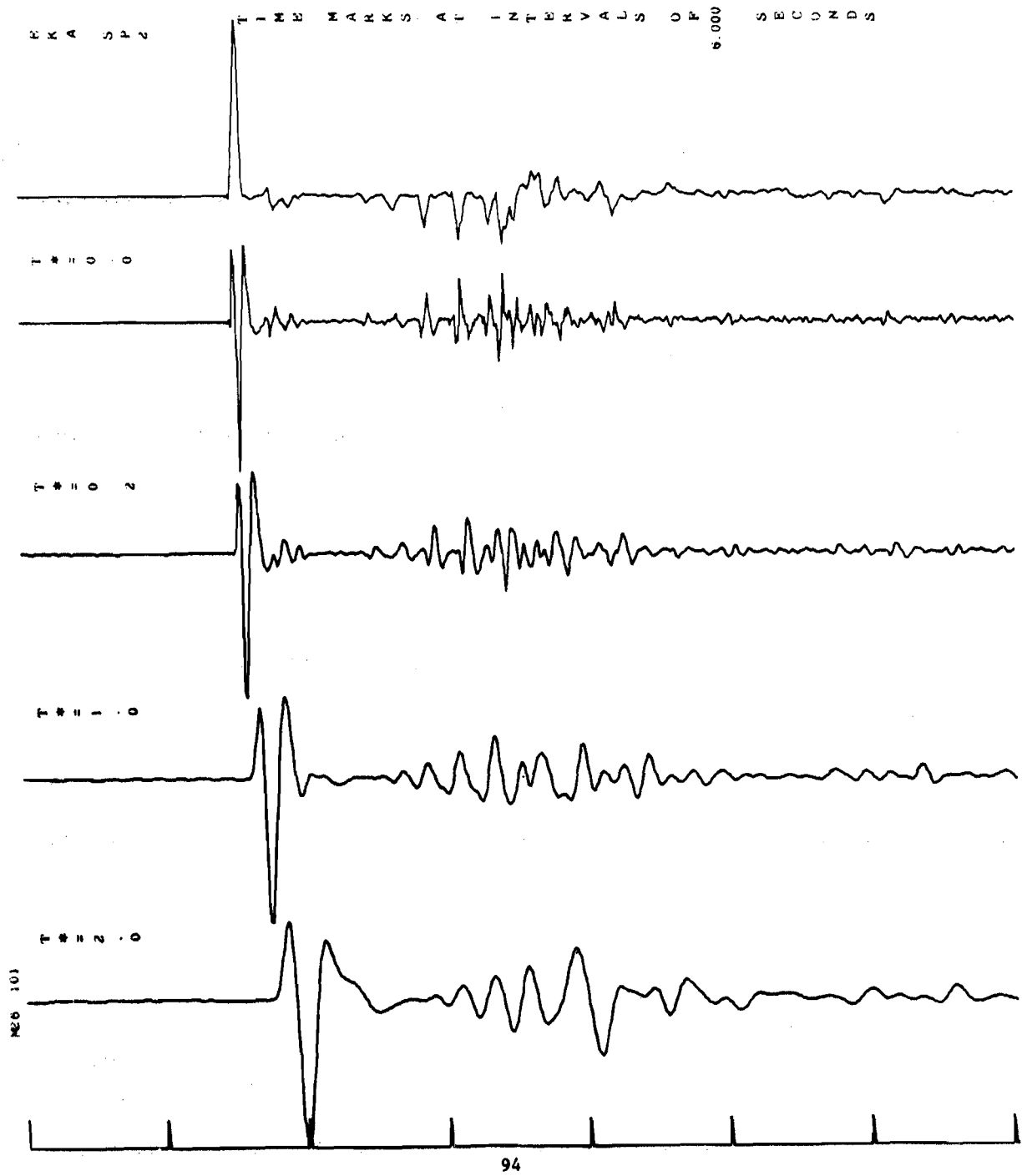
TIME MARKS AT INTERVALS OF 6.000 SECONDS
EKA SP2
T**=0.0
T**=0.2
T**=1.0
T**=2.0
NO 103

Model M27

Dip of fault plane	:	45°
Direction of slip on fault plane	:	-45° to strike
Shape of fault plane	:	circular
Dimensions of fault plane	:	1.0 km radius
Azimuth	:	180°

Amplitudes

	Channel 1	Channel 2	Channel 3	Channel 4	Channel 5
M27K					
Maximum	264.4	283.8	184.0	72.7	33.0
Minimum	-548.3	-472.0	-221.0	-45.9	-19.2
M27SP					
Maximum	264.4	772.7	199.9	11.4	1.0
Minimum	-548.3	-435.5	-110.7	-6.6	-0.8

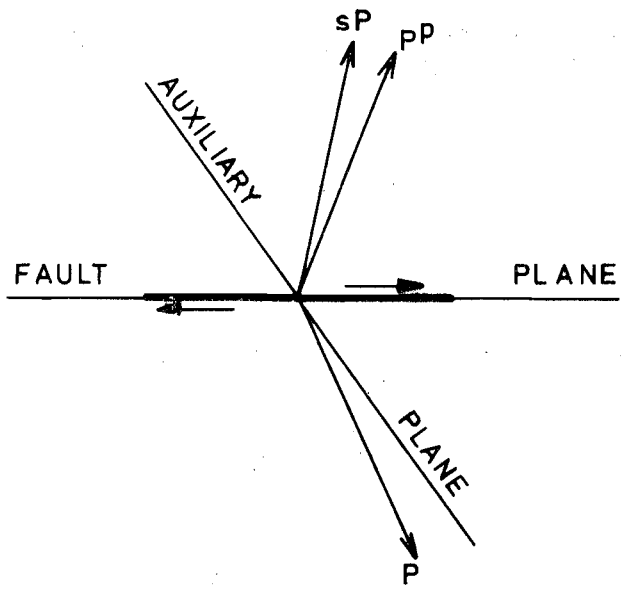

FIGURE 32. CROSS SECTION THROUGH THE SOURCE IN THE PLANE OF THE OBSERVER

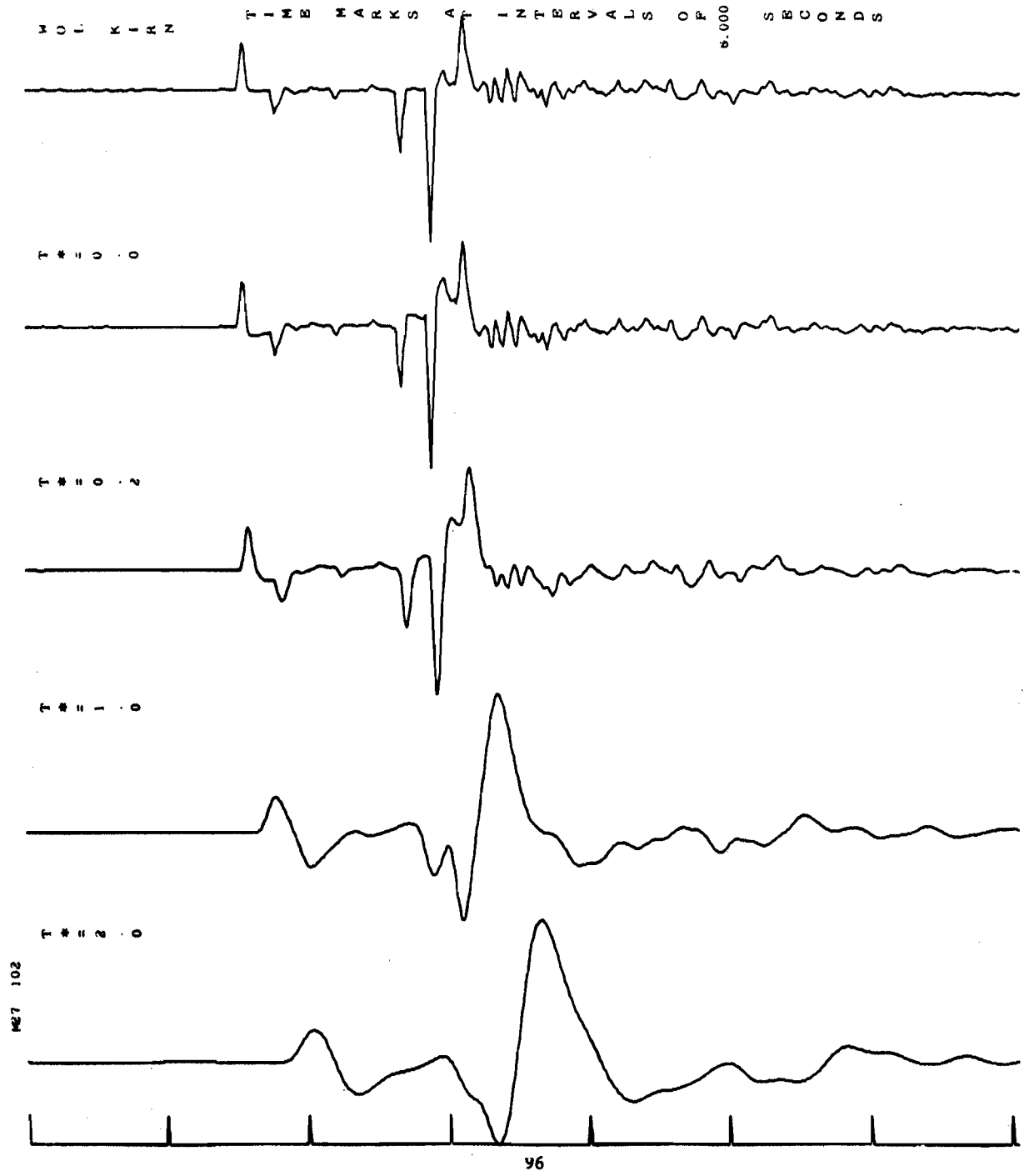
MOL KIRN
TIME MARKS AT INTERVALS OF 6.000 SECONDS
T*=0.0
T*=0.2
T*=1.0
T*=2.0
M27 102
96

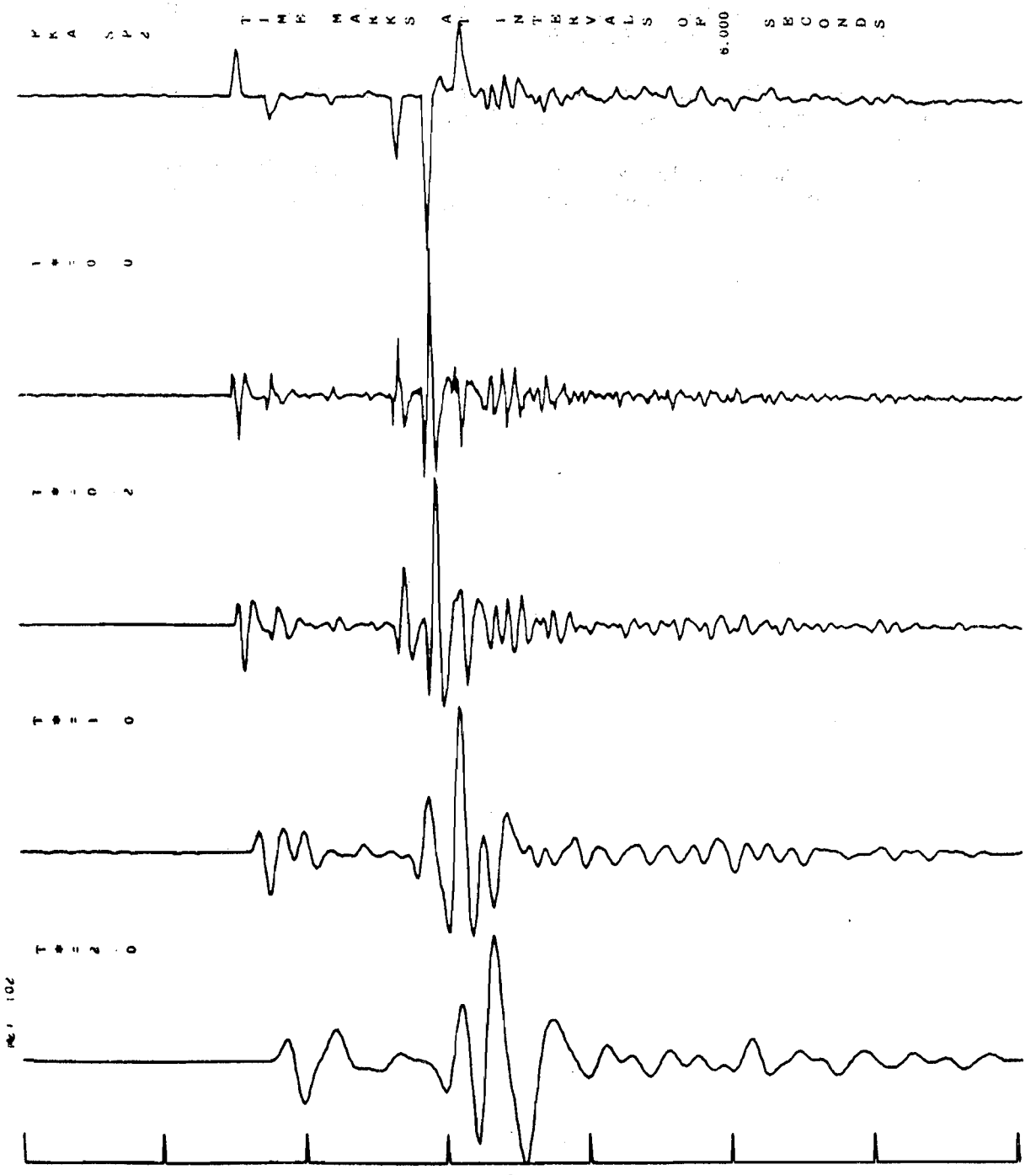
TIME MARKS AT INTERVALS OF 6.000 SECONDS

REFERENCES

1. A Douglas, J A Hudson and C Blamey: "A Quantitative Evaluation of Seismic Signals at Teleseismic Distances. III: Computed P and Rayleigh Wave Seismograms". Geophys J Roy Astr Soc, 28, 385-410 (1972)

2. A Douglas, P D Marshall, J B Young and J A Hudson: "Earthquakes that Look Like Explosions". Geophys J Roy Astr Soc (in press)

3. J C Savage: "Radiation from a Realistic Model of Faulting". Bull Seism Soc Amer, 56, 577-592 (1966)

4. H Kanamori: "Attenuation of P Waves in the Upper and Lower Mantle". Bull Earth Res Inst, Tokyo, 45, 299-312 (1967)

5. R Parks: "Seismic Refraction Networks in the Study of the Earth's Crust" Ph Thesis, University of Edinburgh (1967)